Helsinki University of Technology
Department of Engineering Physics and Mathematics
Low Temperature Laboratory, Brain Research Unit
Espoo 2007

BRAIN MECHANISMS OF AUDIOTACTILE AND AUDIOMOTOR INTERACTIONS

Gina Caetano

Dissertation for the degree of Doctor of Science in Technology to be presented with due permission of the Department of Engineering Physics and Mathematics, Helsinki University of Technology, for public examination and debate in Auditorium F1 at Helsinki University of Technology (Espoo, Finland) on the 21st of December, 2007, at 12 noon.

Helsinki University of Technology
Low Temperature Laboratory
Brain Research Unit

Teknillinen korkeakoulu
Kylmälaboratorio
Aivotutkimusyksikkö

Distribution:
Low Temperature Laboratory
Helsinki University of Technology
P.O.Box 5100
FIN-02015 HUT
Finland
Tel: +358-9-451 5619
Fax: +358-9-451 2969
This thesis is downloadable at http://lib.hut.fi/Diss/2007/isbn9789512291496/

ISBN 978-951-22-9148-9 (printed version)
ISBN 978-951-22-9149-6 (electronic version)

Picaset Oy
Helsinki 2007

ABSTRACT OF DOCTORAL DISSERTATION

HELSINKI UNIVERSITY OF TECHNOLOGY
P.O. BOX 1000, FI-02015 TKK
http://www.tkk.fi

Author Gina Caetano

Name of the dissertation
Brain Mechanisms of Audiotactile and Audiomotor Interactions

Manuscript submitted 10.10.2007 | Manuscript revised 03.12.2007

Date of the defence 21.12.2007

☐ Monograph | ☒ Article dissertation (summary + original articles)

Department	Department of Engineering Physics and Mathematics
Laboratory	Laboratory of Biomedical Engineering
Field of research	Neurosciences
Opponent(s)	Prof. Beatrice de Gelder
Supervisor	Prof. Risto Ilmoniemi
Instructor	Docent Veikko Jousmäki & Prof. Riitta Hari

Abstract

This thesis focuses on audiotactile integration, brain areas activated by vibrotactile stimulation, transfer of vibrotactile information to motor output, and reactivity of the human primary motor and somatosensory cortices in action observation. Human experience of the outside world results from integration of information obtained simultaneously via multiple senses. Accumulating evidence, from studies in both primates and humans, suggests that integration between different sensory modalities also occurs at early stages of cortical processing, in areas classically considered as purely unisensory.

In Study I we studied integration between auditory and somatosensory systems. We showed, in a loudness-matching task, that subjects chose lower intensities for the probe than for the reference tone, when auditory and vibrotactile stimuli were presented simultaneously.

In Studies II and III we explored brain areas involved in processing vibrotactile and tactile information, respectively. We showed that, besides primary and secondary somatosensory areas, auditory areas are also activated. In Study II we characterized the time course of brain activations and showed convergence of vibrotactile information to auditory areas. On the other hand, in Study III we identified, with good spatial accuracy, common neural substrates that process auditory and tactile information in auditory belt areas.

In Study IV we assessed whether frequency information transfers from touch to vocal utterance in normal-hearing female adults. We demonstrated that such information transfer occurs clearly between 150–400 Hz. Based on findings in Studies II and III, we hypothesized that this transfer may involve at least primary and secondary somatosensory and auditory areas.

Our social skills rely on the capability to understand others. In the human brain, the mirror-neuron system matches observation and execution of actions. This system comprises at least the inferior frontal gyrus, premotor areas, primary motor cortex, and the inferior parietal lobule.

In Study V we investigated similarities in sensorimotor oscillatory activity between own, observed, and heard actions. We demonstrated that the primary motor cortex is activated before own and observed actions and stabilizes similarly. We also showed that rhythmic activity in the primary somatosensory cortex recovers later during own actions, which may be related to proprioceptive input and contribute to maintaining the sense of agency.

Keywords audiotactile integration, auditory, mirror-neurons, motor, somatosensory

ISBN (printed)	978-951-22-9148-9	ISSN (printed)	
ISBN (pdf)	978-951-22-9149-6	ISSN (pdf)	
Language	English	Number of pages	58 p. + app. 42p.
Publisher	Low Temperature Laboratory, Helsinki University of Technology		
Print distribution	Low Temperature Laboratory, Helsinki University of Technology		

☒ The dissertation can be read at http://lib.tkk.fi/Diss/2007/isbn9789512291496/

ACADEMIC DISSERTATION

Brain Mechanisms of Audiotactile and Audiomotor Interactions

Author: M.Sc.Tech Gina Caetano
Brain Research Unit, Low Temperature Laboratory
Helsinki University of Technology
Finland

Supervising professor: Professor Risto Ilmoniemi
Laboratory of Biomedical Engineering
Helsinki University of Technology
Finland

Supervisors: Docent Veikko Jousmäki
Brain Research Unit, Low Temperature laboratory
Helsinki University of Technology
Finland

Professor Riitta Hari
Brain Research Unit, Low Temperature Laboratory
Helsinki University of Technology
Finland

Preliminary examiners: Docent Jyrki Mäkelä
BioMag Laboratory, HUSLAB
Helsinki University Central Hospital
Finland

Professor Eduardo Ducla-Soares
Institute of Biophysics and Medical Physics
Faculty of Sciences, University of Lisbon
Portugal

Official opponent: Professor Beatrice de Gelder
Cognitive and affective neuroscience lab
Tilburg University
The Netherlands
&
MGH/MIT/HMS
Athinoula A. Martinos Center for Biomedical Imaging
Charlestown
USA

TABLE OF CONTENTS

LIST OF PUBLICATIONS ..... **I**

ABBREVIATIONS ..... **II**

PREFACE AND ACKNOWLEDGEMENTS ..... **III**

INTRODUCTION **1**

1 LITERATURE REVIEW **2**

1.1 MAGNETOENCEPHALOGRAPHY 2
1.2 FUNCTIONAL MAGNETIC RESONANCE IMAGING 7
1.3 PHYSIOLOGICAL BASES OF MEG AND FMRI 12
1.3.1 Neural current sources *12*
1.3.2 Spontaneous brain rhythms *13*
1.3.3 Neural correlates of BOLD signal *14*
1.3.4 MEG vs. fMRI *14*
1.4 CEREBRAL CORTEX 14
1.5 SOMATOSENSORY SYSTEM 15
1.5.1 Mechanoreceptors and afferent pathways *15*
1.5.2 Somatosensory cortices *17*
1.6 AUDITORY SYSTEM 18
1.6.1 Peripheral auditory system and afferent pathways *18*
1.6.2 Auditory cortices *19*
1.7 AUDIOTACTILE INTEGRATION 21
1.7.1 Multisensory neurons in cat and monkey superior colliculus *22*
1.7.2 Somatosensory convergence in macaque neocortex *22*
1.7.3 Audiotactile integration in humans *23*
1.8 MOTOR MIRROR-NEURON SYSTEM 24
1.8.1 New concepts of the motor system *24*
1.8.2 Mirror neurons in monkeys *26*
1.8.3 The human mirror-neuron system *27*

2 AIMS OF THE STUDY **29**

3 METHODS **30**

3.1 SUBJECTS 30
3.2 RECORDINGS 30
3.2.1 Magnetoencephalography *30*
3.2.2 Functional magnetic resonance imaging *32*
3.3 DATA ANALYSIS 32
3.3.1 Magnetoencephalography *32*
3.3.2 Functional magnetic resonance imaging *33*

4 EXPERIMENTS **34**

4.1 VIBROTACTILE INPUT FACILITATES HEARING AT LOW SOUND-INTENSITY LEVELS (STUDY I) 34
4.2 VIBROTACTILE INPUT ACTIVATES HUMAN AUDITORY AREAS (STUDY II) 35
4.3 TACTILE INPUT ACTIVATES HUMAN AUDITORY AREAS (STUDY III) 38
4.4 FREQUENCY INFORMATION TRANSFERS FROM TOUCH TO UTTERANCES (STUDY IV) 40
4.5 1ST AND 3RD PERSONS MOTOR CORTICES STABILIZE SIMILARLY (STUDY V) 41

5 GENERAL DISCUSSION **44**

5.1 METHODOLOGICAL CONSIDERATIONS 44
5.2 FROM PACINIAN CORPUSCLES TO AUDITORY CORTEX 46
5.3 PRIMARY MOTOR CORTEX VS. MIRROR-NEURON SYSTEM 47
5.4 AGENCY ATTRIBUTION 49

6 CONCLUDING REMARKS **50**

7 BIBLIOGRAPHY **51**

LIST OF PUBLICATIONS

This thesis is based on the following five publications, which are referred to in the text by the respective Roman numeral **I – V**.

I Schürmann M, **Caetano G**, Jousmäki V, and Hari R: Hands help hearing: Facilitatory audiotactile interaction at low sound-intensity levels. *J Acoust Soc Am* 2004, 115: 830–832.

II **Caetano G** and Jousmäki V: Evidence of vibrotactile input to human auditory cortex. *Neuroimage* 2006, 29: 15–28.

III Schürmann M, **Caetano G**, Hlushchuk Y, Jousmäki V, and Hari R: Touch activates human auditory cortex. *Neuroimage* 2006, 30: 1325–1331.

IV **Caetano G** and Jousmäki V: Kenneth, what's the frequency? *TKK Report*, TKK-KYL-018.

V **Caetano G**, Jousmäki V, and Hari R: Actor's and observer's primary motor cortices stabilize similarly after both seen or heard motor actions. *Proc Natl Acad Sci USA* 2007, 104: 9058–9062.

Contributions of the author

All the publications included in this thesis are a result of group effort. I actively participated in the discussions that led to the experimental paradigms of Studies II, III, IV, and V. I was the first author in Studies II, IV, and V, designing the experimental paradigm, conducting the measurements, analyzing the data and writing the publications with input from my co-authors. I performed the pilot experiments that led into the experimental design of Study I, in which I also had a major contribution in data acquisition and analysis. Study III is a continuation of Study II, to which we adapted the already defined experimental paradigm; I had a major contribution in the acquisition and analysis of the data in Study III. I participated in the preparation of the manuscripts in Studies I and III.

ABBREVIATIONS

BA	Brodmann area
BOLD	Blood-oxygenation-level-dependent
ECD	Equivalent current dipole
EEG	Electroencephalography
EMG	Electromyography
EOG	Electro-oculography
EPI	Echo planar imaging
fMRI	Functional magnetic resonance imaging
GLM	General linear model
HDR	Hemodynamic response
HG	Heschl's gyrus
IC	Inferior colliculus
IFG	Inferior frontal gyrus
ISI	Interstimulus interval
M1	Primary motor cortex
MEG	Magnetoencephalography
MGC	Medial geniculate complex
MGd	Dorsal division of MGC
MGm	Magnocellular division of MGC
MGv	Ventral division of MGC
MNS	Mirror-neuron system
MRI	Magnetic resonance imaging
PET	Positron emission tomography
PPC	Posterior parietal cortex
RF	Radiofrequency
SEM	Standard error of mean
SI	Primary somatosensory cortex
SII	Secondary somatosensory cortex
SMA	Supplementary motor area
SOA	Stimulus onset asynchrony
SOC	Superior olivary complex
SQUID	Superconducting quantum interference device
SSP	Signal-space projection
STG	Superior temporal gyrus
STS	Superior temporal sulcus
TFR	Time-frequency representation
TMS	Transcranial magnetic stimulation
TSE	Temporal spectral evolution
VP	Ventroposterior nucleus of the thalamus
VPI	Inferior division of the VP
VTEF	Vibrotactile evoked field

Preface and acknowledgements

I dedicate this thesis in memory of my sweet and beloved mother *Angelina Maria Costa*.

This thesis was carried out at the Brain Research Unit (BRU) of the Low Temperature Laboratory (LTL) and at the Advanced Magnetic Imaging Center of the Helsinki University of Technology (HUT). This work was financially supported by the Foundation for Science and Technology in Portugal, the Academy of Finland (National Centers of Excellence Program 2006– 2011), the Sigrid Jusélius Foundation in Finland, the Instrumentarium Foundation in Finland, and Fundação Calouste Gulbenkian in Portugal. I am also thankful to the Finnish Graduate School of Neurosciences (FGSN).

It has been a privilege to work in such a rich and exciting scientific environment, home of two National Centers of Excellence. Late Academician Olli V. Lounasmaa was the founder of the LTL and its success story, which continues nowadays under the insightful leadership of Prof. Mikko Paalanen. Jointly with the technological development of magnetoencephalography (MEG) in the LTL, the BRU unit was created. The big success and growth of the BRU is owned to Professor Riitta Hari, who has developed an interdisciplinary group highly recognized worldwide.

I thank my supervisors, Doc. Veikko Jousmäki and Prof. Riitta Hari, for all the guidance, support, patience, and positive attitude I had the privilege to experience during these years. I am grateful to my supervising professor, Doc. Veikko Jousmäki, for the inspiring supervision, always filled with great humor, in which I was given total freedom to think, expose ideas, and grow. I am grateful to my supervising professor, Prof. Riitta Hari, for the inspiring leadership, energy, and knowledge which never ceased to amaze me. But most of all, I am very grateful for the support and comprehension I was given while following my mother during her last months of life. I also want to thank Prof. Martin Schürmann and Dr. Yevhen Hlushchuk for the fruitful collaboration.

I thank my supervising professor, Prof. Risto Ilmoniemi for the kindness and guidance when I started the thesis manuscript and asked his advice.

My sincere thanks go to Prof. Ducla Soares and Prof. Jyrki Mäkelä for their effort and time in pre-reviewing my thesis. I also want to thank Prof. Jyrki Mäkelä and Prof. Ari Pääkönen who, as my FGSN follow-up group, gave me guidance and valuable comments while I was developing my thesis work. A special thanks to Prof. Ducla Soares for the always so wonderful and positive attitude, and who has followed my path since I was a graduate student until nowadays.

My deepest gratitude to Mr. Lauri Parkkonen, who besides being a really very nice person I consider as a fabulous mind; thank you for always being available to help and answer questions I may have had. I also want to thank the computer support team, including all the different members it has had; their support has been very important for me as well as for the entire lab. My special thanks to Dr. Cathy Nangini for revising my thesis and making valuable language corrections.

I also want to thank the other senior researchers of this group, Docent Nina Forss, Docent Päivi Helenius, Docent Elina Pihko, Prof. Riitta Salmelin, and Docent Simo Vanni for the enjoyable conversations.

I am grateful to the secretaries and support personnel for helping me with many practical matters since I first arrived to Finland.

I am very happy to have shared these years with all the PhD and graduate students of this group. There were always nice activities, coffee breaks, and conversations. Most of all, I think the friendly atmosphere between the students makes this a very special place. Thank you all for your role as colleagues and dear friends. A special thanks, from the bottom of my heart, to Jan Kujala and Hanna Renvall. I do not need to explain why, you know how much you have helped me.

My sincere thanks to some of my friends outside the working environment: Diogo Beja, Claudia Reis, Diana Pushkina, Giedre Vasiliauskaite, Eunice Pedroso, Ricardo Vigário, Isabel Pinto-Seppä, Erik Westerinen, and Fernando Francisco.

I am deeply grateful to my parents for the support they have given me during these years, and in special I am grateful to my mother for the unconditional love she has always given me. It breaks my heart not to have her here with me today.

Espoo, December 2007

Gina Caetano

INTRODUCTION

The information conveyed by our senses is integrated in the brain, resulting in the illusion of a continuum and a unified world. We are rarely aware of this integration, and because one sensory modality dominates we commonly believe that we only hear, see, or touch. These intrinsic integration processes are most easily identified with incongruent sensory inputs, as is exemplified by the audiotactile parchment-skin illusion (Jousmäki and Hari, 1998) and the audiovisual McGurk illusion (McGurk and MacDonald, 1976). At the neural level, multisensory neurons receive convergent input from two or more senses, and they show enhanced activity when stimuli are spatially concordant and synchronized (Wallace and Stein, 1997). Classically, integration of information from multiple senses was assigned mostly to association areas. The present view posits it also to early stages of cortical processing, in areas previously considered as purely unisensory.

Motor and sensory properties of actions are also tightly linked in the brain: sensory information is transformed into motor commands, and motor actions result in sensory input. Consequently, the sensory space is coded in motor terms. Other properties of actions are also coded in motor terms, as to whether actions are goal-directed and which is the goal. Most strikingly, the latter motor representations are not only valid for the agent but also for observing third parties. Neurons that code visual and motor representations of goal directed actions were found a decade ago in primates, and designated as “mirror neurons” (Gallese et al., 1996; Rizzolatti et al., 1996a). A system that matches observation and execution of actions was also found in the human brain — the mirror-neuron system (for a review, see Rizzolatti and Craighero, 2004).

In this thesis work I focus on the influence of tactile input on auditory processing and on motor output (Studies I–IV), as well as on the sensory representation of motor actions (Study V). Studies I–III unravel: *(i)* behavioral correlates of integration between auditory and tactile inputs that have similar temporal patterns, *(ii)* auditory areas that also process tactile information, and *(iii)* temporal dynamics and accurate sites of auditory areas responsive to vibrotactile and touch information. Study IV aims at defining the efficacy of frequency information transfer from touch to vocal utterance in normal-hearing adults. Finally, in Study V we searched for neural correlates of action processing in performed, seen, or heard tasks.

1 Literature Review

The following literature review is divided into seven sections that first introduce magnetoencephalography (MEG) and functional magnetic resonance imaging (fMRI), and then discuss briefly somatosensory and auditory systems, audiotactile integration, and the motor mirror-neuron system.

1.1 Magnetoencephalography

Magnetoencephalography (MEG) is a completely non-invasive method to detect weak magnetic fields generated by neuronal activity, on the order of 10 fT to 1 pT. In 1970, James Zimmerman introduced the Superconducting Quantum Interference Device (SQUID), which can conveniently measure weak fluxes of magnetic fields. Soon after, David Cohen, from the Massachusetts Institute of Technology, used the SQUID technology, simultaneously with electroencephalography, to measure the alpha rhythm from a healthy subject and spontaneous brain activity of an epileptic patient (Cohen, 1972). Consequently, the interest in the field increased, and few years later the first studies on magnetic brain activity evoked by external stimuli appeared (Brenner et al., 1975; Teyler et al., 1975). MEG instrumentation has gradually developed from single-channel to whole-head devices, enabling investigation of spontaneous and evoked brain activity in basic and clinical research. The location of neuronal current sources is found by solving the neuromagnetic inverse problem on the basis of the detected magnetic-field distribution and appropriate assumptions about neuronal activity. MEG allows investigation of brain activity with a millisecond-scale temporal resolution, and a spatial discrimination of about 2–3 mm under favorable circumstances.

The following introduction to MEG is mainly based on the extensive review by Hämäläinen et al. (1993).

Maxwell's equations

The laws of electromagnetism, fundamental also for MEG, are described by Maxwell's equations:

$$\nabla \cdot \mathbf{E} = \frac{r}{e_0}, \tag{1.1}$$

$$\nabla \times \mathbf{E} = -\frac{\partial \mathbf{B}}{\partial t}, \tag{1.2}$$

$$\nabla \cdot \mathbf{B} = 0, \tag{1.3}$$

$$\nabla \times \mathbf{B} = m_0\left(\mathbf{J} + e_0 \frac{\partial \mathbf{E}}{\partial t}\right) \tag{1.4}$$

where **E** and **B** are the electric and magnetic fields, **J** is the total current density, r is the charge density, t is time, and e_0 and m_0 are the permittivity and permeability of the vacuum, respectively.

At the cellular level, bioelectrical signals are below 1 kHz, and in neuromagnetism the frequencies of interest are usually below 150 Hz. As derived by Hämäläinen et al. (1993), changes in magnetic field over time only influence the electric field on a much longer length scale than the head diameter. Therefore, equations (1.2) and (1.4) can be simplified using the

quasi-static approximation, in which time-dependent phenomena contribution is negligible. Consequently, the electric field can be expressed as the gradient of an electric (scalar) potential $\mathbf{E} = -\nabla V(r)$.

The current density $\mathbf{J}(r)$ produced by neuronal activity is the sum of the primary current $\mathbf{J}_p(r)$ and volume current $\mathbf{J}_v(r)$:

$$\mathbf{J}(r) = \mathbf{J}_p(r) + \mathbf{J}_u(r) = \mathbf{J}_p(r) - s(r)\nabla V(r) \quad \textbf{(1.5)}$$

Here, the volume current $\mathbf{J}_v(r)$ describes the effect of the macroscopic electric field on charge carriers in the conducting medium, i.e., the volume current that flows passively in the whole brain. The primary current $\mathbf{J}_p(r)$ is the source of brain activity generated by neuronal activity, from the macroscopic point of view. Finally, $s(r)$ is the macroscopic conductivity of the brain, modeled as a homogeneous conductor.

Calculation of magnetic fields

The magnetic field at location **r** outside the head, generated by current distribution at location **r**' within the brain, can be calculated using the Ampère-Laplace law:

$$\mathbf{B}(r) = \frac{m_0}{4p}\int \frac{\mathbf{J}(\mathbf{r}') \times (\mathbf{r} - \mathbf{r}')}{|\mathbf{r} - \mathbf{r}'|^3} dn', \quad \textbf{(1.6)}$$

Combining equations (1.4)**,** (1.5), and (1.6)**,** we obtain the bases to solve the forward problem, from current to magnetic field:

$$\mathbf{B}(\mathbf{r}) = \frac{m_0}{4p}\int \left(\mathbf{J}_p(\mathbf{r}') + V\nabla' s\right)\frac{(\mathbf{r} - \mathbf{r}')}{|\mathbf{r} - \mathbf{r}'|^3} dn', \quad \textbf{(1.7)}$$

Conductor models

The head as a volume conductor can be quite well approximated by a spherically symmetric model, in which the macroscopic conductivity $s = s(r)$ is a function of the distance to the sphere origin. The sphere model is computationally fast and fits the overall brain geometry well, including the areas studied in this thesis: auditory, motor, and somatosensory cortices, respectively.

For symmetry reasons, radial primary currents do not produce fields outside the sphere since their magnetic fields exactly cancel the fields of the associated volume currents. Thus the magnetic field outside a sphere is due to tangential components of the primary currents, including the associated volume currents. MEG is optimal for measuring primary currents with a tangential component and is mainly sensitive to neuronal activity in the fissural cortex, where most of the primary sensory projection areas are located.

More realistic head models take into account the exact shape of the brain using anatomical information obtained from magnetic resonance images. Although these models are computationally more time consuming and need detailed anatomical information, for example from MRI, better results are obtained in more frontal and deep brain regions (Tarkiainen et al., 2003). Moreover, the signal-to-noise ratio seems to limit the detectability of convexial cortex sources more than source orientation per se (Hillebrand and Barnes, 2002). Thus, the use of realistic brain models depends mostly on the areas of interest.

Source modeling

As shown previously (see Eq. 1.7), the forward problem consists of the calculation of the magnetic field **B**. This computation requires information about both the primary current and the volume current (or macroscopic conductivity geometry, $s(r)$). The goal in MEG is to solve the inverse problem, i.e., to estimate the primary current $\mathbf{J}_p(r)$ that explains the measured distribution of the magnetic field. This so-called neuromagnetic inverse problem does not have a unique solution, because an infinite number of current distributions could, in principle, produce the same electromagnetic distribution outside the volume conductor. Thus, besides the volume conductor, it is necessary to define e.g. anatomical or physiological constraints for the sources.

The equivalent current dipole (ECD) model is the simplest and most widely used model to describe the primary currents, i.e. neuronal sources, generated in the brain. A current dipole **Q** is a point-like source with specific location $\mathbf{r}_\mathbf{Q}$, orientation, and strength that can be defined with the help of Dirac's delta function:

$$\mathbf{J}_\mathbf{p}(\mathbf{r}) = \mathbf{Q}d(\mathbf{r} - \mathbf{r}_\mathbf{Q}) \qquad \textbf{(1.8)}$$

This model is physiologically and physically plausible if the activated brain area is small compared with the distance to the measurement sensors, as is often the case during early and middle latency evoked responses.

Once the volume conductor geometry, the current model, and constraints are defined, the inverse problem can be solved using computational iterative methods. An initial guess on the ECD site is done and the resulting magnetic field is calculated (forward problem). Iteratively, the ECD parameters that minimize the difference between the recorded and predicted magnetic fields are found by a least-squares search. The goodness-of-fit value (g) can be computed to indicate in percentage how much of the measured magnetic field variance is accounted for by the ECD.

When multiple cortical regions are activated, it is possible to apply a multi-dipole model in which sources can be separated either temporally or spatially. For each of these areas, the 3-D locations and orientations of the ECDs are found, one at a time, with a least-squares search. The single- and multi-dipole models can be further evaluated by fixing the ECD locations and orientations, but allowing the strengths to change as a function of time when all the channels are taken into account.

Besides the point-like source model, distributed source models can be used to explain the measured neuromagnetic signals. These models put no, or only minor constraints, on the source configuration; they only assume that source currents are distributed within a volume or surface (Hämäläinen et al., 1993; Uutela et al., 1999).

SQUIDs and pick-up coils

Neuromagnetic fields are about 10^{-8} to 10^{-9} of the earth's static geomagnetic field. These fields can be measured with Superconducting Quantum Interference Device (SQUID) sensors inside a magnetically shielded room. Contemporary neuromagnetometers are based on DC SQUIDs (Fig. 1.1a), which consist of a superconducting loop interrupted by two insulating layers, the Josephson junctions. The current flows in the superconducting loop without resistance up to a critical current I_c that characterizes the Josephson junctions.

In practice, the SQUID is coupled to a flux transformer: a pickup coil senses the external magnetic field and a signal coil couples to the SQUID (Fig. 1.1a). Since both the flux transformer and the SQUID are based on superconductivity, the whole unit is immersed in liquid helium at 4 K. The impedance of the SQUID loop depends on the magnetic flux (Φ) that passes through it, and the voltage $\boldsymbol{V}$ across the loop can be measured by feeding a bias

current (I_b) to the loop. This voltage is a periodic function of the magnetic flux (Fig. 1.1b), but the SQUID loop is kept at constant magnetic field by means of a feedback coil that cancels changes in the magnetic flux Φ (Fig. 1.1a). The feedback current, required to keep the SQUID loop locked to its working point, gives an indirect measure of the external magnetic flux.

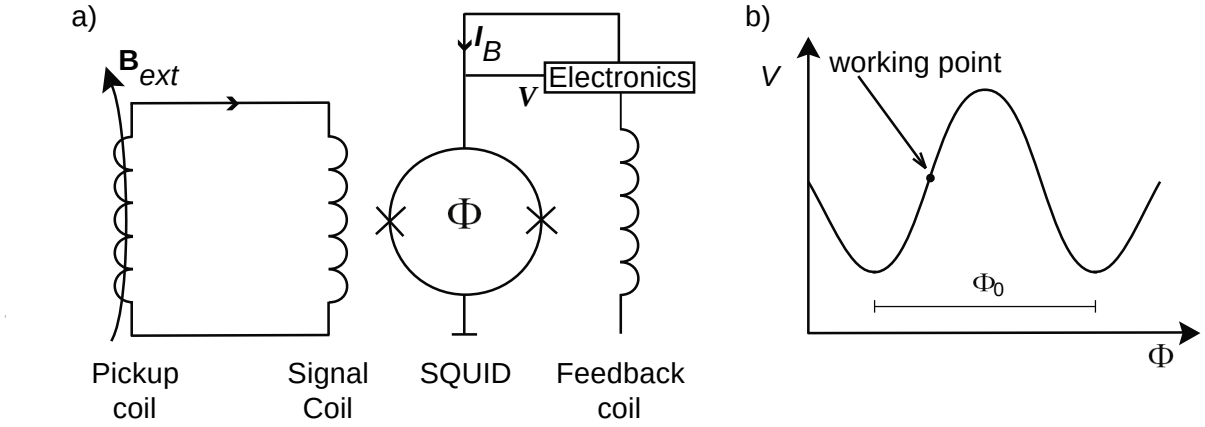

Fig. 1.1 Example of a DC SQUID sensor and its working point**.** a) The flux transformer couples the external magnetic field to the SQUID loop. The two Josephson junctions are represented by the symbol ×. The feedback coil and electronics keep the voltage ***V*** and the magnetic flux Φ constant. b) The voltage ***V*** is a periodic function of Φ, but the feedback circuitry keeps the SQUID loop locked to its working point. Adapted from Hämäläinen et al. (1993).

The pickup coil can have different configurations (Fig 1.2). A magnetometer consists of a single-loop pickup coil that is able to detect activity from deep sources in the brain, but is also sensitive to ambient noise. A gradiometer consists of two or more loops wound in opposite directions and can have either planar or axial design. First-order gradiometers detect inhomogeneous magnetic fields produced by nearby sources, and cancel effectively the approximately homogeneous magnetic field produced by distant sources.

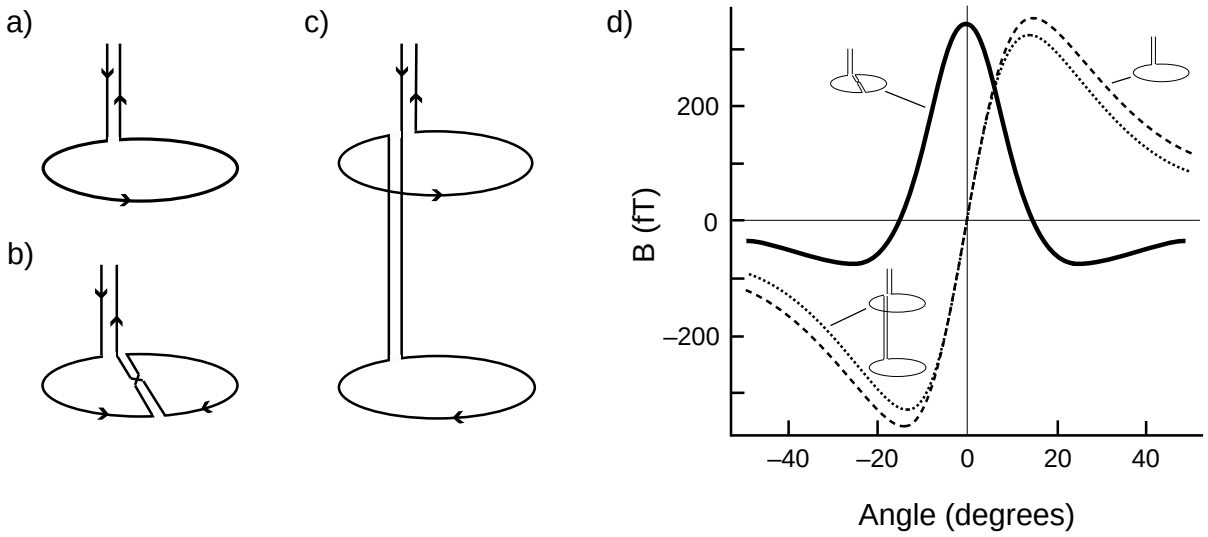

Fig. 1.2 Examples of pickup coil designs and their sensitivity profile. a) Magnetometer. b) First-order planar gradiometer. c) First-order axial gradiometer. d) Sensitivity profile for the different sensor designs, for an ECD at location 0 degrees. A first-order planar gradiometer measures the strongest amplitude of magnetic signal (**B**) just above the source (solid line), whereas a magnetometer and a first-order axial gradiometer pick-up maximum magnetic signal on both sides of the source (dashed lines). Adapted from Hämäläinen et al. (1993).

Present whole-head neuromagnetometers consist of a sensor-array with a helmet-shaped design, and the composition of the recording elements depends on the manufacturer. Figure 1.3 illustrates the device used in this thesis, the 306-channel neuromagnetometer manufactured by the Neuromag company (*Vectorview*™, Neuromag Ltd., Helsinki, Finland).

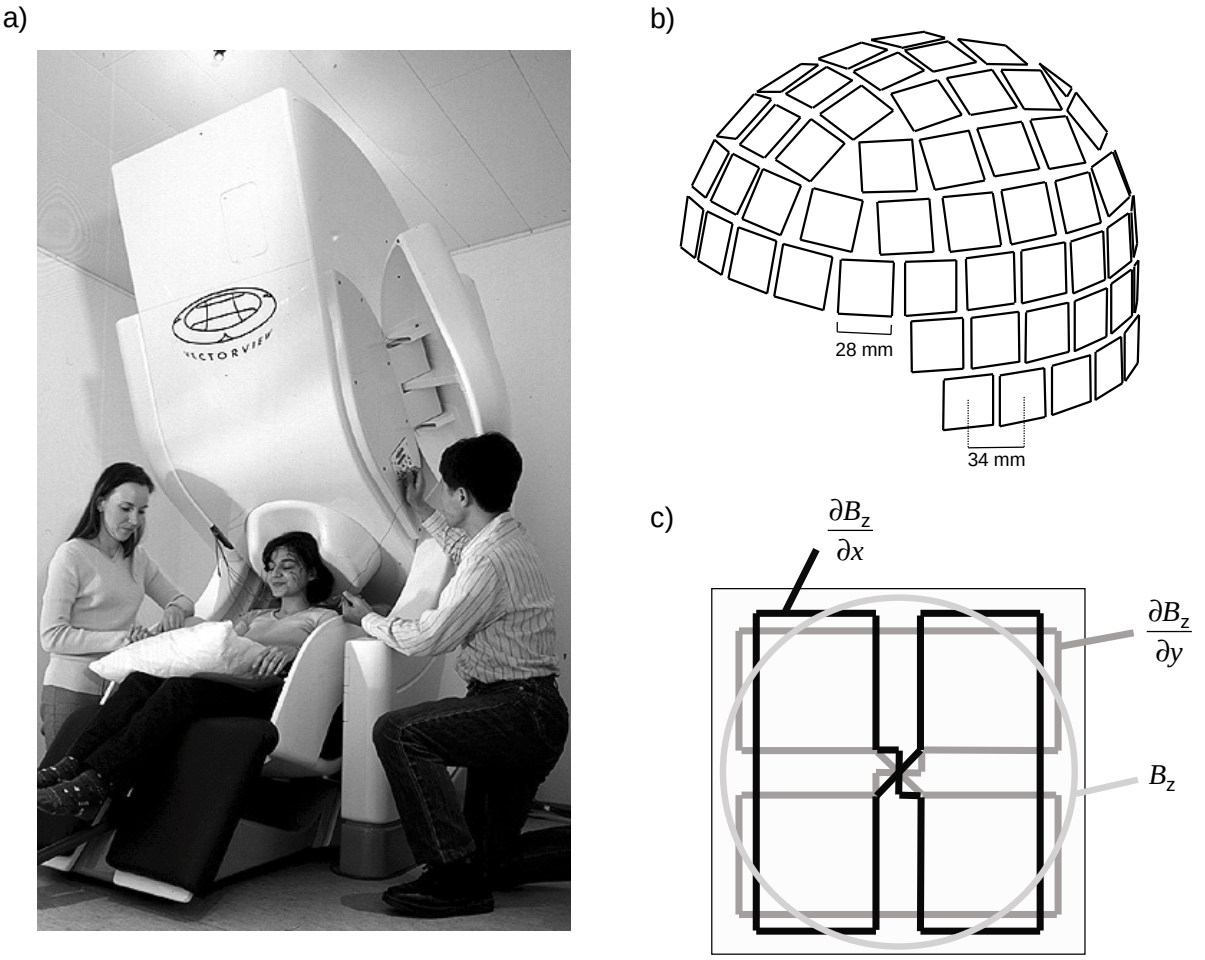

Fig. 1.3 a) The Vectorview™ system. b) The helmet-shaped array is composed of 102 sensor elements. c) Each sensor element consists of two orthogonal first-order planar gradiometers and one magnetometer. The orthogonal planar gradiometers give independent measures of changes in the magnetic field normal to the helmet surface.

Applications of magnetoencephalography

MEG has been mainly used for basic research, although relevant medical applications have been developed (for a review, see Hari, 2004). In basic research, sensory processing has been widely studied, such as visual (Brenner et al., 1975), somatosensory (Brenner et al., 1978; Hari and Forss, 1999), and auditory (Hari et al., 1980) systems. Other areas have been explored as, for example, pain (Hari et al., 1983b), oscillatory activity (Salmelin and Hari, 1994; Hari and Salmelin, 1997), cortex-muscle coherence (Salenius et al., 1997a), language perception and production (Salmelin, 2007), multisensory processing (Raij et al., 2000), and the human mirror-neuron system (Hari et al., 1998a).

Clinical applications of MEG include localization of epileptic foci (Paetau et al., 1990), pre-surgical mapping (Mäkelä et al., 2001), and investigation of specific neurological disorders.

Methodological development in magnetoencephalography is of main importance, whether it implies instrumentation, stimulation systems, monitoring devices, models to localize active areas, or integration of information with other neuroimaging methods. A new

promising analysis method is the dynamic imaging of coherent sources, which enables investigation of neuronal cooperation between different brain areas (Gross et al., 2001; Salmelin and Kujala, 2006).

1.2 Functional magnetic resonance imaging

Functional magnetic resonance imaging (fMRI) is a noninvasive technique, based on the property of nuclear magnetic resonance (NMR), which measures oxygen availability in active brain areas. A strong steady magnetic field, weaker magnetic field gradients, and radiofrequency (RF) signals are used to produce images of the brain.

NMR was observed for the first time in purified gases at the end of 1930s (Rabi et al., 1938), and soon afterwards the same phenomenom was observed in bulk matter (Purcell et al., 1945; Bloch et al., 1946). The application and development of this technique, in the analysis of chemical composition and structure of various materials, has led to theoretical and technological development in NMR. In the 1970s, a very important step was achieved with the implementation of RF signals together with analysis techniques related to the Fourier transform. It then became possible to study more diluted solutions and to use other nuclei (besides ^{1}H) as a signal source. Furthermore, a new variety of techniques emerged: high resolution spectroscopy, bidimensional NMR, and MR imaging (MRI). One of the latest, and possibly the most striking development in MRI is functional MRI (fMRI), a neuroimaging technique that reflects changes in brain function over time. This technique reflects changes in cerebral blood flow, cerebral blood volume, and blood oxygenation level as a result of neural activity.

The following introduction to MRI and fMRI is mainly based on a textbook by Huettel et al. (2004).

Nuclear spin and Zeeman effect

"In vivo" human magnetic resonance uses high intensity magnetic fields (usually from 1.5 to 4 T, but nowadays also 7 T magnets). In medicine, ^{1}H and ^{31}P nuclei are used because they have the adequate nuclear properties necessary for magnetic resonance, and because they are found in abundance in the human body. In this thesis, techniques based on nuclear magnetic resonance used only the excitation of ^{1}H nuclei, or proton.

Nuclear magnetic resonance is based on the properties of atomic nuclei in their fundamental state. Atomic nuclei have a spin angular momentum, also known as nuclear spin, characterized by the spin quantum number (I). The nuclear spin depends on the number of protons and neutrons, i.e. nucleons. For even-even nuclei, with equal number of protons and neutrons, I = 0, whereas for nuclei with an uneven number of nucleons, the nuclear spin is determined by the intrinsic spin of the unpaired nucleon[1]. Moreover, a nucleus of spin I will have 2I+1 possible orientations. The ^{1}H nuclei, or proton, has a nuclear spin I = ½. Thus, the proton can have 2 possible orientations that correspond to the spin values ½ and –½. In the absence of an external magnetic field, these two configurations have the same energy. In addition, the rotating nucleus (proton, in this case) generates a small magnetic field, the magnetic moment $\boldsymbol{\mu}$.

When a homogeneous and static magnetic field $\mathbf{B_0}$ is applied to the hydrogen nucleus, the magnetic moment of the proton interacts with the applied field. The degenerate energy levels split, and the proton can take two different energy states (Zeeman effect). The

[1] Note: the situation with an uneven number of both protons and neutrons will not be discussed here.

difference between the two energy states, ΔE, is proportional to the intensity of the static magnetic field:

$$\Delta E = g \frac{h}{2p} B_0 \qquad \textbf{(1.9)}$$

g is the gyromagnetic ratio (g = 2,67×10^8 rad/s/T, for the proton), h is the Planck constant, and B_0 is the density of the magnetic flux.

When the magnetic moment of the nucleus is parallel to $\mathbf{B_0}$, the energy of the system is lower and the system is more stable than in the situation when the magnetic moment of the nucleus is antiparallel to $\mathbf{B_0}$. The static magnetic field is assumed to be applied in the z-direction from now on.

Spin precession and Larmor frequency

When a homogeneous and static magnetic field $\mathbf{B_0}$ is applied, the proton precesses about the direction of $\mathbf{B_0}$ (Fig. 1.4a) at the Larmor frequency (resonant frequency) n :

$$n = \frac{g}{2p} B_0 \qquad \textbf{(1.10)} \qquad\qquad \Delta E = hn \qquad \textbf{(1.11)}$$

These equations also indicate the energy of the photons that should be applied such that a nucleus can transit from the lower energy (parallel) state to the higher energy (antiparallel) state. For hydrogen protons, n /B = 42.5 MHz/T.

Bulk magnetization

When studying bulk matter, such as the human brain, we are interested in the group behaviour of nuclear spins (protons, in this case). In the absence of an external magnetic field, the nuclear spins are oriented in random directions. When an external magnetic field $\mathbf{B_0}$ is applied, the alignment of individual magnetic moments in the parallel or in the antiparallel state follows the Boltzmann distribution under thermal equilibrium:

$$\frac{N_+}{N_-} = \exp\left(\frac{\Delta E}{k_B T}\right) = \exp\left(\frac{\hbar g B_0}{k_B T}\right) \approx 1 + \frac{\hbar g B_0}{k_B T} \qquad \textbf{(1.12)}$$

$$N_+ - N_- \approx \frac{\hbar g B_0}{2 k_B T} \qquad \textbf{(1.13)}$$

provided $k_B T >> \Delta E$ at room temperature. N_- and N_+ are the number of spins in the antiparallel and parallel states respectively, k_B is the Boltzmann constant, and T is the absolute temperature. It results that there are more parallel than antiparallel spins (20 parts per million at 37°C and 3 T).

The bulk magnetization will align in the direction of $\mathbf{B_0}$. At this stage, there is no component perpendicular to the static magnetic field, since the phases of individual magnetic moments are random and the resulting summation in the perendicular plane is zero. The net magnetization points along the magnetic field direction, and it precesses at the Larmor frequency.

Radiofrequency excitation of spins

When applying RF electromagnetic pulses at the Larmor frequency and perpendicular to the static magnetic field $\mathbf{B_0}$, the magnetic component $\mathbf{B_1}$ interacts with the spins' magnetic

moment in the *xy* plane. The electromagnetic energy is absorbed and some spins change from the parallel to the antiparallel state. Moreover, the RF pulses induce phase coherence between spins, i.e. spins start to precess about the longitunal axis in synchrony. As a result, the net magnetization undergoes a nutation and will follow a spiral wobbling motion. The process is illustrated in Figure 1.4b, as observed from the laboratory reference system. The angle at which the net magnetization rotates relative to the **z**-axis is determined by the duration of the applied RF pulse and is defined as the flip angle.

The longitudinal component of the net magnetization $\mathbf{M}_z$ decreases, whereas a transverse component in the xy-plane appears, with components $\mathbf{M}_x$ and $\mathbf{M}_y$ that rotate at the Larmor frequency. The rotating $\mathbf{M}_{xy}$ component, which is a changing magnetic field, induces electric currents in receiving coils. Therefore, we create a measurable MR signal during resonance conditions.

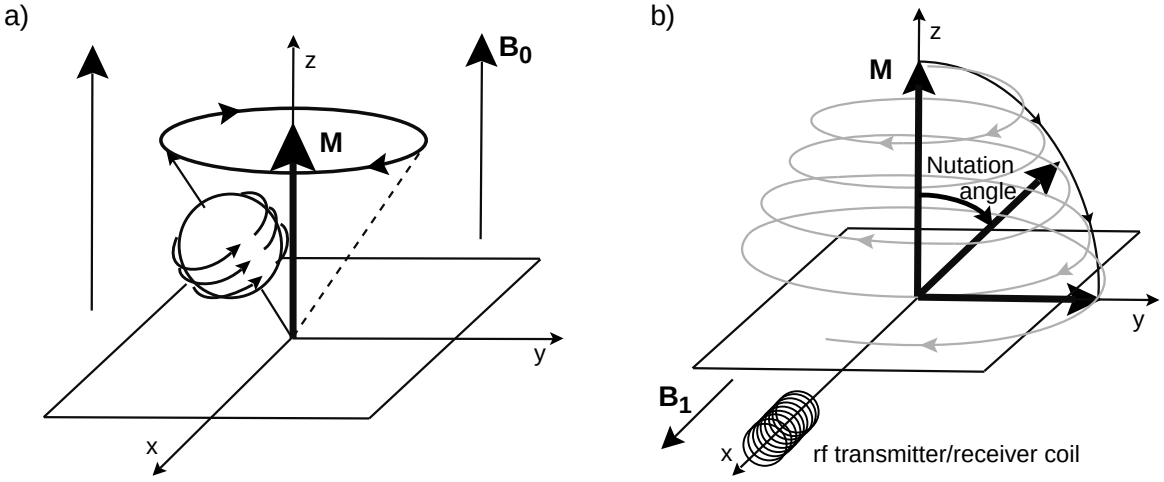

Fig. 1.4 Net magnetization in a static magnetic field, in the laboratory reference system. a) ^1H nuclei precess about the direction of the static magnetic field $\mathbf{B_0}$ at the Larmor frequency, and the net magnetization **M** is parallel to $\mathbf{B_0}$. b) When RF electromagnetic pulses are applied, the net magnetization undergoes a nutation, with the angle defined by the duration of RF signal. The $\mathbf{M_{xy}}$ component precesses at Larmor frequency and induces electric currents in the receiver coil. Adapted from Huettel et al. (2004).

Spin relaxation and the Bloch equation

When the RF signal is turned off, spins will gradually loose the energy absorbed during the excitation by emitting photons. This phenomenon is known as spin relaxation and is composed of two processes: longitudinal or spin-lattice relaxation, and transverse or spin-spin relaxation.

Longitudinal relaxation – spins in the antiparallel state loose energy to the lattice of nuclei by emitting photons when going back to their original parallel state. As a result, the net magnetization returns to its original position, i.e. parallel to $\mathbf{B_0}$. The recovery of the longitudinal component of the net magnetization is associated with the time constant $\mathbf{T_1}$.

Transverse relaxation – the excitation pulse induces phase coherence between spins, and that is why a transverse component of the net magnetization is observed. This coherence is lost over time, leading to a loss of the net magnetization within the transverse plane. The process is independent of the longitudinal relaxation, and has two distinct contributions. One contribution is intrinsic, the so called spin-spin interaction, with interaction effects between spins in parallel and antiparallel states. Whereas protons in the parallel state add to the magnetic field $\mathbf{B_0}$, protons in the antiparallel state decrease the local magnetic field. Although these temporal and local fluctuations of the magnetic field are very small, spins start precessing at different local Larmor frequencies, and the relative phases of the spins gradually fan out over time. This spin-spin interaction is characterized by the time constant

$\mathbf{T_2}$. The second contribution is extrinsic, caused by inhomogeneities of the external magnetic field. The relaxation process due to the combined effect of spin-spin interaction and external field inhomogeneities is characterized by the time constant $\mathbf{T_2^*}$, with $\mathbf{T_2^*} < \mathbf{T_2}$. The behavior of the net magnetization can be described in a single equation, the Bloch equation:

$$\frac{d\mathbf{M}}{dt} = g\ \mathbf{M}\times\mathbf{B} + \frac{1}{T_1}\left(\mathbf{M}_0 - \mathbf{M}_z\right) - \frac{1}{T_2}\left(\mathbf{M}_x + \mathbf{M}_y\right) \qquad \textbf{(1.14)}$$

Contrast in MRI

Image formation is based on spin frequency-phase encoding. The basic procedure is the following: first, a slice selection gradient $\mathbf{G_z}$ is applied; second, a phase-encoding gradient $\mathbf{G_y}$ is turned on and then off allowing the spins to accumulate different phases in the selected slice; third, a frequency-encoding gradient $\mathbf{G_x}$ is turned on during the acquisition allowing the spins' Larmor frequencies to vary over space. Many different acquisition sequences exist, with distinct encoding schemes, but the basic idea remains the same, i.e. frequency-phase encoding.

The spin density[2] and time constants $\mathbf{T_1}$ and $\mathbf{T_2}$ are inherent tissue properties, and they play an important role in MRI contrast (Table 1.1). Two additional parameters are essential in defining the type of contrast: the repetition time **TR**, which is the time interval between successive excitation pulses, and the echo time **TE**, which represents the time interval between the excitation pulse and the signal acquisition (Table 1.2, Fig. 1.5). Equation **1.15** describes the transverse component of the net magnetization and provides the foundation for manipulating the signal obtained from a particular tissue type:

$$M_{xy}(t) = M_0\left(1 - e^{-\frac{TR}{T_1}}\right)e^{-\frac{TE}{T_2}} \qquad \textbf{(1.15)}$$

	T_1 (ms)	T_2(ms)	T_2^*(ms)
White matter	830	80	45
Gray matter	1330	110	45

Table 1.1 Average relaxation times T_1, T_2 and T_2^* for white and grey matter at 3.0 Tesla (Wansapura et al., 1999).

	Short TE	Intermediate TE
Intermediate TR	T1	-
Long TR	PD	T2

Table 1.2 TR and TE parameters can maximize tissue contrast, such that MR images are T1-weighted, T2-weighted or proton-density (PD) related.

[2] Brain's tissue spin density depends on water content: ~71% for grey matter and ~84% for white matter.

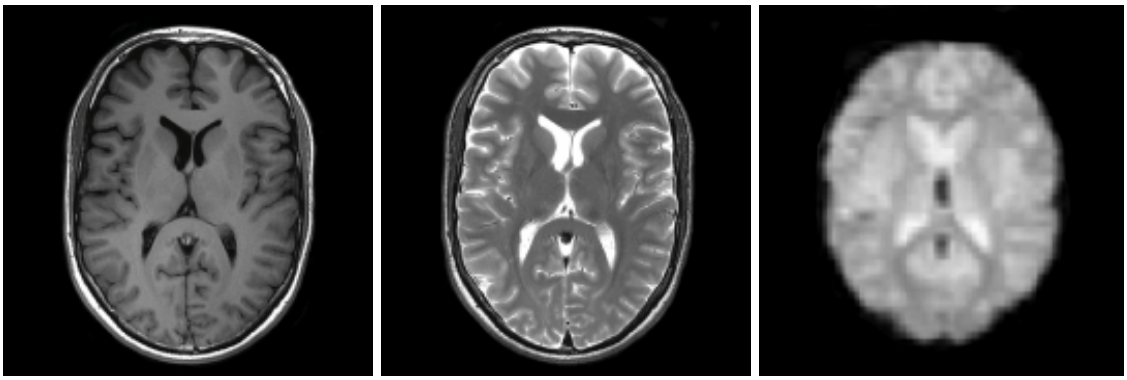

Fig. 1.5 T_1, T_2, and T_2^* weighted images of the human brain at 3 T; transaxial slices (from AMI Centre at TKK).

Principles of fMRI

Functional magnetic resonance imaging (fMRI) commonly refers to the blood-oxygenation-level-dependent (BOLD) contrast imaging method, which tracks signal differences in T_2^*-weighted images as a function of the level of deoxyhemoglobin. However, the physiological mechanisms of BOLD contrast are still under study [see section 1.3.3]. Several influencing factors have already been determined: cerebral blood flow, cerebral blood volume, and blood oxygenation.

BOLD contrast relies on the magnetic properties of the hemoglobin molecule: oxygenated hemoglobin is diamagnetic and deoxygenated hemoglobin is paramagnetic. The stronger magnetic susceptibility of deoxygenated hemoglobin results in dephasing of water protons and faster decay of the transverse magnetization (decreased T_2^*). Also, the transverse relaxation time of water protons depends on the square of the magnetic field strength (Thulborn et al., 1982).

The first BOLD contrast was achieved in Bell laboratories in anesthetized rodents (Ogawa et al., 1990). Correlation between neuronal activity and BOLD contrast in humans was first demonstrated in 1992 by several research groups (Bandettini et al., 1992; Kwong et al., 1992; Ogawa et al., 1992) using gradient-echo EPI sequences.

The BOLD contrast reveals the hemodynamic response (HDR) triggered by neuronal activity, because increased inflow of oxygenated blood to active areas results in a decrease in the amount of deoxygenated hemoglobin. Thus, BOLD contrasts are generally related to an increase in MR signals in the activated brain regions. When short stimuli are used, MR signals from active brain regions start to increase at about 2 s and reach a maximum value at about 5 s, whereas when stimuli are presented in blocks of long duration the neuronal activity is prolonged and the peak extends to a plateau of activation. After reaching its maximum, the response decreases below baseline, because the rapid decrease in blood flow causes a rise in deoxygenated hemoglobin until the blood volume goes back to baseline. The HDR is also influenced by other factors such as the type of stimulation used and the brain region. In some studies an initial drop in the BOLD HDR has been found at 1–2 s after the stimulation time (Huettel et al., 2004). However, these results are not consistently replicable and no general consensus has been reached yet.

The positive BOLD responses seem to be correlated with neuronal postsynaptic activity as reflected by local field potentials (Logothetis et al., 2001; Mukamel et al., 2005; Niessing et al., 2005). On the other hand, negative BOLD responses have been shown in monkey visual cortex (Smith et al., 2004) and in human primary somatosensory cortex (Hlushchuk and Hari, 2006). The negative BOLD responses in the monkey primary visual cortex were correlated with decreased neuronal activity observed in intracranial recordings (Schmuel et al., 2006).

1.3 Physiological bases of MEG and fMRI

This section focuses on the physiological bases of MEG and fMRI. First, the underlying neural current sources will be described, followed by introductory remarks about the brain's oscillatory activity. Neuronal correlates of the BOLD signal are discussed, and a brief comparison between MEG and fMRI is presented. This section is mainly based on extensive textbooks on neurophysiology, neuroscience, and neuroimaging (Kandel et al., 1991; Guyton and Hall, 1996; Huettel et al., 2004).

1.3.1 Neural current sources

The cerebral cortex has two types of cells: neurons and glia. The neurons are the basic active units that process, transmit, and integrate information in the brain (Fig 1.6). A neuron consists of *(i)* cellular body (soma), the metabolic and integrative center of the cell, *(ii)* dendrites, afferents that bring information into the soma, *(iii)* axon, efferent that transmits information to other neurons, and *(iv)* pre-synaptic terminals that establish the communication between neurons, either via direct contact of the membranes — electrical synapse — or most commonly mediated via neurotransmitters — chemical synapse. There are at least 10^{10} neurons in the cerebral cortex, forming a complex network with about 10^{14} synapses.

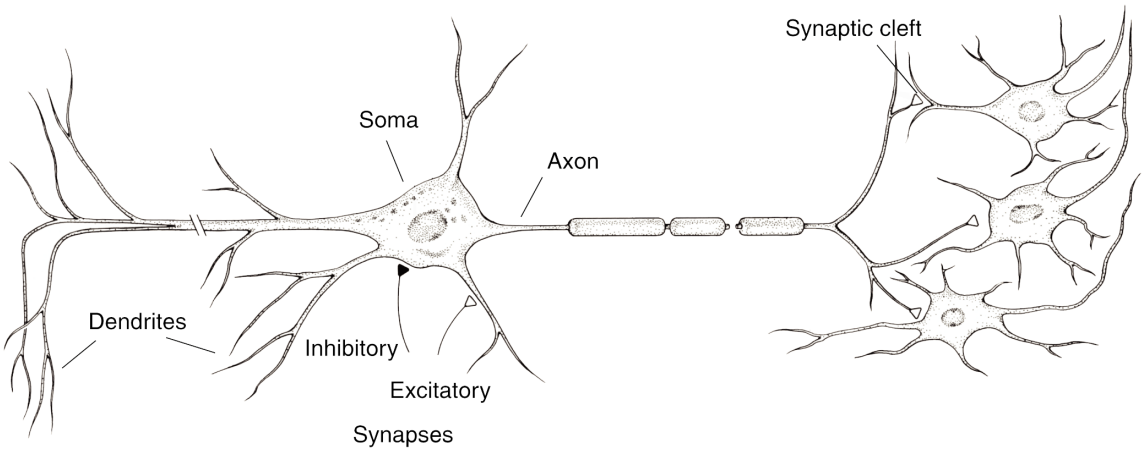

Fig. 1.6 Schematic illustration of a neuron and points of contact with other nerve cells. Modified from Kandel (1991).

The ability of nerve cells to process and transmit information depends on their membrane properties. The membrane resting potential is about –60 mV to - 70 mV with respect to the extracellular environment. When the axon hillock is depolarized to a threshold of about –50 mV, it initiates a depolarization front, followed by a repolarization front, that travels along the axon. This "action potential" typically lasts ~2 ms and is responsible for the transmission of information along the axon (Fig. 1.7a).

The action potential reaches the axon terminal and causes the pre-synaptic nerve cell to release neurotransmitters into the synaptic cleft that bind to specific chemical receptors of the post-synaptic nerve cell. A nerve cell typically has hundreds of synapses and the spatial and temporal summation of the respective contributions determines the post-synaptic potential duration and amplitude (Fig 1.7b). Post-synaptic potentials are on the order of tens of milliseconds, thus much longer than action potentials.

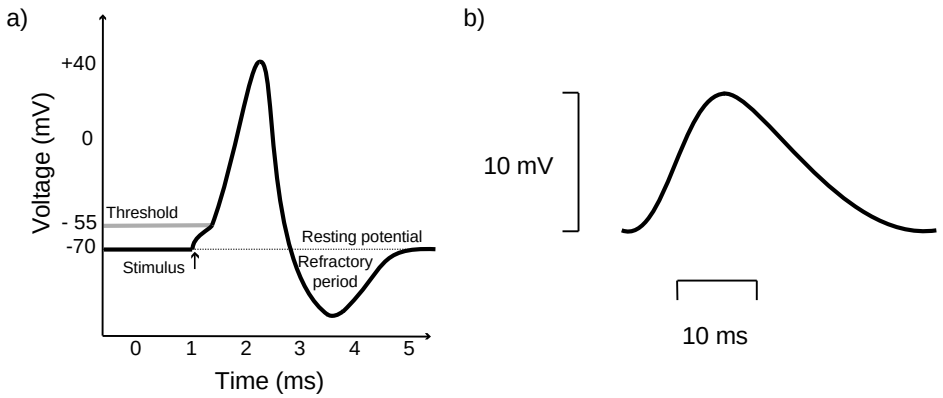

Fig. 1.7 a) Action potential. b) Post-synaptic potential. Modified from Hämäläinen et al. (1993).

Because apical dendrites of cortical pyramidal cells lie parallel to each other and approximately perpendicular to the surface of the cortex, they are thought to give rise to magnetic signals measurable with MEG. Action potentials are brief in duration and the associated quadrupolar magnetic field decreases rapidly with the distance, as $1/r^3$. Thus, MEG signals reflect mainly postsynaptic currents in dendrites (primary currents), which produce measurable dipolar magnetic fields that decrease as $1/r^2$ with the distance r. Besides primary currents, extracellular volume currents flow in the surrounding medium in the opposite direction and close the current loop, so that no charge accumulates. A detectable MEG signal is created by tens of thousands of neurons activated synchronously, which allows temporal and spatial summation of the dipolar magnetic fields generated by the respective postsynaptic currents (Hari, 1990; Murakami and Okada, 2006).

1.3.2 Spontaneous brain rhythms

The human brain exhibits intrinsic oscillations that have characteristic frequencies. Macroscopic neuronal rhythmic activity is mainly found in thalamic nuclei and cortical areas. The best known macroscopic cortical oscillations are α and μ rhythms, which can easily be detected with EEG and MEG. The α rhythm (8–13 Hz) is located over the posterior parts of the brain, predominantly in the parieto-occipital and occipital areas, and is best observed during rest with eyes closed. The level of the α rhythm decreases when the subject opens the eyes, and also during visual stimulation, visual imagery, and visual memory tasks (for a review, see Hari and Salmelin, 1997; Hari, 2004). The μ rhythm, generated in rolandic areas, has a "comb-like" shape. The magnetic μ rhythm will be explained below in some detail because it was used to probe the functional state of the sensorimotor cortices in Study **V**.

The magnetic Rolandic μ rhythm has two components: the ~20-Hz component that arises mostly from the primary motor (M1) cortex, and the ~10-Hz component that receives a major contribution from the primary somatosensory (SI) cortex (Salmelin and Hari, 1994; Hari and Salmelin, 1997). The levels of both the ~10-Hz and the ~20-Hz components are suppressed during brisk movements and increase again after the movement, a phenomenon known as "rebound". The suppression of the μ rhythm is strongest for contralateral limb movements and starts about 1–2 s before a voluntary movement, followed 0.5–2.5 s afterwards by an increase in the rhythmic activity. The rebound is much stronger and about 0.3 s faster for the ~20-Hz than the ~10-Hz component (Salmelin and Hari, 1994). In addition to voluntary and reflex movements, the μ rhythm reacts during somatosensory stimulation, electric stimulation of peripheral nerves (Salenius et al., 1997b), motor imagery (Schnitzler et al., 1997), and action observation (Hari et al., 1998a). Furthermore, the ~20-Hz component arising from the M1 cortex follows the somatotopic organization for the body

part that is moved, whereas the ~10-Hz component is consistently localized close to the somatosensory hand area (Salmelin et al., 1995).

1.3.3 Neural correlates of BOLD signal

Positive and negative BOLD contrasts have been observed in neuroimaging studies (see Section 1.2). However, a model that would correlate the neuronal activity with BOLD contrast and fully explain the underlying metabolic mechanisms is still under study.

Neuronal activity consists of changes in membrane potential and release of neurotransmitters. Energy supply is needed to support metabolic processes, especially to restore concentration gradients after depolarization. The vascular system supports those energy requirements by supplying glucose and oxygen, the latter bound to hemoglobin.

Positive BOLD signals are generally considered to be driven by the metabolic cost of neuronal activity and consequent changes in blood supply, and to correlate strongly with the level of postsynaptic activity (Logothetis et al., 2001; Mukamel et al., 2005; Niessing et al., 2005). However, recent studies suggest that blood flow may also correlate with other factors. First, hemodynamic changes occur not only in the region of synaptic activity, but also in areas located a few millimeters away and with no synaptic activity (Iadecola et al., 1997; Iadecola, 2002). Second, negative BOLD responses were found to be correlated with decreased neuronal activity (Schmuel et al., 2006). Third, BOLD responses were suggested to reflect neuronal signaling via the release of neurotransmitters, which act as vasoactive substances (Attwell and Iadecola, 2002). Finally, dendritic calcium channels, sensitive to synaptic inhibition in pyramidal cells, seem to also control the amplitude of the vascular signal (Lauritzen, 2005). Thus, it is likely that several processes contribute simultaneously to the amplitudes of BOLD signals.

1.3.4 MEG vs. fMRI

MEG has a sub-millisecond temporal resolution and measures signals generated by synchronized postsynaptic primary currents. The signals reflect direct measures of the neuronal activity, and clear responses are obtained at the single subject level. Source localization accuracy is about 5mm, reaching 2–3 mm under favorable circumstances (Hämäläinen et al., 1993).

Whereas MEG signals represent electrophysiological events at the macroscopic level, BOLD signals in fMRI are an indirect measure of neuronal activity through related hemodynamic changes. Statistical processing of the data is more complex, and results are usually visualized at group level. fMRI presents an advantage, however, as it can detect active areas in sulci, gyri, and deep brain regions. The spatial resolution of this technique is on the order of few millimeters, constrained by the architecture and dynamics of the vascular blood supply. Higher spatial resolution may be obtained at higher field strength, e.g. 7 T; methods are currently under development. In contrast to MEG, fMRI temporal resolution is at best on the order of hundreds of milliseconds (Huettel et al., 2004).

1.4 Cerebral cortex

The human cerebral cortex is 2–4 mm thick, and is in general composed of six layers that are characterized by different properties. The layers' numbering starts from the surface of the cortex inward, and the pyramidal layers III and V mainly contain the bodies of pyramidal neurons. Characteristic connections between layers are structurally organized into cortical columns.

The cerebral cortex is heavily folded into sulci and gyri, with two thirds of the surface buried in the sulci. The first classification of distinct areas, on the basis of morphology and laminar distribution of nerve cells, was performed by Brodmann in a single human brain; 52 cytoarchitectonic areas were classified into Brodmann areas (BAs). Currently, the human cerebral cortex is thought to contain 100–200 distinct areas, with distinct functional behavior (Van Essen and Dierker, 2007). Important methodological developments have been made in recent years, linking and defining cytoarchitecture, brain function, and neuroimaging techniques (e.g., Eickhoff et al., 2005; 2007).

Figure 1.8 illustrates the human brain and the functional areas related to the studies in the present thesis: auditory, somatosensory, and motor areas.

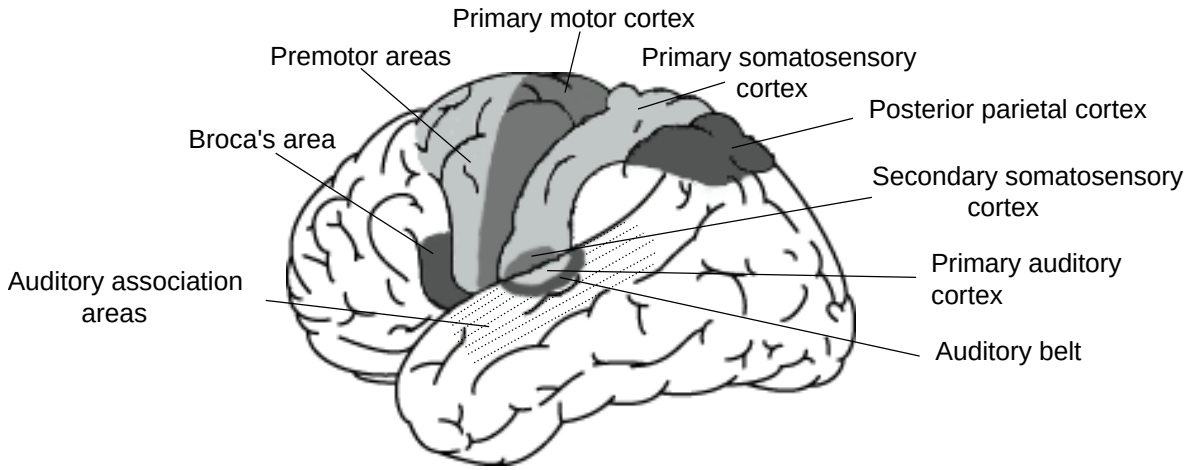

Fig. 1.8 Schematic illustration of human motor, somatosensory, and auditory areas. Adapted from Kandel (1991).

1.5 Somatosensory system

Somatosensation refers to sensations arising from the body itself and the interaction of the body surface with the environment. Somatosensation is divided into four distinct modalities: *touch*, which provides information about the environment via mechanical stimulation of the body surface, *proprioception*, which allows us to perceive the body position by mechanical displacements of muscles and joints, *pain*, which provides information about present or potential tissue damage, and *temperature*, for detecting heat and cold.

The following text focuses on touch, with an emphasis on tactile detection of vibration along the lines presented by Kandel (1991).

1.5.1 Mechanoreceptors and afferent pathways

Mechanoreceptors

Touch and proprioception are mechanoreceptive somatic senses, i.e., the mechanical force is transduced into sensory signals by specialized neurons with *encapsulated* pressure-sensitive tips. Mechanoreceptors that mediate touch are classified into two functional groups: *slowly* adapting receptors, which respond during a persistent stimulus, and *rapidly* adapting receptors, which respond to the onset and the offset of the stimulus. The superficial glabrous skin has mechanoreceptors that can perform fine spatial discrimination due to their small

receptive field: Meissner´s corpuscle, a rapidly adapting receptor, and Merkel's receptor, a slowly adapting receptor. The subcutaneous tissue in both glabrous and hairy skin has mechanoreceptors with larger receptive fields: Ruffini's and Pacinian corpuscles, which are slowly and rapidly adapting receptors, respectively (Fig 1.9a). However, hairy skin has mostly hair follicle receptors.

Rapidly adapting receptors are best suited for detecting sinusoidal mechanical stimuli. Meissner's corpuscles are most sensitive to low-frequency stimuli, whereas Pacinian corpuscles are most sensitive to high-frequency stimuli (Fig 1.9). Pacinian corpuscles have their lowest sensitivity threshold at 200–300 Hz (Gescheider et al., 2002; 2004).

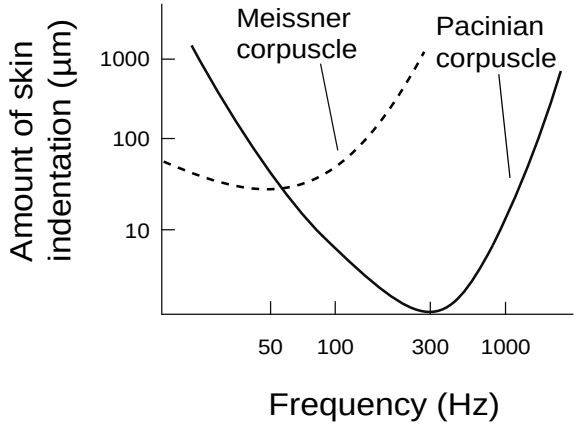

Fig. 1.9 Frequency sensitivity profile as a function of skin indentation for Pacinian and Meissner corpuscles. Modified from Kandel (1991).

In humans, the lips and fingertips are the most sensitive regions to touch, containing a high density of mechanoreceptors. For example, the glabrous skin of palm and fingers is innervated by about 17 000 receptors (Johansson and Vallbo, 1979). In particular, the fingertips have a good tactile acuity for vibration. The distribution of Pacinian corpuscle afferents in the hand amounts to about 350 per finger and 800 in the palm (Johnson et al., 2000).

Limb proprioceptive information arrives via mechanoreceptors located in joint capsules, muscle spindle receptors that transduce stretch of skeletal muscles, and cutaneous mechanoreceptors. The combined information from these receptors is necessary for proper sense of proprioception.

Afferent pathways

Touch and limb proprioceptive inputs reach the cerebral cortex via the dorsal column-lemniscal system (Fig 1.10a), which consists of thick myelinated fibers that carry input from the contralateral side of the body at velocities of 30–110 m/s (Guyton and Hall, 1996). Fibers originating from the same part of the body remain together, thus besides a functional organization, a somatotopic organization is already present at the level of the spinal column. The first synapse occurs in the medulla: in the cuneate nucleus for the upper part of the body, and in the gracile nucleus for the lower part of the body. The second-order neurons cross to the other side of the body and ascend to the contralateral thalamus as the medial lemniscus. From the thalamus, the third-order neurons project further from the ventral posterior lateral and medial nuclei to the SI cortex, and to a lesser extent to the SII cortex and to the posterior parietal cortex (PPC).

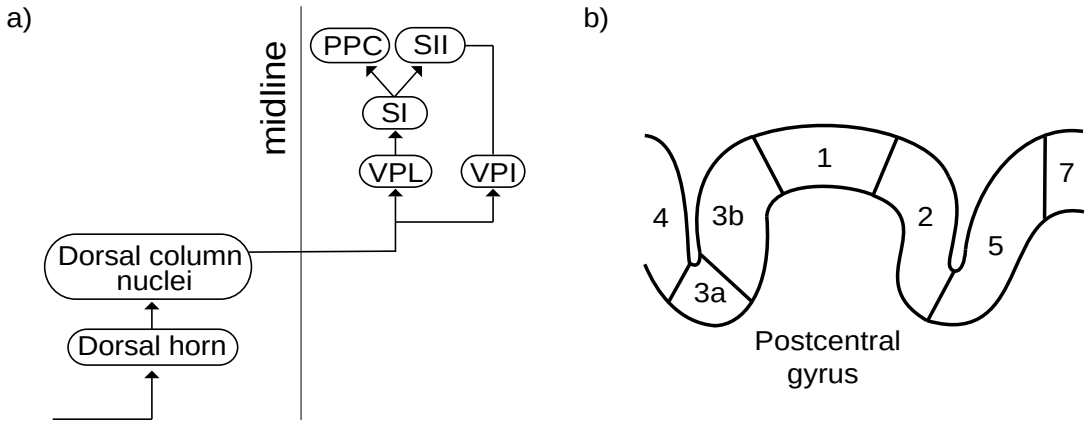

Fig. 1.10 a) Levels and connections in the dorsal lemniscal system of primates. Thalamic nuclei are indicated as VPL, ventroposterior lateral nucleus, and VPI, ventroposterior inferior nucleus. b) Cytoarchitectonic subdivisions of the SI cortex, shown in a cut transverse to the postcentral gyrus. Modified from Kandel (1991).

1.5.2 Somatosensory cortices

Primary somatosensory cortex

The SI cortex is located in the fundus and posterior bank of the central sulcus, and in the crown and posterior wall of the postcentral gyrus (Fig 1.8). The SI cortex is subdivided in four distinct cytoarchitectonic regions: Brodmann areas 3a, 3b, 1, and 2 (Geyer et al., 1999; Geyer et al., 2000; Grefkes et al., 2001). Each area has its own input pattern: most thalamic relay neurons project to BA 3b and 3a, and to a lesser extent to BA 1 and 2. In addition, BA 3b and 3a project backwards to areas 1 and 2.

Projections from the thalamus are functionally and somatotopically organized. Proprioceptive input goes mostly to areas 3a (muscle tissues) and 2 (joints and other deep tissues), whereas information from skin mechanoreceptors is mainly processed in areas 3b and 1 (Fig 1.10b). Each of the four subregions in SI is somatotopically organized, with lower limbs represented medially, followed by trunk, arms, hands, and finally the face represented laterally.

The density of receptors in a certain area of the body determines the size of its representation in the SI cortex (Penfield and Jasper, 1954). For example, lips and fingertips have disproportionally large representations compared with other body parts. In addition to the connections within the SI cortex, each region (mostly BA 3a and 2) has few reciprocal connections to its homologue on the contralateral SI cortex via callosal fibers (Killackey et al. 1983). SI also has reciprocal connections to the ipsilateral M1 cortex (BA 4), ipsi- and contralateral SII cortices, and PPC (BA 5 and 7).

Secondary somatosensory cortex (SII)

The SII cortex is located on the superior bank of the Sylvian fissure within the parietal operculum, somewhat posterior and lateral to the SI cortex (Fig 1.8), where it occupies a relatively small cortical area compared with the SI cortex. The SII cortex also shows somatotopic organization, though less fine-grained than the SI cortex (Hari et al., 1993; Ruben et al., 2001). Recent histological studies (Eickhoff et al., 2006a; 2006b) have shown the existence of four distinct cytoarchitectonic areas in the human parietal operculum. Two of those areas may not respond optimally to pure somatosensory stimuli, and thus may not contribute to the functions assigned to the SII cortex. Further studies have to be done in order to understand the role of the four areas defined.

SII cortex receives thalamic projections, as well as cortical connections from the contralateral SI and SII cortices via the corpus callosum, and from the ipsilateral SI cortex. The connections from bilateral SI cortices come from all four cytoarchitectonic areas. The role of serial and parallel information processing in human SII cortex is still under debate, but most probably both occur in the cortical somatosensory network (Pons et al., 1987; Garraghty et al., 1991; Turman et al., 1992; Fabri et al., 1999; Forss et al., 1999; Simões et al., 2003). SII neurons project to contralateral SII cortex, ipsilateral M1, supplementary motor area (SMA), and PPC.

Whereas contralateral SI cortex is activated by unilateral tactile stimulation, SII cortex is activated bilaterally (Hari et al., 1983a; Kaukoranta et al., 1986) and with a longer latency on the ipsi- than on the contralateral side. The functional roles assigned to SII cortex include: integration of information from both body halves (Simões and Hari, 1999; Simões et al., 2001; Alary et al., 2002), maintainance of body scheme (Hari et al., 1998b), integration of somatosensory and motor information (Huttunen et al., 1996; Forss and Jousmäki, 1998; Lin et al., 2000), tactile learning and memory (Ridley and Ettlinger, 1976), and texture discrimination (Murray and Mishkin, 1984).

Other somatosensory cortices

The PPC is located just posterior to SI cortex. PPC includes BA 5 in the superior parietal lobe, and BA 7 in the posterior part of the superior parietal lobe. Later studies assigned part of the PPC also to BA 39 and BA 40 (Zilles and Palomero-Gallagher, 2001; Caspers et al., 2006). PPC receives direct thalamic input, and besides reciprocal connections with SI and SII cortices, PPC neurons project to SMA. BA 5 is involved in higher level processing of both tactile and proprioceptive input, i.e. integration of somatosensory information, whereas BA 7 integrates both somatosensory and visual information. In addition, the mesial frontal and mesial parietal (supplementary sensory area) cortices contribute to somatosensory processing (Penfield and Jasper, 1954).

1.6 Auditory system

Audition refers to sensations arising from compression and rarefaction patterns of air transformed into neural signals by the ear and processed in the brain. The auditory system is composed of afferent and efferent pathways that run parallel but in opposite directions. Processing of auditory information is complex and occurs at multiple levels of the central auditory pathway, with six relay neurons up to primary cortical areas, in contrast to three relay neurons in the somatosensory system.

The following text gives an introduction to the peripheral auditory system and afferent pathways (Kandel et al., 1991), and describes the most recent findings on the organization of auditory cortices in monkeys and humans.

1.6.1 Peripheral auditory system and afferent pathways

The pattern of mechanical vibrations in the cochlea was unraveled in the 1920’s and 1930’s by Georg von Békésy, who later won the Nobel Prize for his research. Sound energy sets up a traveling wave in the cochlear incompressible fluid. The consequent displacement of the basilar membrane induces changes in electric conductance of the hair cell membranes, and transmitters are released to the nerve endings. Hair cells and their afferent fibers are maximally tuned to high frequencies at the cochlear base and to low frequencies at the apex. The tonopic organization, already present in the auditory nerve, is preserved in fibers and synapses within auditory pathways.

Figure 1.11a represents schematically the most important neural pathways and nuclei, from the active cochlea to the auditory cortices, in the primate brain. The superior olivary complex (SOC) has a critical role in spatial localization of sounds. Some neurons tuned to lower frequencies compare interaural time differences of auditory signals, whereas neurons tuned to higher frequencies detect interaural differences in sound intensity. The inferior colliculus (IC) also projects to other areas: premotor areas, superior colliculus, reticular formation, and cerebellum. These connections might be related to orientation or audiomotor reflexes. The medial geniculate complex (MGC) projects primarily to the primary auditory cortex (BA 41) in the temporal lobe, but also establishes connections to forebrain regions.

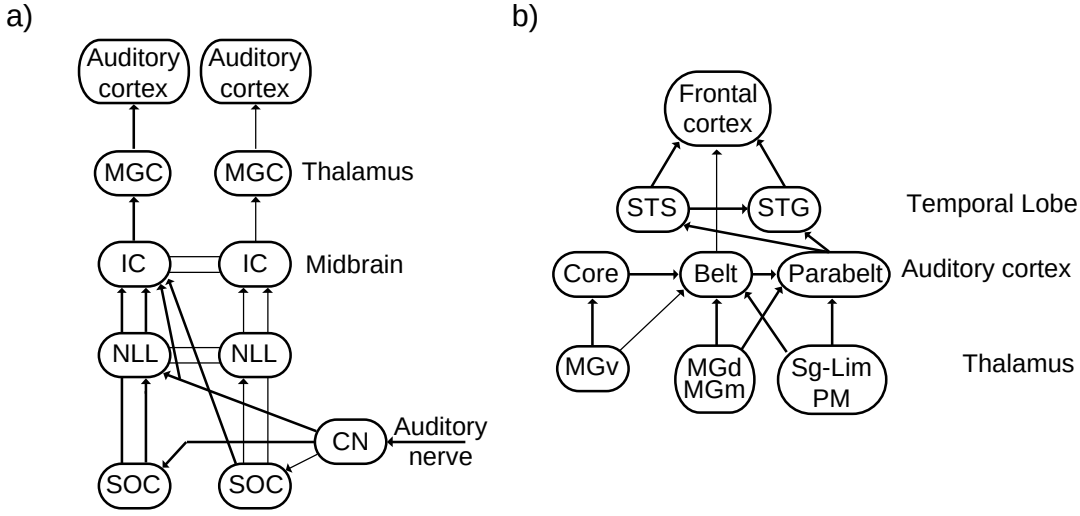

Fig. 1.11 Levels and connections in the primate auditory system. Thick solid lines denote major connections. a) Neural pathways and nuclei from the auditory nerve to the auditory cortex, for stimuli presented to the left ear. CN = cochlear nucleus; SOC = superior olivary complex; NLL = nucleus lemniscus lateralis; IC = inferior colliculus; MGC = medial geniculate complex. Modified from Kandel (1991). b) Schematic illustration of major cortical connections. MGv/d/m = ventral/dorsal/magnocellular divisions of MGC; Sg-Lim = suprageniculate and limitans nuclei; PM = medial pulvinar nucleus; STS = superior temporal sulcus; STG = superior temporal gyrus. Modified from Kaas et al. (1999).

1.6.2 Auditory cortices

Primates

Animal studies have long been the best source of information on the functional organization of the auditory cortex. The information available on non-human primate auditory cortex has been tested and summarized in recent studies (Hackett et al., 1998; Kaas et al., 1999; Kaas and Hackett, 2000; Hackett et al., 2001), which will be shortly described below. Based on cochleotopic organization, interconnections, and architectonic features, the nonhuman primate auditory cortex can be divided into three regions (Fig 1.11b): *core* (primary cortex), *belt* (secondary cortex), and *parabelt* (association/higher-order cortex).

The central core is currently divided in three cochleotopically organized fields: AI (caudal field), R (rostral field), and RT (rostral temporal field). These three core areas have features of primary sensory areas: koniocellular architecture, dense myelination, dense thalamic input from the ventral division of the MGC (MGv), neurons that respond with short latencies to best frequency pure tones, within other properties (Hackett et al., 1998; Kaas et al., 1999; Hackett et al., 2001). RT field is the least similar and uncertain member of the core area. Ipsilaterally, each of the core areas interconnect densely with their neighbor and also with neighboring belt areas. Core areas also have major callosal projections to the auditory core (tonopically) and adjacent belt areas in the other hemisphere (Hackett et al., 2001).

The core is surrounded by a 2- to 4-mm narrow belt area composed of six or seven subdivisions (Hackett et al., 1998; Kaas et al., 1999; Kaas and Hackett, 2000). Belt areas are most densely interconnected with adjacent belt subdivisions and parabelt areas, but they also project to more distant belt and parabelt areas and to the frontal lobe (Kaas et al., 1999; Kaas and Hackett, 2000). The belt has a mediator role in information flow from the primary auditory areas to higher-order auditory and association areas on the superior temporal gyrus.

The parabelt area, situated along the lateral surface of the superior temporal gyrus, is at the third stage of auditory cortical processing (Hackett et al., 1998; Kaas and Hackett, 2000), probably comprising two to three fields. The parabelt has callosal connections to contralateral homotopic regions of the parabelt and and belt areas (Hackett et al., 1998; Kaas and Hackett, 2000).

Whereas the core areas extract spectral and temporal features of sounds, belt and parabelt areas integrate the information, performing the analysis of complex auditory stimuli necessary for mental representation of auditory objects (Hackett et al., 1998; Kaas et al., 1999; Kaas and Hackett, 2000; Hackett et al., 2001). Additionally, the parabelt is interconnected to upper and lower regions of the superior temporal sulcus, parietal cortex, and projects to four major regions of the frontal lobe, which include cortex near and within the frontal eye field and the orbitofrontal cortex (Kaas and Hackett, 1999). These targets can be considered as a fourth-level of auditory processing that include space perception and auditory memory (Kaas and Hackett, 1999; Kaas and Hackett, 2000).

Humans

Human auditory cortical areas are located bilaterally in the superior regions of the temporal lobe, and classically comprise BA 41, 42 and 22 (Fig 1.12a). The primary auditory cortex (BA 41) is located in the lower bank of the Sylvian fissure, in Helsch's gyri, and is defined as a "core" system (Rivier and Clarke, 1997; Morosan et al., 2001; Rademacher et al., 2001). On the other hand, "belt" (BA 42) and higher-order auditory association areas (BA 22) surround the primary auditory cortex, in the planum temporale and planum polare (Rivier and Clarke, 1997; Hackett et al., 2001). New areas are being defined (Fig 1.12b), e.g. area Te3 in the superior temporal gyrus (Morosan et al., 2005).

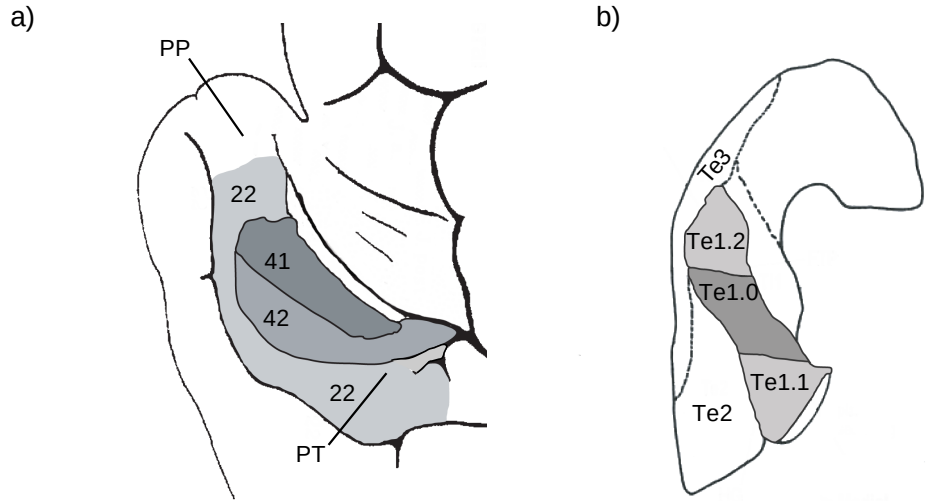

Fig. 1.12 Human auditory areas in the superior temporal plane, as viewed in a slice section through the Sylvian fissure. a) Topography of auditory cortices in the cytoarchitectonic map of Brodmann. b) Topography of subdivisions within the primary auditory cortex (BA 41) — Te1.2, Te1.0, Te1.1; and partial view of the auditory belt (BA 42) — Te2 — and of a new area defined within BA 22, Te3. Modified from Morosan et al. (2001).

Comparison of auditory architectonic features between primate and human suggest that a similar organization may exist in the human auditory system (Hackett et al., 2001; Rademacher et al., 2002). The core area of the human auditory cortex occupies an elongated region of the superior temporal plane, between the planum polare and the planum temporale. This area is mostly confined to the first gyrus of Heschl, even when more than one gyrus is present (Rivier and Clarke, 1997; Hackett et al., 2001). Recent findings suggest that the human primary auditory cortex may also be composed of three distinct areas (Fig 1.12b), but no general consensus exists yet (Morosan et al., 2001; Rademacher et al., 2001).

As shown previously, intrinsic connections within the primary auditory cortex involve mainly nearby units, while surrounding auditory areas have reciprocal connections to more distant units (Tardif and Clarke, 2001). The human primary auditory cortex is surrounded by at least six non-primary belt auditory areas (Rivier and Clarke, 1997). Pure tones activate primarily the auditory core, whereas belt areas prefer complex sounds, indicating the latter integrate auditory features (Wessinger et al., 2001).

Higher order auditory processing seems to be organized in at least two main streams, but controversy still surrounds these notions in human auditory processing. Tracing of auditory cortical connections and functional studies in nonhuman primates have shown evidence for distinct “where” dorsal and “what” ventral processing streams (Kaas and Hackett, 1999; Romanski et al., 1999; Rauschecker and Tian, 2000; Poremba et al., 2003). In humans, the superior temporal gyrus (STG) has been known for processing speech or phonological decoding. Presently, studies suggest that distinct “what” and “where” networks may selectively respond to sound recognition and sound location (Maeder et al., 2001; Ahveninen et al., 2006).

1.7 Audiotactile integration

In daily life, we receive sensory information simultaneously through multiple senses and combine the inputs into a single integrated experience of the world. The ability to combine information from different senses is also known as multisensory integration. In the brain, multisensory neurons respond to inputs from two or more senses and their activity is enhanced when the different sensory channels are stimulated simultaneously (Wallace and Stein, 1997). Typically, there is a temporal window during which multisensory integration may take place.

Multisensory integration is often hidden due to the dominance of one sensory modality. It can be readily studied by creating incongruence in sensory inputs that result in either illusions or altered perceptions. A well known example is the audiovisual McGurk-effect (McGurk and MacDonald, 1976), where the observation of an incongruent syllable articulation results in modified percept of the simultaneously presented auditory syllable. Another striking example is the parchment-skin illusion (Jousmäki and Hari, 1998), in which modulation of the frequency of the auditory feedback, when rubbing hands, alters the tactile percept between rough and smooth.

Multisensory integration in humans has long been assumed to take place only in higher order association areas, after processing of information in each unisensory modality within its pathway. However, multisensory integration also occurs in areas classically viewed as unisensory (for a review, see Calvert et al., 2004). Moreover, most of the cortex is not unimodal (Kaas and Collins, 2004). For example, auditory parabelt cortical areas, in macaque monkey, also project to the primary visual cortex and extrastriate visual areas (Falchier et al., 2002; Rockland and Ojima, 2003).

This section describes multisensory neurons in animals, convergence of somatosensory information in macaque neocortex, and the first studies on auditory and tactile integration in humans.

1.7.1 Multisensory neurons in cat and monkey superior colliculus

The neural substrate for multisensory integration relies on neurons, or ensembles of interconnected neurons, that receive convergent input from two or more senses. Integration of multiple sensory information takes place in the midbrain, thalamus and cortex (Stein and Meredith, 1993). Pioneering studies in cat superior colliculus (SC), in the midbrain, have described how information from auditory, somatosensory, and visual modalities is integrated at the neuronal level, later complemented by studies in the macaque monkey (Wallace et al., 1993; Wallace and Stein, 1997; Stein, 1998; Wallace et al., 1998; Wallace and Stein, 2001).

The SC plays a significant role in overt attentive and orientation behavior in cats and contains several types of neurons (Wallace et al., 1993). Unimodal neurons (outer layers) respond only to one type of sensory input, whereas multimodal neurons (deep layers) respond to either two or three types of sensory input. Neuronal organization in SC (both unimodal and multimodal) corresponds to the spatial location of stimuli in sensory space, thus SC multisensory neurons respond to different types of sensory input when the different receptive fields overlap.

SC multisensory neurons respond more vigorously when inputs from two or more senses are spatially concordant: the activity is higher than when elicited by a single sense and sometimes even larger than the predicted sum of activations elicited by unsynchronized stimulation (Wallace and Stein, 1997).

Spatially discordant stimuli reduce or abolish the neuronal response (Stein, 1998). Furthermore, stimulus synchronization is essential in multisensory integration, i.e. if the time lag between stimuli is too long, the inputs will be treated as belonging to independent events. Most of the SC neurons integrate information up to a time lag of 100 ms time lags, some up to 200 ms, and some, more rarely, up to 1 s (Wallace and Stein, 1997).

The multisensory integration in SC is mediated by two cortical areas: the anterior ectosylvian sulcus and the rostral lateral suprasylvian sulcus (Wallace et al., 1993; Wilkinson et al., 1996; Jiang et al., 2001). Principally, the capacity for multisensory integration in SC is not innate, but is rather the result of real life experience with cross-modal cues (Wallace and Stein, 1997, 2001).

1.7.2 Somatosensory convergence in macaque neocortex

The classical view in neuroscience divides the neocortex into sensory, motor and association cortices. Multisensory convergence can be found in parietal, temporal, and frontal lobes of the monkey neocortex. Candidate structures that integrate auditory and somatosensory information have been identified with intracranial recordings: at least PPC (Hyvärinen and Poranen, 1974), the temporo-parietal cortex (Leinonen and Nyman, 1979), and the superior temporal sulcus (Hikosaka et al., 1988). However, most of the cortex is not purely unimodal, although cortical areas often have a dominant modality (Kaas and Collins, 2004). The assumption that multisensory integration only takes place in high-order association cortices was challenged recently, when multisensory convergence was found to occur in early cortical processing, in structures formerly considered as unisensory in function. For example, visual and somatosensory inputs were shown to activate caudio-medial (CM) auditory belt areas in monkeys (Schroeder et al., 2001; Schroeder and Foxe, 2002; Schroeder et al., 2003).

Monkey CM auditory belt areas respond to both auditory and somatosensory inputs at early stages of cortical processing (Schroeder et al., 2001; Fu et al., 2003). Responsiveness to

somatosensory stimuli may also inlcude other belt and parabelt auditory areas, but not the primary auditory cortex. In the former study (Schroeder et al., 2001), binaural clicks, pure tones, and band-passed noise were used as auditory stimuli, and contralateral median nerve stimulation were used as a pure somatosensory input. The CM belt area had similar timing and laminar profile activation for both auditory and somatosensory inputs. In both cases the response showed a feed-forward profile, i.e., the initial excitation began in and near lamina 4 and spread to extragranular laminae. The latter study (Fu et al., 2003) aimed at defining what body parts and somatosensory submodalities activate the CM belt area. Cutaneous stimulation, proprioceptive stimulation at the elbow, and vibrotactile stimulation, all activated the CM belt area, with a clear bias towards cutaneous representation of head and neck. Additionally, isolation of single multisensory neurons showed that responses occurred at a slightly longer latency for cutaneous compared to auditory input. At present, there are several possibilities for somatosensory input to CM belt areas, including both feedforward and feedback/lateral inputs.

1.7.3 Audiotactile integration in humans

Despite the increasing interest in audiotactile integration in humans (Jousmäki and Hari, 1998; Foxe et al., 2000; Foxe et al., 2002; Guest et al., 2002; Lütkenhöner et al., 2002; Gobbelé et al., 2003), the underlying neural basis is still poorly understood. Audiotactile integration is present in everyday life, but in most situations the somatosensory information dominates. For instance, when we scratch ourselves, turn over a page, touch a surface texture, or rub our hands together, the related sound is faint. However, absent or modified auditory input changes the percept to some degree. Paul von Schiller (1932) reported for the first time that sounds – tones or noise bursts – affect roughness perception. More recently, manipulating the frequency content of touch-related sounds (Jousmäki and Hari, 1998; Guest et al., 2002), when the subject is rubbing the hands together or touching abrasive surfaces, has been shown to modify the percept.

As mentioned in Section 1.7.1, audiotactile integration occurs if a neural substrate receives convergent input from auditory and somatosensory modalities. The first study in humans that shed light on this matter was performed on a congenitally deaf subject with MEG. Levänen et al. (1998) delivered 100-ms vibrotactile stimuli to the hand-palm via a plastic blind-ended tube in an old-ball paradigm. Consistent activation of the auditory cortex and a clear difference between the MEG responses to both 180-Hz and 250-Hz stimuli were found. The findings were related to cross-modal plasticity due to the absence of auditory input or reorganization of thalamo-cortical connections. However, inherent somatosensory input to auditory areas may also happen in humans (Schroeder and Foxe, 2002).

Non-invasive brain-imaging studies using electroencephalography (EEG), MEG, and fMRI, have revealed possible neural correlates of audiotactile integration in humans. Such correlates were found in auditory belt areas, SII cortex, and PPC (Foxe et al., 2000; Foxe et al., 2002; Lütkenhöner et al., 2002; Gobbelé et al., 2003).

In a high-density EEG study by Foxe et al. (2000), audiotactile integration was shown in early stages of cortical processing, at ~65 ms in the hand representation area of the postcentral gyrus, and at ~80 ms in the posterior auditory cortices. A complementary fMRI study (Foxe et al., 2002) indicated convergence of auditory and somatosensory inputs to BA 22/39, a sub-region of the human auditory cortex along the superior temporal gyrus and human homologue of the macaque monkey CM belt area. Moreover, the results revealed facilitatory audiotactile integration in the convergence region, as the activity exceeded the predicted sum from the unimodal responses.

Audiotactile integration has also been studied with MEG (Lütkenhöner et al., 2002; Gobbelé et al., 2003). The former study showed suppressive audiotactile integration in the hemisphere contralateral to the tactile stimuli, at ~140ms and ~220 ms, which may reflect

partial inhibition of the neurons in SII cortex (Lütkenhöner et al., 2002). The latter MEG study identified audiotactile integration at about 75–85 ms, in the contralateral posterior parietal cortex, and at about 105–130 ms in the contralateral operculum, between SII and auditory cortices. In contrast to the first study, these results may reflect suppression in auditory processing during audiotactile integration (Gobbelé et al., 2003).

The differences observed between the MEG, EEG, and fMRI studies may be influenced by several factors: *i*) relative dominance of the auditory or somatosensory stimulus, *ii*) different stimulation techniques, *iii*) temporal and spatial coincidences between auditory and somatosensory stimuli, *iv*) attention, and *v*) the neuroimaging techniques themselves.

The study by Levänen et al. (1998) triggered our interest in temporal correlates and neural substrates of vibrotactile stimuli in normal-hearing people. Vibrotactile and auditory stimuli are essentially similar temporal patterns, and both senses can detect low-frequency vibrations. As emphasized by von Békésy (1960) in his early studies in cochlear mechanisms, there are many similarities between skin sensation and hearing. Therefore, the auditory system may also have a role in processing vibrotactile information in normal-hearing people.

1.8 Motor mirror-neuron system

Humans have an intense social nature: social cognition is ubiquitous whether it occurs in terms of verbal or non-verbal cues. A large part of our social interaction relies on the observation of facial expressions, gaze direction, posture, and gestures of others in order to understand their intentions, feelings, and motivations. Thus, in social environments, the interpretation of motor acts is a key element, as they are monitored continuously and automatically without effort.

The mechanisms underlying interpretation of motor acts are still poorly understood, but a growing set of evidence suggests that a “mirror-neuron system” in humans could support action understanding and imitation (Rizzolatti and Craighero, 2004). Mirror neurons were first identified in the monkey frontal lobe as neurons that respond both when the monkey performed and observed the same goal-directed action (Gallese et al., 1996; Rizzolatti et al., 1996a). Therefore, similar brain mechanisms in the actor’s and observer’s brains can make the bridge in action understanding (Rizzolatti and Craighero, 2004). These findings are also related to new concepts about the parcellation and organization of the motor cortex (Rizzolatti et al., 1998; Luppino and Rizzolatti, 2000; Rizzolatti and Luppino, 2001).

This section describes: *(i)* new concepts of the motor system, (*ii)* mirror neurons in the monkey brain, and *(iii)* the human mirror-neuron system.

1.8.1 New concepts of the motor system

From the classical point of view, the motor cortex consists of primary motor and premotor areas (Fig 1.8). The human M1 cortex is located in the anterior wall of the central sulcus and in the precentral gyrus (BA 4), presenting a somatotopic organization rather similar to that of the SI cortex. BA 6 is divided into: *i)* premotor cortex, which forms the ventrolateral part of BA 6 and is roughly somatotopically organized, *ii)* SMA, which forms the dorsomedial part of BA 6.

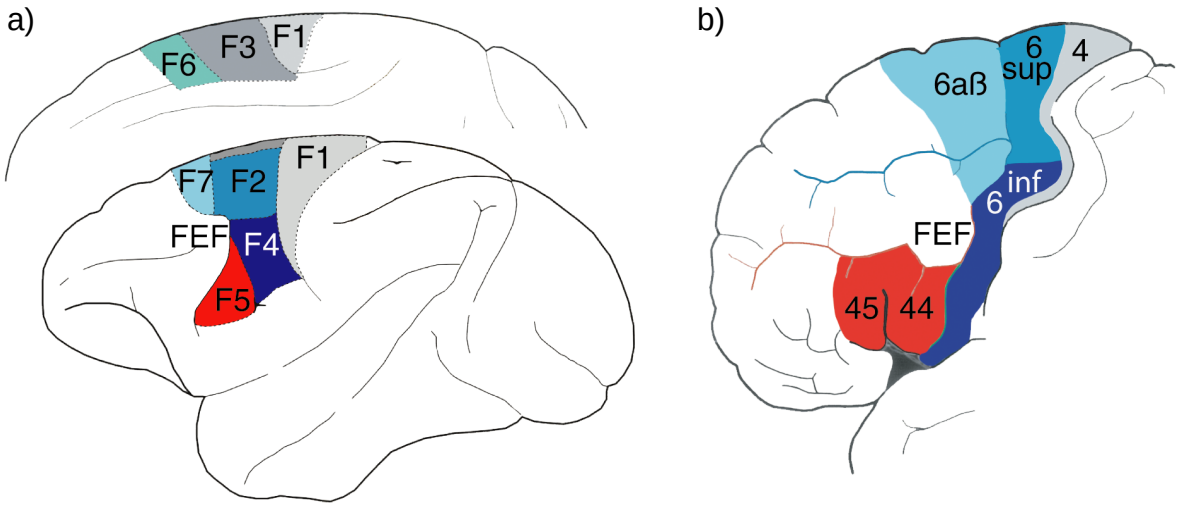

Fig. 1.13 Homologous premotor areas between monkey and human brains. a) Mesial and lateral views of the monkey brain, with motor fields F1–F7 represented by different colors. b) Lateral view of the human brain. Homologous areas are illustrated with the same color. Adapted from Rizzolatti et al. (1998)

From recent anatomic and functional studies in the monkey brain, a very different perspective on motor processing has emerged (for a review see, Rizzolatti et al., 1998; Luppino and Rizzolatti, 2000). The monkey motor cortex is composed of seven fields (F), where F1 corresponds to BA 4 (Fig 1.13a). In turn, the classic BA 6 is divided into six motor areas with distinct afferent and efferent connections and specific functional properties (Fig 1.13a). Some of these areas are mostly involved in transforming sensory information into motor commands, whereas other areas control this sensory-motor transformation. The strongest corticospinal connections originate in F1, but areas F2, F3, F4 and F5 also have spinal connections besides cortico-cortical connections with F1. Thus, all of these areas are more or less directly involved in motor execution.

Afferent inputs to the frontal motor areas originate from SI, the parietal cortex, the prefrontal lobe, and the cingulate cortex. The parietal cortex, similar to areas F2–F5 of motor cortex, is composed of independent areas with specific functional properties (sensory information and effector type). Reciprocal connections exist between distinct parietal and frontal motor areas, forming sets of highly segregated anatomic circuits dedicated to specific aspects of sensory-motor transformation. In addition, because posterior parietal areas are also activated during motor actions, the functional units of the cortical motor system may consist of those parietofrontal circuits (Rizzolatti et al., 1998). On the other hand, areas F6 and F7 of the frontal motor cortex are mainly connected with the prefrontal and cingulate cortices, which play a role in working memory, temporal planning of actions, and motivation. Dense interconnections exist between the different areas of the frontal motor cortex, enabling integration of sensory-motor transformation with higher-order aspects of motor control (Rizzolatti et al., 1998; Luppino and Rizzolatti, 2000).

Precise homology between monkey and human brains is difficult to establish. Based on general similarities of the cytoarchitecture and organization, possible homologies for the human motor cortex parcellation was suggested by Rizzolatti et al. (1998), as illustrated in Figure 1.13.

Interpretation of motor acts is a key element in social cognition. Information about other people's actions is conveyed by visual and/or motor input. Accordingly, sensory and motor input may bind in the brain into an already integrated abstract representation of action. Thus, it is of importance to understand first how sensory and motor processing of own actions relates at the neuronal level.

Neurons in area F4, which have motor properties with rough somatotopy, respond to both somatosensory and visual information (Gentilucci et al., 1988; Fogassi et al., 1996). These neurons code visual space in motor terms, as a consequence of motor interaction with the environment (Gentilucci et al., 1988; Graziano et al., 1994; 1997). F4 stores potential motor vocabulary to move body parts towards specific space locations, with local reference systems defined in motor terms.

In turn, area F5 contains a somatotopic representation of hand (dorsally) and mouth (ventrally) movements (Okano and Tanji, 1987; Rizzolatti et al., 1988). F5 "hand" neurons are mainly active during goal-directed actions related to objects, such as grasping, manipulating, tearing, and holding (Rizzolatti et al., 1988). Similar non-goal directed hand movements (e.g. pushing away) do not lead to activation of F5 neurons. Most F5 neurons represent grasping actions and can have very specific spiking responses. For example, some neurons are active during the entire grip movement, others are most active during finger-hand opening or during finger closure, others during precision grip, finger prehension, or whole hand prehension. In addition, some neurons are goal specific, independent of whether the left or right hand or mouth is used to achieve the action. These results suggest that F5 area stores a set of goal-directed motor vocabulary (Rizzolatti et al., 1988), in contrast to F1 that seems to store motor vocabulary independently of the context. In addition, F5 neurons have goal-directed sensory properties. These studies of Parma neuroscientists led to the discovery of mirror-neurons in the monkey brain (Gallese et al., 1996; Rizzolatti et al., 1996a).

1.8.2 Mirror neurons in monkeys

Besides motor properties, F5 neurons also respond to visual and auditory stimuli (Gallese et al., 1996; Kohler et al., 2002). F5 visuomotor neurons can be divided into canonical neurons and mirror neurons (Gallese et al., 1996; Rizzolatti et al., 1996a; Murata et al., 1997). Canonical neurons are mainly located in the region of F5 buried inside the arcuate sulcus, and they discharge in the visual presence of graspable objects (Rizzolatti et al., 1988; Murata et al., 1997). These neurons are congruently selective to one or a specific type of object in terms of both motor actions and visual properties. Therefore, canonical neurons seem to be important for object-to-hand movement transformation.

The second category of visuomotor neurons—the mirror neurons—are located in the cortical convexity of F5. They become active both when the monkey acts on an object and when it observes another individual performing a goal-directed action towards an object, with hands or mouth (di Pellegrino et al., 1992; Gallese et al., 1996; Rizzolatti et al., 1996a). These neurons "resonate" with another individual's goal-directed interactions with objects, and not to the presentation of objects, food, or tool grasping (e.g. pliers). In agreement with motor characterization of F5 neurons (Rizzolatti et al., 1988), mirror neurons are most sensitive to grasping, placing, manipulating, and holding observed actions. Also, they are congruent in terms of both motor and visual properties, being selective of the action and how it is performed (Rizzolatti and Craighero, 2004). Some mirror neurons are activated by mouth ingestive actions, such as sucking and breaking food (Ferrari et al., 2003).

Evidence for a more abstract representation of goal-directed actions was obtained by Umiltá et al. (2001), who proved that mirror neurons are goal-directed action coding neurons. Indeed, they still discharge when the final part of a goal-directed hand-object interaction (grasping) is hidden behind a screen, but they do not discharge if the monkey is aware that the object behind the screen has been removed. In this case, the monkey predicted whether a goal-directed action was going to occur or not.

More recently, a new class of mirror neurons was found—audiovisual mirror neurons (Kohler et al., 2002). These neurons become active when the object-related goal-directed action is performed, seen, or heard. Furthermore, in half of the neurons tested by Kohler et al. (2002), the amplitude of the response did not depend on whether the action was only heard,

only seen, or both seen and heard simultaneously. Based on firing rate, at the single audiovisual mirror-neuron level, it was possible to discriminate between two actions in two-thirds of the neurons tested, independently of the action being heard, seen, or performed (Keysers et al., 2003). Thus audiovisual mirror neurons code and discriminate information in an abstract manner, independently of the source of information. In contrast, other types of sounds, such as white noise or several monkey vocalizations, do not evoke significant responses in these neurons.

Mirror-neuron type behavior has also been found in the monkey inferior parietal lobule, area PF (Fogassi et al., 1998), in agreement with the existing reciprocal connections to the frontal motor areas. Moreover, neurons in the superior temporal sulcus (areas STSa) discharge during the observation of biological motion and goal-directed hand actions, but these neurons lack clear motor properties and therefore do not fulfill the requirements of motor mirror neurons.

In summary, the functional role of F5 neurons is related to motor vocabulary that codes actions, whether they are performed or internally represented (Rizzolatti and Craighero, 2004). Canonical and mirror neurons address the same "motor vocabulary" in a different fashion. Whereas canonical neurons may be at the basis of the sensorimotor transformation that adapts the hand to the observed object, mirror neurons may be at the basis of action imitation and action understanding (Rizzolatti and Craighero, 2004). Thus, mirror neurons enable the individual to recognize someone else's action, observed or heard, because our own inner representation of that action is activated. The mirror-neuron observation–execution matching system may be at the basis of interindividual gestural understanding (Rizzolatti and Craighero, 2004), since monkey area F5 is believed to be the precursor of the human Broca's region (BA 44 and BA 45) (Rizzolatti and Arbib, 1998; Rizzolatti and Luppino, 2001).

1.8.3 The human mirror-neuron system

Once mirror neurons were discovered in the monkey brain, the scientific community tried to find out if such an observation–execution matching system, the mirror-neuron system (MNS), also existed in the human brain (for a review, see Rizzolatti and Craighero, 2004). The first evidence that mirror neurons may exist in the human brain was obtained with transcranial magnetic stimulation (Fadiga et al., 1995). Stimulation of the left motor cortex, while subjects observed both transitive hand actions (grasping objects) and intransitive arm movements, resulted in increased motor-evoked potentials from the right hand and arm muscles. However, it could not be determined if this effect took place due to facilitation in M1 or facilitatory input to the spinal cord. A subsequent neuroimaging study attempted to identify human mirror-neurons using positron emission tomography (PET) (Rizzolatti et al., 1996b). Results showed activation of the inferior frontal gyrus (IFG), in BA 45, during action observation, but no overlap was found with the area activated during action execution itself. Moreover, the monkey area F5 is considered to be the homologue of BA 44 in the IFG (Rizzolatti et al., 1998). The first direct evidence of human mirror-neurons was obtained in an MEG experiment (Hari et al., 1998a), which showed reactivity of the M1 cortex to both performed and observed actions.

Later research showed that besides M1 reactivity, the human MNS comprises at least the inferior frontal gyrus (IFG), i.e. BA 44 and its right hemisphere homologue (Rizzolatti et al., 1996b; Iacoboni et al., 1999; Nishitani and Hari, 2000; Buccino et al., 2001; Iacoboni et al., 2001; Decety et al., 2002; Nishitani and Hari, 2002). These studies showed that observation of actions made by another person activates a large network in the human brain, but only IFG and M1 were commonly active during execution and observation. This complex network comprised visual areas, the superior temporal sulcus, the inferior parietal lobe and finally IFG and M1.

The human MNS seems to code movements that form an action (Fadiga et al., 1995; Levänen et al., 2001; Maeda et al., 2002; Patuzzo et al., 2003), and not only objected-related goal-directed actions as the monkey area F5. This function could play an important role in the human capacity to imitate other's actions. The observation of transitive actions activates both the inferior parietal lobule and the IFG (*pars opercularis*), whereas intransitive hand-actions seem to activate only the IFG (Iacoboni et al., 1999; Koski et al., 2002; Koski et al., 2003; Fogassi et al., 2005). In addition, the human MNS is more sensitive than what could be predicted from monkey data: presentation of static pictures of hand-object interaction is sufficient to activate bilaterally the precentral and inferior frontal gyri (Johnson-Frey et al., 2003), and the presentation of tools or other graspable objects activates the dorsal premotor cortex (Grafton et al., 1997).

Audiovisual mirror neurons in the monkey brain are activated by action-related sounds (Kohler et al., 2002; Keysers et al., 2003). Similar behavior may be expected in humans, as actions can be readily recognized as either heard, observed, or performed. A TMS study showed lateralized left-hemisphere motor corticospinal excitability of hand muscles to bimanual action-related sounds, like typing or tearing paper (Aziz-Zadeh et al., 2004), which suggests coding of auditory, visual, and motor components of actions on the left hemisphere, whereas on the right hemisphere only visual and motor components of actions seem to be coded.

The existence of an action execution–observation matching system activated when one performs, observes, or hears an action leads to the problem of agency. It has been suggested that understanding other's actions, imitation, and motor learning is achieved through internal simulation of similar actions, and also prediction of other people's goal-directed movements. But at the neural level, how can one distinguish self from other? Proposals to solve the problem of agency include: efference copies from the movement preparation areas, afferent copies when performing movements (proprioceptive input), and weaker activation of the MNS when the action is solely observed (Ruby and Decety, 2001; Flanagan and Johansson, 2003; MacDonald and Paus, 2003; Farrer et al., 2004; Hari and Nishitani, 2004; Vogeley et al., 2004; Jackson et al., 2006).

In summary, the human MNS includes the posterior part of the inferior frontal gyrus, the lower part of the precentral gyrus, and the rostral part of the inferior parietal lobule (Fadiga et al., 1995; Rizzolatti et al., 1996b; Hari et al., 1998a; Iacoboni et al., 1999; Nishitani and Hari, 2000, 2002). Within the MNS, Broca's region has a central role between perception and action understanding (Nishitani et al., 2004). More precisely, Broca's region links time-sensitive perceptual and motor functions underlying interindividual communication. Besides action understanding (Grèzes et al., 1999; Rizzolatti et al., 2001), the human MNS may also play a crucial role in motor learning (Buccino et al., 2001), imitation (Iacoboni et al., 1999; Nishitani and Hari, 2000, 2002), attribution of mental states (Avikainen et al., 1999; Avikainen et al., 2003; Nishitani et al., 2004), as well as in some aspects of language perception (Rizzolatti and Arbib, 1998).

2 Aims of the study

The aim of this study was to investigate, by means of behavioral tasks and non-invasive neuroimaging techniques, human audiotactile integration, transfer of information between sensory modalities, and brain rhythmic activity related to performed and observed actions. The specific goals of each individual study were:

I to find out whether integration of vibrotactile and auditory stimuli exist and can be quantified in a behavioral loudness-matching task (Study I).

II to characterize, by means of whole-scalp MEG, brain activation sequences elicited by vibrotactile stimuli, and to find out whether human auditory areas are activated by such stimuli (Study II).

III to adapt the experimental setup from Study II for fMRI, to determine with good spatial accuracy areas co-activated by auditory and tactile stimuli (Study III).

IV to test frequency information transfer from somatosensation to motor output in normal-hearing adults (Study IV).

V to monitor sensorimotor MEG rhythmic activity to unravel similarities between performed vs. seen or heard actions (Study V).

3 Methods

3.1 Subjects

Altogether 56 healthy, right-handed volunteers were studied, some of them in several experiments, after informed consent. The experiments were conducted in accordance with the Declaration of Helsinki, and with approval from the local ethics committee. The table below shows the number of subjects in different studies, the subjects' age range, and the experimental paradigms.

Study	Number of subjects	Age range	Task and stimulation
I Behav	9	24–41	Loudness matching task, with pairs of 200-Hz vibrotactile and auditory stimuli presented in a 2-s cycle. Reference tone (900 ms) constant in intensity, probe tone (500 ms) varying in intensity, ISI = 0.1 s.
II MEG	10	21–43	Vibrotactile stimulation with 200-Hz 500-ms sinusoidal signals, SOA = 8.0 ± 0.5 s. Auditory stimulation with 1-kHz 100-ms pure tones, SOA = 1.0 s. Alternate electric stimulation of left and right median nerves, SOA = 1.5 s.
III fMRI	13	22–39	Vibrotactile stimulation with 200-Hz 500-ms sinusoidal signals, SOA = 1.5 ± 0.7 s. Auditory stimulation with 500-ms white noise bursts, SOA = 1.5 ± 0.7 s. Pulsed-tactile stimuli, 282 ms in duration, applied to fingers II–IV of the right hand, SOA = 0.4 ± 0.1 s.
IV Behav	11	21–29	Vibrotactile stimulation, 2000 ms in duration, of 150, 200, 250, 300, 350, and 400 Hz, ISI = 0.5 s.
V MEG	13 (25)	25–40	Tapping of a drum membrane with right index finger by the subject and by another person. Four conditions: own action with sound, own action without sound (ISI ~3–6 s), observation of action, listening to action-related sound (ISI ~4–5 s).

3.2 Recordings

3.2.1 Magnetoencephalography

Neuromagnetometer

The MEG studies were carried out at the Brain Research Unit, Low Temperature Laboratory, with a 306-channel neuromagnetometer (Vectorview™, Elekta Neuromag Oy, Helsinki, Finland) that houses 102 identical triple-sensor elements in a helmet-shaped array. Each sensor unit consists of two orthogonal planar gradiometers and one magnetometer, providing three independent measures of the magnetic field. The planar gradiometers measure the two orthogonal tangential derivatives of the magnetic field component that is normal to the helmet surface at the sensor location, and they detect the largest signal just above a local dipolar current source.

Before recordings

When the subject was prepared for the recording, four head position indicator coils were attached to the subject's head and four electrodes were placed to record electro-oculograms (EOGs) during the measurement. The coils were used to determine the head position of the subject before/during/after the measurement. The locations of the coils were determined relative to three anatomical landmarks (left and right pre-auricular points, and nasion) using a 3-D digitizer (Isotrak 3S10002; Polhemus Navigation Sciences, Colchester, VT, USA). Moreover, additional points were digitized on the subject's head, which together with the anatomical landmarks were used to align MEG and MRI coordinate systems. Magnetic fields generated by currents fed into the coils were measured when the subject was in position to start the experiment, and they gave information on coil locations with respect to the sensor array. For the studies in this thesis, T1-weighted MRIs of the subjects' brains were acquired using a 1.5-T Siemens Magnetom (Department of Radiology, Helsinki University Central Hospital) or a 3-T General Electric Signa system (Advanced Magnetic Imaging Centre, Helsinki University of Technology).

During recordings

During MEG recordings, the subject was sitting comfortably in a magnetically shielded room, with the head firmly resting against the helmet-shaped neuromagnetometer. The subject was asked to keep the head immobile, eyes open, and avoid eye blinking during the stimulation. The MEG signals were recorded with a 0.03–172 Hz passband and digitized at 600 Hz. Vertical and horizontal EOGs were recorded simultaneously. MEG epochs with EOG amplitudes exceeding 150-μV peak-to-peak were rejected from the analysis and online averaging, because magnetic fields created by eye blinks and saccades can mask signals arising from brain activity.

Noise reduction

The measurements were conducted inside a magnetically shielded room, which consists of two aluminum and μ-metal layers (Holmlund et al., 2001). The shielded room is equipped with active shielding, i.e. the room has coils embedded in the walls that measure the external magnetic field continuously, in three orthogonal directions. The active shielding is provided by the generation of compensating currents in coils outside the room.

Further noise reduction was achieved using the Signal Space Projection (SSP) method, which allows elimination of various artifacts (Uusitalo and Ilmoniemi, 1997). In practice, SSP vectors are based on empty room recordings, and the information is used to perform noise cancellation beyond what planar gradiometers can achieve. For example, a projection operator for gradiometers is calculated containing information on homogeneous gradients and higher order derivatives. The method assumes that these components are relatively stable over a period of days or weeks.

Further noise reduction was achieved by signal averaging, because the signal-to-noise ratio of stationary signals increases with the square root of the number of averaged responses. Besides EOG monitoring, single-trials were rejected whenever signal-quality criteria were not met in all sensors. Additionally, non-functional or noisy sensors were discarded from the averaging, and also from the SSP projection.

3.2.2 Functional magnetic resonance imaging

MRI scanner

The fMRI study in this thesis was conducted at the Advanced Magnetic Imaging (AMI) Centre at Helsinki University of Technology, with a Signa VH/i 3.0 T MRI scanner (GE Healthcare, Chalfont, StGiles, UK) and a quadrature transmission-and-receiver head coil. The MRI scanner is inside a magnetically shielded room to reduce noise by environmental contamination.

Functional images were acquired with a gradient-echo EPI sequence defined at the AMI Centre. Each volume was composed of 31 axial-oblique slices that covered the whole brain: 3.1 × 3.1 mm^2 in plane-resolution, 4.0 mm slice with no gap between slices, FOV = 200 mm × 200 mm, matrix size 64 × 64 voxels, TR = 2.5 s, TE = 32 ms, and 90° flip angle. Additionally, structural T1 images were acquired using a standard fast-spoiled gradient-echo pulse sequence (GE SPGR) with 1.4 × 1.4 × 1.4 mm^3 resolution.

3.3 Data analysis

3.3.1 Magnetoencephalography

Source modeling

Source analysis was performed with Neuromag software (Neuromag Ltd., Helsinki, Finland) on signals from 204 planar gradiometers. Sources of brain activation were modeled with ECDs, in a spherical volume conductor (see Section 1.1), with the origin found on the basis of individual MR images. In our coordinate system, the *x* axis goes from left to right pre-auricular point, *y* axis runs towards nasion, and *z* axis goes upward perpendicular to the *xy* plane.

To model ECDs, we selected time windows and sensors with stable magnetic field patterns of dipolar appearance; only sources with goodness of fit > 80% were accepted. In Studies II and V, ECDs in postcentral and Rolandic regions, respectively, were modeled with a subset of at least 18 channels. In Study II we used multidipole models, including sources accepted for different regions of the brain. ECDs in parietotemporal regions were modeled with subsets of 30–46 channels overall, after projecting out the contribution from the SI source with the SSP method (Uusitalo and Ilmoniemi, 1997). In the multidipole model, the source locations and orientations were kept fixed, the strength was allowed to change as function of time, and all channels were taken into account. The multidipole model was validated by comparing both the predicted waveforms with the measured signals and the modeled magnetic field patterns with the measured magnetic field patterns. Peak latencies and amplitudes were measured from the source waveforms, with respect to the base-level (–200 ms to –10 ms, in Study II), and statistical differences in source latencies and locations were evaluated with the Student's two-tailed paired t-test.

Temporal spectral evolution

Data analysis was performed using Neuromag software (Neuromag Ltd., Helsinki, Finland) and the software package Matlab 6.5 (http://www.mathworks.com/products/matlab/).

The level of brain oscillatory activity was assessed (in Study V) using temporal spectral evolution (TSE) (Salmelin and Hari, 1994). According to the frequency band of interest, signals were first bandpass filtered: 8–13 Hz (~10-Hz band) and 14–30 Hz (~20-Hz band).

Then, the filtered signals were rectified and time-locked averaged to the stimuli. In each subject, we selected the channel over the left Rolandic cortex that showed the strongest ~20-Hz reactivity during the *Own Action* condition. We then calculated the average of the ~10- and ~20-Hz activity levels from –3 s to 3 s, relative to the drum trigger. The baseline, corresponding to the spontaneous activity level when no motor actions were performed, observed, or heard, was set from –2.9 s to –2.4 s.

Time-frequency representation

Time-frequency representations (TFRs) were calculated using the 4D-Toolbox, developed by Ole Jensen (currently at F.C. Donders Centre for Cognitive Neuroimaging, Nijmegen, The Netherlands). TFRs were calculated in each subject from the channels selected for TSE. Frequencies ranging from 5- to 35-Hz with steps of 0.25 Hz were analyzed in a –3 s to 3 s time window, using wavelets with a width of seven cycles. The grand-average across the 13 selected subjects was calculated in all four experimental conditions.

3.3.2 Functional magnetic resonance imaging

The data analysis was performed using the Statistical Parametric Mapping software package developed by members and collaborators of the Wellcome Department of Imaging Neuroscience, London, UK (SPM99, http://www.fil.ion.ucl.ac.uk/spm/software/spm99/).

Preprocessing

The first four volumes of each fMRI run were excluded from the analysis to ensure that only volumes with full magnetic saturation were taken into account. Functional images were realigned (3D movement correction) and high-pass filtered. Normalization (EPI-to-EPI) to standard MNI space (Montreal Neurological Institute) on subsampled data ($1.5 \times 1.5 \times 2.0$ mm^3) was performed with a smoothing kernel corresponding to the original voxel size ($3.1 \times 3.1 \times 4.0$ mm^3).

Individual subject analysis

General linear model (GLM) analysis was performed on individual data, and contrasts between experimental conditions were calculated. In each subject, areas of co-activation between auditory and vibrotactile stimuli were found (conjunction analysis, with pulsed-tactile activation voxels exclusively intersected). The clusters of co-activation in each of the subjects (or the closest to the group activation loci), in both left and right hemipsheres, were used to extract individual subject time-courses and amplitudes of activations. The time-courses were averaged across each specific stimulation–rest block.

Group analysis

A random-effects analysis was performed at the group level from the individual contrast images, with thresholds of $P < 0.001$ (uncorrected) at the voxel level and $P < 0.05$ (corrected) at the cluster level. Two types of smoothing kernels were used: original voxel size and 3 × original vovel size ($9.3 \times 9.3 \times 12$ mm^3).

4 Experiments

4.1 Vibrotactile input facilitates hearing at low sound-intensity levels (Study I)

The purpose of this study was to search for an intermodal bias in perception of sound intensity when vibrotactile stimuli are presented simultaneously. Normal-hearing subjects adjusted the intensity of the probe tone such that the perceived intensity was as loud as the reference tone (Fig 4.1). This loudness-matching task comprised two distinct conditions: 1) without vibrotactile information (*Sound only*); 2) with vibrotactile information presented simultaneously with the probe tone (*Sound+Touch*).

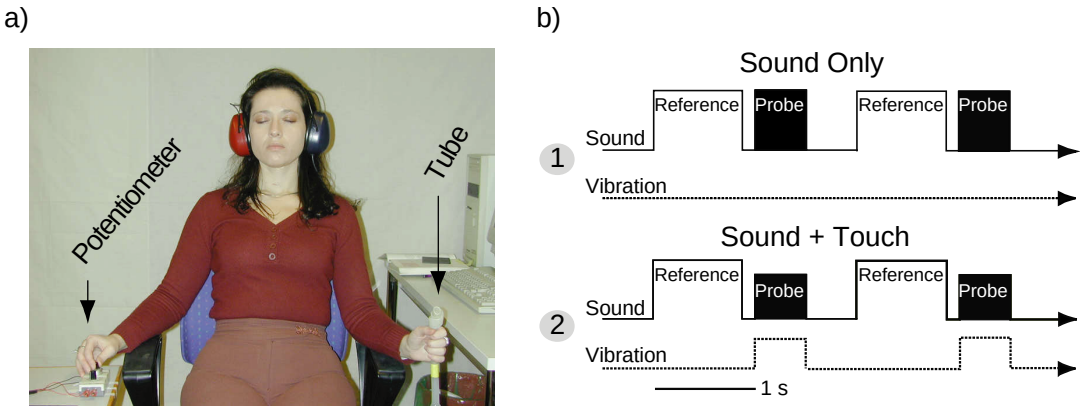

Fig. 4.1 Experimental setup. a) The probe and reference tones were presented via headphones, while the subject adjusted the probe-tone intensity with a semi-log potentiometer. Vibrotactile stimuli were delivered to the subject's left-hand fingers via a blind-ended silicone tube attached to a custom-built stimulator. b) Within a 2-s cycle, two pairs of 200-Hz tones were presented binaurally: the reference and the probe tone respectively, with a 100-ms pause in between. The tones were embedded in continuous masking white noise, 60 dB above hearing threshold, and kept constant for all subjects. The intensity of the 900-ms reference tone was adjusted individually to 10 dB above hearing threshold within masking noise, while the 500-ms probe tone was adjusted by the subject. In condition 2, the vibrotactile stimuli (200-Hz, 500-ms signals; constant intensity across subjects) were presented simultaneously with the probe tone. Reprinted with permission from Schürmann M, Caetano G, Jousmäki V, Hari R: Hands help hearing: Facilitatory audiotactile interaction at low sound intensity levels. J Acoust Soc Am 2004, 115, 830–832 Copyright (2004), American Institute of Physics.

The data were recorded and subsequently analyzed using the Matlab 6.5 software package (http://www.mathworks.com/products/matlab/). Root-mean-square intensities for the probe tone were calculated in "*Sound only*" and "*Sound + Touch*" conditions. Median amplitudes amplitudes for the "*Sound only*" condition were normalized to 1.0 for each subject.

On average, subjects chose 12.4% lower intensities for the probe tone in *Sound + Touch* than in *Sound only* condition ($p = 0.007$, Wilcoxon's signed rank test for paired samples). At the individual level, 7 out of the 9 subjects showed statistically significant differences between the two experimental conditions ($p < 0.05$, Wilcoxon's rank sum test for independent samples).

Conclusion

These results suggest facilitatory audiotactile integration between pure tones and vibrotactile stimuli at low sound-intensity level in normal-hearing subjects.

4.2 Vibrotactile input activates human auditory areas (Study II)

Our aim was to find out, by means of whole-scalp MEG, whether auditory areas in normal-hearing adults would be activated by vibrotactile stimuli. For that purpose, we designed an experiment consisting of two sessions with vibrotactile stimulation, and additional sessions to identify SI, SII, and auditory cortices.

Experimental setup

In the two sessions with vibrotactile stimulation, the subject touched the *touch* tube with fingertips, without squeezing, and the *no-touch* tube was placed close to the *touch* tube for control purposes (Fig 4.2). The tubes were stimulated alternatingly, once every 4.00 ± 0.25 s, with 500-ms 200-Hz signals. Replicability of the evoked fields elicited by the vibrotactile stimulation (VTEFs) was verified between the two sessions.

The SI and SII cortices were identified by recording responses to alternate stimulation of the subject's left and right median nerves, above the motor threshold, once every 1.5 s with 0.2-ms electric contant-current pulses. The auditory cortices were identified by recording responses to presentation of binaural 100-ms 1-kHz tone bursts.

At least a total of 200 responses were averaged for both *touch* and *no-touch* tubes (100 responses per session), about 130 responses were averaged for median nerve stimulation (left- and right-sided stimuli), and approximately 250 responses were averaged for auditory stimuli.

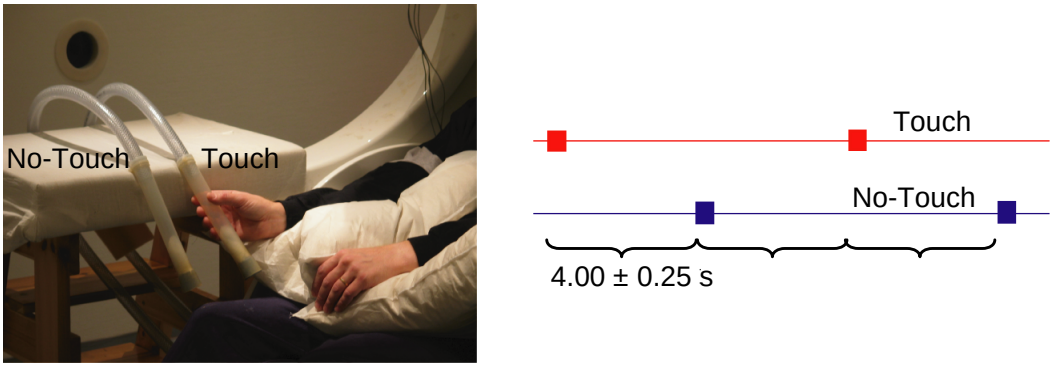

Fig. 4.2 Experimental setup. Vibrotactile stimuli were delivered to the subject's right-hand fingertips via a blind-ended silicone tube attached to a purpose-built stimulator (different from stimulator in Study I). The perceived intensity of the vibrotactile stimuli was on average 19.5 dB above the individual tactile detection threshold (15–22 dB, N = 9). Subjects used earplugs to prevent any possible contamination from ambient noise or vibrotactile stimuli. Adapted from Caetano and Jousmäki (2006).

Results

After the experiment, the subject described in their own words the percepts during the experiment. All subjects reported a weak percept of vibration at the fingertips, a percept of a sound when vibrotactile stimuli were applied to the *touch* tube, and perceived nothing when the *no-touch* tube was stimulated.

Figure 4.3a shows the spatial distribution of VTEFs in a representative subject, for both *touch* (red) and *no-touch* (blue) tubes. The traces show replicability of the VTEFs between sessions. The encircled channels, enlarged on the right (Fig. 4.3b), illustrate the latencies of the evoked responses elicited by vibrotactile stimuli. The first deflection occurred in the contralateral postcentral area (channel A) about 60 ms after the stimulus onset. This deflection was followed bilaterally by transient responses in parietotemporal areas, peaking

at 140 ms (channel B) and 165 ms (channel C) respectively, and by a sustained field that outlasted the stimulus duration. In the ipsilateral hemisphere, a second transient peaked at 170 ms (not illustrated in the enlarged channels).

Across all subjects, the contralateral VTEFs consisted of two transient responses, the first peaking at about 60 ms in postcentral areas, and the second peaking at about 100–200 ms in parietotemporal areas. Contralateral sustained activity was observed in only two of the ten subjects. The ipsilateral VTEFs comprised at least one transient response peaking at 100–200 ms, followed by a sustained field.

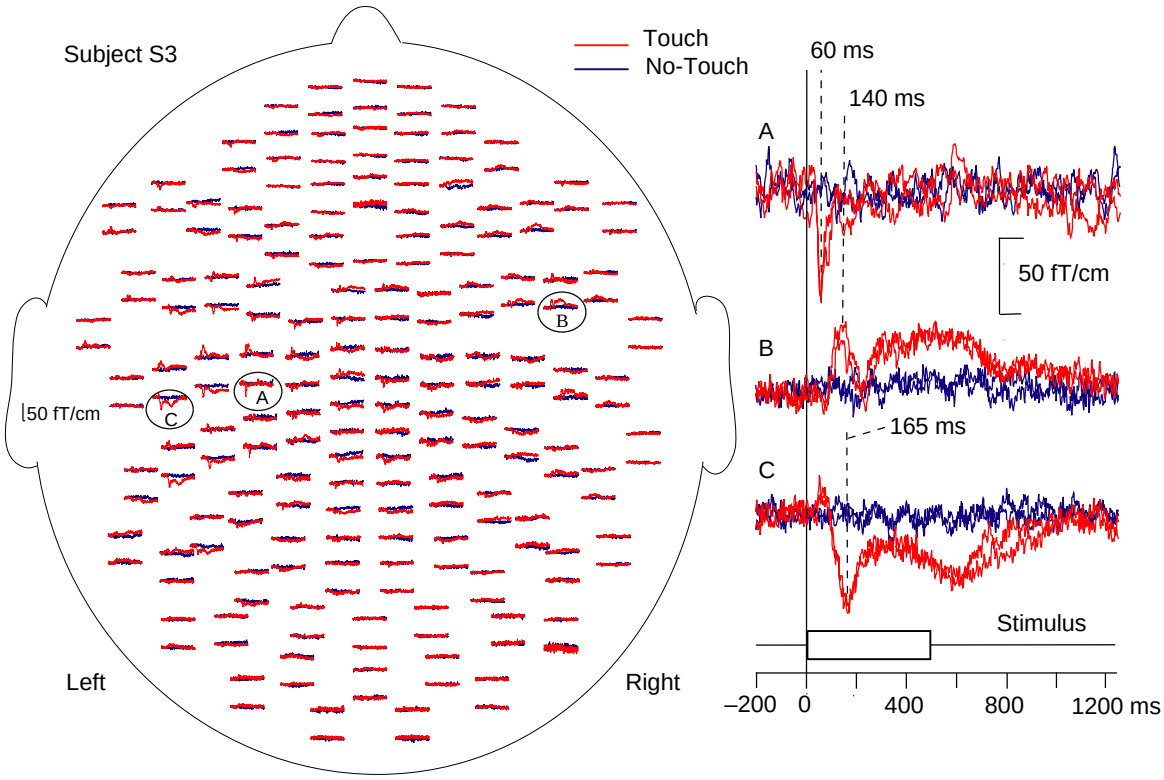

Fig. 4.3 VTEFs from a representative subject. a) Whole-scalp spatial distribution of MEG signals. The pairs of gradiometers, visualized as traces, represent the longitudinal and latitudinal derivatives of the magnetic field at each sensor location. b) Encircled channels are enlarged, with transient peak latencies indicated by dashed lines. The red traces show VTEFs to the *touch* tube, and the blue traces to the *no-touch* tube. The data were digitally low-pass filtered with a cut-off frequency of 140 Hz, and with a notch filter at 50 Hz and 100 Hz. The base-level of brain activity was defined from –200 to –10 ms. Adapted from Caetano and Jousmäki (2006).

SI sources peaked at about 60 ms, and their contribution was projected out with the SSP method to identify parietotemporal sources. The stability and robustness of sources in parietotemporal areas was assessed with sequential ECD modeling at 4-ms steps. If the sources formed distinct clusters for at least 20 ms, the area was accepted as activated by vibrotactile stimuli.

Figure 4.4a shows the results of the sequential ECD modeling in two of the subjects, with information on the time of the activation color-coded. Clusters of sources were located in both lower and upper banks of the Sylvian fissure. Figure 4.4b summarizes the number of subjects with consistent clusters of activation, in either the lower or upper banks of the Sylvian fissure. The criteria applied in sequential ECD modeling ($g > 80\%$) may have led to the discard of possible clusters of activation in both auditory and SII cortices.

The results suggest that a first transient response at 100–200 ms, in parietotemporal areas, was equally probable in both upper and lower banks of the Sylvian fissure ($p = 0.69$ in left hemisphere, $p = 0.38$ in right hemisphere; sign test). In addition, sustained activity was

only present in the lower bank of the Sylvian fissure (p = 0.008 in right hemisphere; sign test).

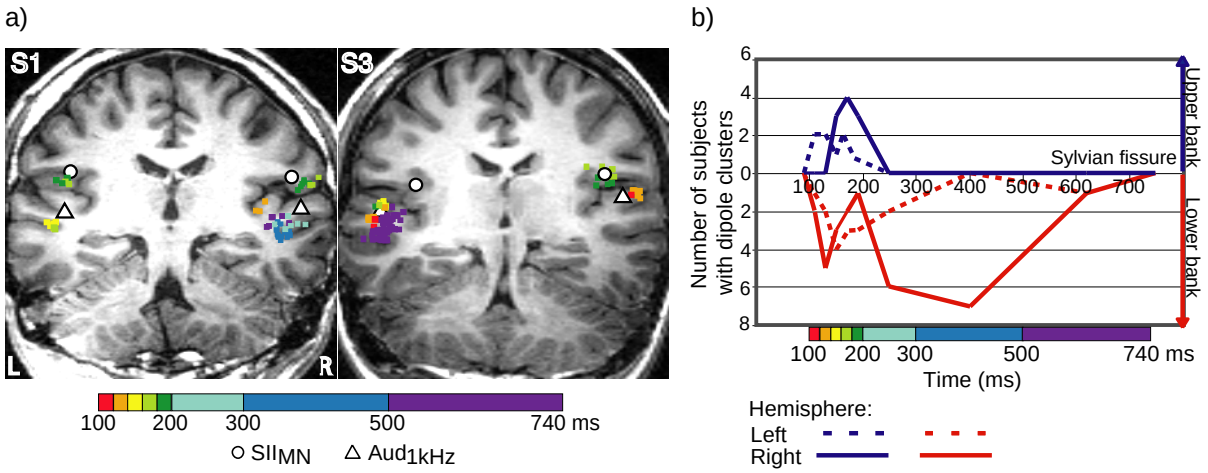

Fig. 4.4 Results of sequential dipole fitting, with temporal information color-coded in the horizontal bar. a) Clusters of single sources are superimposed on individual MR images, perpendicular to the Sylvian fissure. The sources within ± 15 mm were projected onto the selected MR image. Additionally, the functional landmarks for SII and auditory cortices are shown by a white circle and triangle, respectively. b) Number of subjects with source clusters, in upper (blue) and lower (red) banks of the Sylvian fissure, as a function of time. The left and right hemispheres are represented by dashed and solid lines, respectively. Adapted from Caetano and Jousmäki (2006).

The accepted sources were included, for each subject, in a time-varying multi-dipole model. Overall, the model had 2–5 sources, including the contralateral SI source. Activation of auditory cortical areas was identified in all subjects, either bilaterally (N = 5) or ipsilaterally (N = 5), whereas activation of SII cortices was identified in six out of ten subjects, both contralaterally (N = 3) and ipsilaterally (N = 4). Vibrotactile sources peaked 81 ms (N = 5) or 49 ms (N = 9) later than the 100-ms response (N100m) elicited by tone pips, in the left and right hemispheres, respectively. The mean locations of the sources in auditory areas did not differ between vibrotactile or tone stimuli in either hemisphere.

Conclusion

The results suggest that, in normal-hearing adults, vibrotactile stimuli elicit transient activations of SI, SII, and auditory cortices, as well as sustained activation in auditory areas that resembles sustained activation elicited by long auditory stimuli (Hari et al., 1980). Most strikingly, the vibrotactile stimuli elicit a perception of a sound, which may be related to the activation of auditory areas. Auditory sensations can arise without stimulation of the cochlea, as for example during auditory seizures, hallucinations, or electric stimulation of the temporal lobe (Penfield and Jasper, 1954). Pacinian corpuscles (stimulated in this experiment) react to a frequency range that overlaps with audition. Thus, the auditory system may have a role in processing vibrotactile temporal information. The studies by von Békésy (1960) on cochlear mechanisms have demonstrated and emphazised the similarity of skin sensations and hearing.

Our results suggest convergence of vibrotactile input to auditory cortex in normal-hearing adults, in agreement with results previously obtained in a congenitally deaf adult (Levänen et al., 1998).

4.3 Tactile input activates human auditory areas (Study III)

The aim of this study was to find out by means of fMRI, and based on findings of Studies I and II *i)* the extent of auditory areas activated by VT and pulsed-tactile stimuli, and *ii*) areas co-activated by auditory and tactile stimuli. Similar to the MEG experiment in Study II, we had two sessions of VT stimuli alone (with a two-tubes setup), and separate sessions with functional localizers for auditory, SI, and SII cortices.

Experimental setup

Before starting the experiment, we presented all stimuli to the subject to minimize novelty effects. The vibrotactile stimuli were delivered via the *touch* tube to the subject's right hand fingers and palm. The *touch* and *no-touch* tubes were stimulated alternatingly, for periods of 25 s, with 500-ms 200-Hz signals (SOA 1500 ± 700 ms). The SI and SII cortices were identified using pulsed-tactile stimuli (282 ms duration, SOA 400 ± 100 ms) in random order to fingers II–IV of the right hand. Auditory cortices were identified using 500-ms bursts of white noise (SOA 1500 ± 700 ms) delivered binaurally via headphones, while subjects used earplugs. All sessions consisted of 25-s periods of stimulation (VT, pulsed-tactile, auditory) alternated with 25-s periods of non-stimulation (rest condition for auditory and pulsed-tactile stimuli, and control condition for the *no-touch* tube in the vibrotactile sessions).

Results

The group results, illustrated on a coronal MR image in Figure 4.5a, showed most consistent activations in *i*) contralateral (left) SI and SII cortices with extension into the superior temporal sulcus for pulsed-tactile stimuli, *ii*) contralateral SII cortex with extension into the superior temporal gyrus for vibrotactile stimuli, and *iii*) bilateral auditory cortices to auditory belt areas for auditory stimuli. Figure 4.5b shows, on a sagittal MR image, the areas of co-activation for both vibrotactile–auditory and pulsed-tactile–auditory conditions. At the group level, co-activation was observed in the left hemisphere, in a single area posterior to the primary auditory cortex.

Similar analysis was performed, at the individual subject level, identifying voxels of vibrotactile–auditory co-activation in single subjects (exclusively intersected with pulsed-tactile–rest). The clusters were selected with minimal smoothing and superimposed on an averaged structural scan, as illustrated in Figure 4.6. The peak voxels in the left hemisphere (MNI –45 –36 12) corresponded to seven subjects, whereas those in the right hemisphere (MNI 66 –20 7) corresponded to five subjects. Furthermore, 9 out of 13 subjects had clusters of co-activation bilaterally, and 12 out of 13 subjects had clusters of co-activation in the left hemisphere.

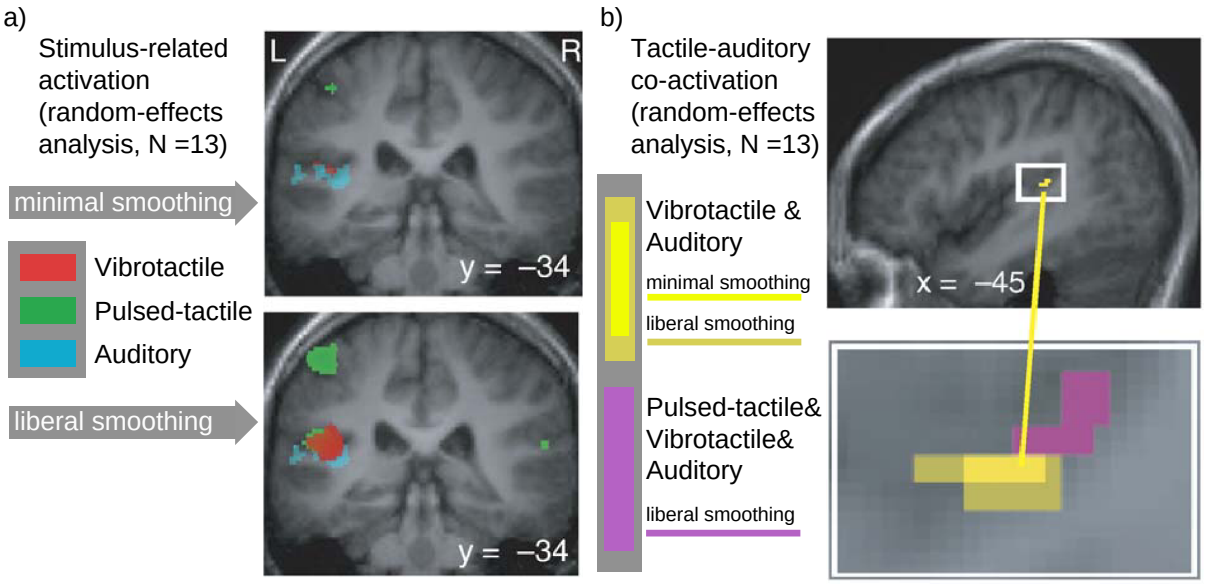

Fig. 4.5 Random-effects analysis at the group level (N = 13) and areas of co-activation, with both minimal smoothing (kernel of original voxel size 3.1 × 3.1 × 4.0 mm^3) and liberal smoothing (kernel 3 × original voxel size), in upper and lower rows, respectively. The results are superimposed on 13 individual normalized structural images. a) Red, green, and blue represent the stimulus-related activation for vibrotactile, pulsed-tactile, and auditory stimulation, respectively. Right-hemisphere activation was not observed above the defined thresholds, independent of the smoothing used. b) Areas of vibrotactile–auditory (yellow) and pulsed-tactile–auditory (purple) co-activations in the left superior temporal gyrus, corresponding to auditory belt areas. Adapted from Schürmann, Caetano, Hlushchuk, Jousmäki, and Hari (2006).

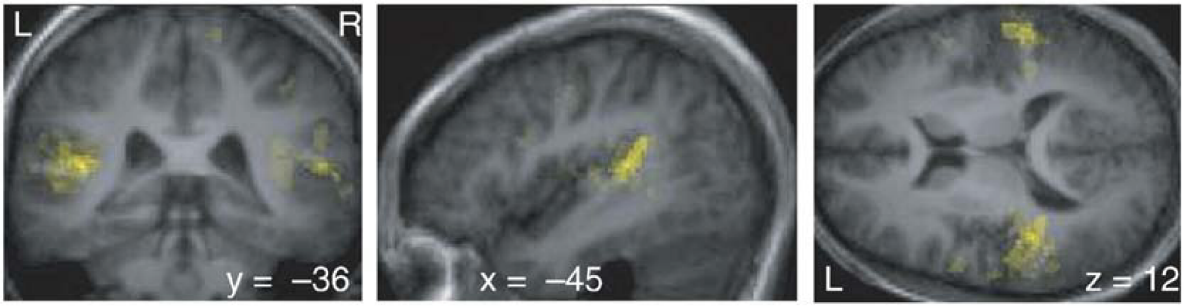

Fig. 4.6 Areas of vibrotactile–auditory co-activation displayed as a population map across 13 subjects. Adapted from Schürmann , Caetano , Hlushchuk , Jousmäki , and Hari (2006).

Conclusion

In summary, this experiment allowed us to identify a common neural substrate in auditory belt areas that processes both vibrotactile and auditory stimuli (and to a lesser extent also pulsed-tactile stimuli). This finding agrees with the results of Study II, and it provides better spatial accuracy on the location of auditory areas activated by vibrotactile stimuli.

4.4 Frequency information transfers from touch to utterances (Study IV)

The purpose of this study was to find out the efficacy of frequency information transfer from touch to vocal utterance in normal-hearing adults. In a humming–vibration matching task, the subject was asked to hum the pitch of the vibrotactile stimulus delivered to the right-hand fingertips. All participants were female with no professional vocal or musical training. Sinusoidal 2-s vibration bursts were delivered to the subject's right-hand fingertips via a blind-ended silicone tube. Subjects wore earplugs and headphones through which white noise was delivered as an auditory masker. The sinusoidal bursts (150, 200, 250, 300, 350, or 400 Hz) were presented once every 0.5 s in a random fashion.

The data were recorded and analyzed using the software package Cool Edit 2000 (http://www.mp3-converter.com/cool_edit_2000.htm). The hummed pitch was calculated offline with fast fourier transform (FFT), and the most prominent frequency value was selected. The results were compared using the autocorrelation method of the software package Praat (http://www.fon.hum.uva.nl/praat/).

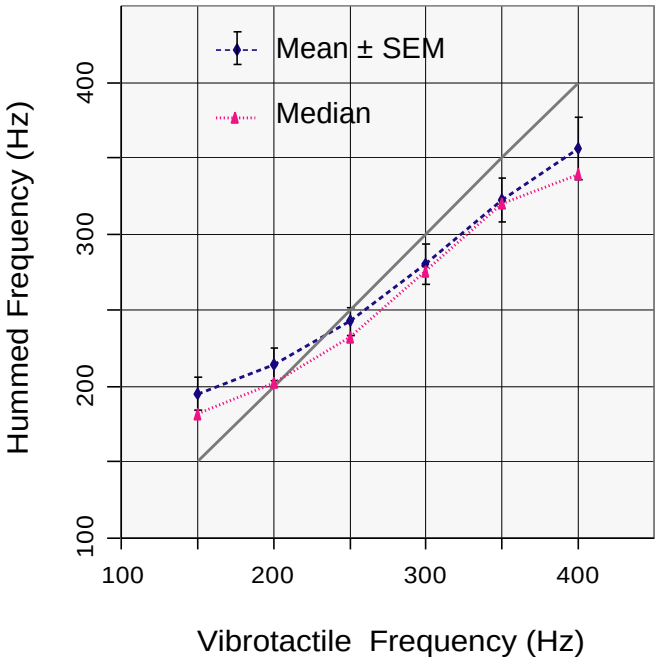

Fig. 4.7 Mean ± SEM and median of the frequency hummed by the subjects as a function of the frequency of the vibrotactile stimulus. The grey line represents equal values for humming and for vibrotactile stimulus. Adapted from Caetano and Jousmäki (Submitted).

The results indicate a clear transfer of frequency information from touch to vocal utterances in normal-hearing subjects. The results were very similar when analyzed with the software Praat. Overestimation occurred at low frequencies and underestimation at high frequencies.

In summary, information is transferred from touch to motor output. Neural correlates of such process could involve SI, SII, and auditory areas.

4.5 1st and 3rd persons motor cortices stabilize similarly (Study V)

The goal of this study was to monitor sensorimotor oscillatory activity, by means of whole-scalp MEG, to find similarities between own, observed, and heard motor actions.

Experimental setup

The experiment consisted of five conditions (Figure 4.8a), in which the subject (*i*) was at rest, (*i*) tapped a drum membrane with the right index finger (*Own Action*), (*iii*) tapped a drum membrane without listening to the drum-related sound (*Own Action No Sound*), (*iv*) observed similar action performed by another person (*Observation*), or (*v*) heard the drum-related action (*Drum Sound*).

The tapping intervals varied from 3 to 6 s for individual subjects, and from 4 to 5 s for the experimenter. On average, 91 epochs of spontaneous activity were collected per condition. From the original set of 25 subjects, we selected 13 who showed a clear ~20-Hz reactivity—at least 10fT/cm—after *Own Action*.

Results

Modulation of the ~20-Hz oscillatory activity was clearly visible in the raw data, for both *Own Action* and *Observation*, as is shown in Figure 4.8b; the level of the ~20-Hz oscillations increased within 1 s after each action event (done or observed), while EMG activity was only visible for own actions. Also, we confirmed previous results on the location of ~20-Hz and ~10-Hz oscillations, in M1 and SI cortices respectively (Figure 4.8c).

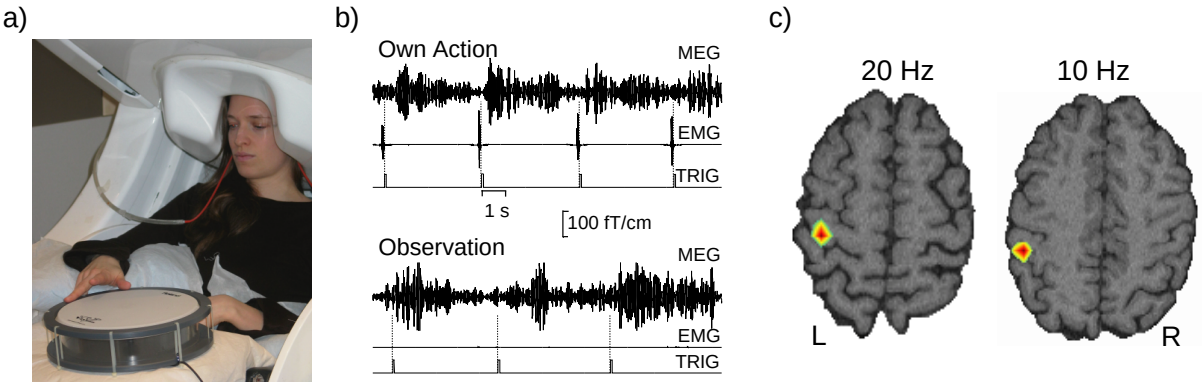

Fig. 4.8 Experimental setup, reactivity of the MEG signals and source locations of rhythmic activity in a representative subject (note: MEG signals and sources do not belong to the person in the figure). a) The subject is tapping the drum membrane with her right index finger, while looking at her hand. b) MEG ~20-Hz oscillations from a representative channel over the left motor cortex, EMG activity from the right first interosseous muscle, and the trigger (TRIG) from the drum, during *Own Action* and *Observation* conditions. c) Density plot of the ~20-Hz and ~10-Hz sources, located in M1 and SI cortices, respectively (software inbuilt at the Brain research Unit by Jan Kujala). The ECDs for ~20-Hz and ~10-Hz oscillations were modeled for *Own Action* from single epochs between 0.5–2.0 s after the drum tap. Adapted from Caetano, Jousmäki, and Hari (2007).

Figure 4.9 illustrates the average TSE across the 13 subjects selected. The level of the ~20-Hz oscillations began to decrease about 2 s before the subject tapped the drum (*Own Action*, *Own Action No Sound*) and about 0.8 s before the subject observed another person perfom the same action (*Observation*). The maximum suppression occurred ~150 ms after the tap, and it was followed by an increase in intensity that peaked at approximately 600 ms. The value of maximum suppression for the *Observation* condition was only 42 ± 9% of that

during *Own Action* ($P < 0.005$), and no statistically significant differences were observed between *Own Action* and *Own Action No Sound*. There was a clear rebound for the *Action Sound* condition, but suppression was not identified. In all four conditions, no systematic differences were found in rebound amplitude, rebound onset, or peak latencies.

Similarly, the level of the ~10-Hz oscillations started to decrease about 1.8 s before own actions, whereas such a decrease in *Observation* and *Drum Sound* conditions only occured after the tap. The suppression reached its maximum at ~270 ms, in all four conditions, followed by a tiny rebound that peaks ~600 ms later for own actions compared to observed conditions; however the rebound did not reach statistical significance in any of the conditions. Again, no difference in maximum suppression latency was observed between conditions, and suppression during *Observation* was only 46 ± 16% ($P < 0.05$) of that during *Own Action*.

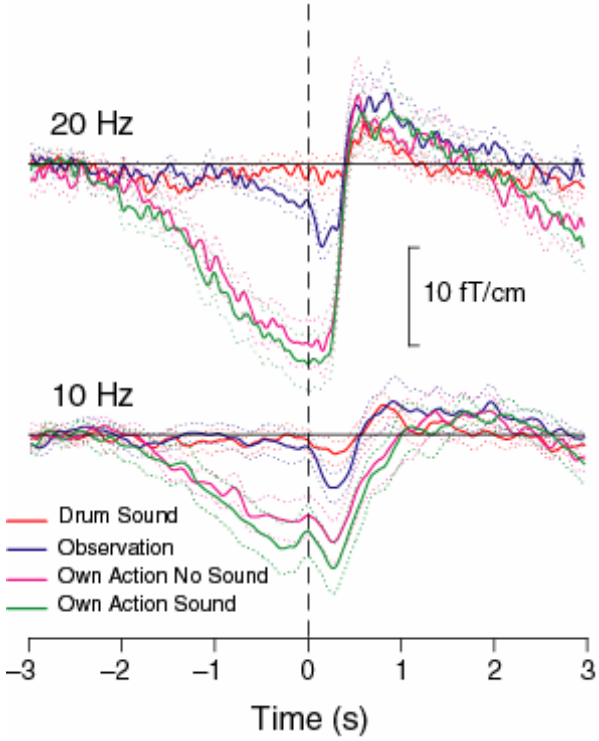

Fig. 4.9 Results obtained from TSE analysis in the selected group of 13 subjects, with baseline applied from –2.9 to –2.4 s. The curves represent the mean ± SEM level (solid and dotted lines, respectively) for ~20- and ~10-Hz oscillations, in all four conditions. Adapted from Caetano, Jousmäki, and Hari (2007).

Similar results were seen in TFRs (Fig 4.10). Rebounds for the ~20-Hz oscillations were observed in all conditions, but they were weaker for *Observation* and *Drum Sound*. The ~10-Hz level returns back to baseline later than the ~20-Hz level in *Own Action* conditions, in contrast to *Observation* and *Drum Sound* conditions.

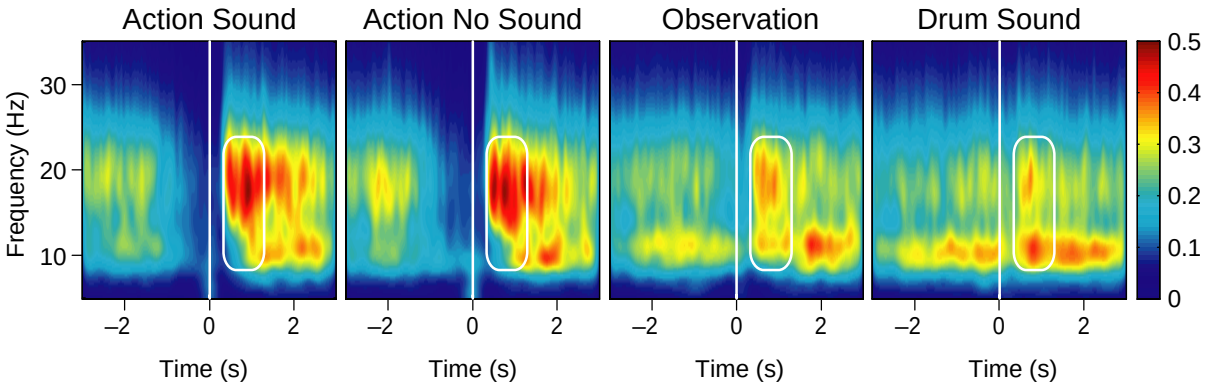

Fig. 4.10 Average TFRs calculated from the selected group of 13 subjects, in [–3, 3] s time window, and [5, 35] Hz frequency range; the color bar indicates the amplitude scale $(fT/cm)^2$. Adapted from Caetano, Jousmäki, and Hari (2007).

Conclusion

In summary, both M1 and SI cortices (main generators of the ~20- and ~10-Hz oscillations, respectively) were activated when the subjects performed or observed similar hand actions. The ~20-Hz post-movement rebound, indicative of M1 stabilization, peaked at about the same time after performed, observed, or heard actions. In addition, activation of the M1 cortex started much earlier for self-performed than observed actions, and in the latter case was indicative of action prediction. Besides the similarities in M1 neural mechanisms, we also showed that the ~10-Hz oscillations returned ~600 ms later to base-level during own than observed actions; this difference suggests that afferent somatosensory input influences the modulation of SI rhythmic activity. Thus, SI modulation in observation conditions (with no afferent input) suggests that during motor simulation of the observed act, reciprocal cortical connections between M1 and SI cortices play a role in SI activation—which might indicate simulation of sensory consequences of the referred action. Overall, our data suggest the importance of M1 for understanding other's actions and that besides having weaker activations in M1 during observed actions, the somatosensory cortex may play an important role in distinguishing self from others on the basis of sensory and proprioceptive feedback.

5 General Discussion

The studies in this thesis focus on audiotactile integration, brain processing of vibrotactile information, and sensorimotor reactivity during own and observed actions.

We identified and quantified integration of vibrotactile and auditory information in a loudness-matching task. At low sound–intensity levels, hearing was facilitated by about 12% by simultaneous presentation of vibrotactile information with the same frequency (Study I). This effect clearly demonstrates integration between the two senses. The corresponding neural correlates may be found in auditory areas (Studies II and III).

In Study II, we characterized, by means of whole-scalp MEG, brain activation sequences elicited by vibrotactile stimuli, showing activation of auditory areas in association with the illusory sound perception by touch. Study III defined more accurately the auditory belt areas that were co-activated by vibrotactile and auditory stimuli, and to a lesser extent by pulsed-tactile and auditory stimuli. In agreement with the close connections between vibrotactile and auditory stimuli, the frequency of the vibrotactile information was transferred to vocal utterances with great efficiency, as was demonstrated in normal-hearing female adults (Study IV). Finally, Study V showed similarities between performed vs. seen or heard actions, and demonstrated for the first time that *i)* both visual and auditory action perception are transformed into internal motor representations of the same action, *ii)* the primary motor cortex stabilizes similarly in actor's and observer's brain, and that *iii)* the problem of attribution of agency may partially be solved by the presence or absence of proprioceptive input.

5.1 Methodological considerations

Auditory contamination

Vibrotactile stimuli elicited by a blind-ended silicone tube may produce faint sound. For this reason, different strategies were used in each study. First, in Studies I–IV we presented very weak vibrotactile stimuli, at about 19–28 dB above the tactile sensation level. Second, in both behavioural experiments (Studies I and IV), auditory masking was successfully achieved with white noise at about 60 dB and 80 dB above hearing sensation level, respectively. Furthermore, in Study IV, the subjects reported difficulty in performing the humming task due to lack of auditory feedback.

In Studies II and III, we used a double-tube setup, with the *no-touch* tube as a control for any possible auditory contamination. In Study II, the clear absence of MEG responses for the *no-touch* tube stimulation indicated that responses from the *touch* tube stimulation were transmitted via touch and not via hearing. We performed control measurements in which *(i)* no evoked responses were elicited when the subject did not touch any tube, and *(ii)* no significant difference occurred in the evoked responses when the roles of the *touch* and *no-touch* tubes were reversed. In Study III, the double-tube setup proved as effective, as no activations were found when control subjects did not touch any tube.

In addition, the perception of a sound when low-intensity vibrotactile stimuli are applied to fingertips is not caused by bone conduction but rather results from auditory imagery. Extensive work in occupational health and safety has shown that above 150 Hz, vibrations are not effectively transmitted beyond the hand, because the energy is dissipated in hand and finger tissues (Griffin, 1990; Bovenzi, 1998; Dong et al., 2005).

Additionally, we performed control recordings with vibrotactile stimulation, on two occasions, on a patient with right median-nerve injury (unpublished data). The first and

second recordings were conducted 7.5 weeks and 9 months after the injury, respectively. The clinical state of the patient was the same in both measurements: sensation had been recovered at the thenar (from wrist to mid-palm), but not in the palmar side of thumb, index, and middle fingers. During the first measurement, vibrotactile stimulation was applied over distal fingers, onto the intermediate phalanges, whereas during the second measurement, only the fingertips were stimulated. In both measurements, vibrotactile stimulation of normally sensing fingers elicited clear MEG responses at ~65 ms over the contralateral SI cortex, and at about 140 ms and 165 ms over left parietotemporal areas.

When the non-sensing fingers were stimulated, no clear SI responses were observed. During the first measurement, the subject reported sensation of the stimulation on the palm of the hand, and a low-amplitude response peaked at ~280 ms over left parietotemporal areas. During the second measurement, the subject reported no sensation and no MEG responses were observed. Furthermore, the subject reported perceiving a sound only when the normally-sensing fingers were stimulated. These results demonstrate that the vibration was attenuated in the tissues of fingers and hand, and that activation of parietotemporal areas is due to transmission of information by peripheral mechanoreceptors.

In Studies II and III, the auditory cortex was activated in response to 500-ms vibrotactile stimuli under passive conditions, i.e. when subjects attended to the stimuli without any further task. A recent MEG study, showed the influence of attention on identifying SII and auditory areas in response to 20–30 ms vibrotactile stimuli (Iguchi et al., 2007). Therefore, a stricter control of attention may have helped in identifying the sites of activation in Studies II and III.

Effect of baseline on MEG signals

In Study V, subjects predicted the observed actions, so the selection of a baseline had to exclude prediction in the observer's brain or movement preparation in the actor's brain. This led to selection of the base-level from –2.9 to –2.4 s prior to tapping the drum. This baseline was sometimes influenced by the former rebound, and thus rebound amplitudes may be underestimated for own actions.

Prediction of observed actions was possible because they occurred more or less regularly, with about 4–5 s intervals. In contrast to the study by Kilner et al. (2004), in which the observed movements were totally predictable with the presentation of a visual cue 1.5 s prior to the movement, our experimental setup had some variability on the time of the observed action. This factor has likely slightly weakened and delayed the ~20-Hz suppression.

Group analysis of fMRI data

The group analysis of Study III had some limitations. The goal was to obtain an accurate estimate of cortical areas co-activated by both auditory and tactile stimuli. Group analysis identified left-hemispheric vibrotactile-auditory co-activation in auditory belt area, but not in the right hemisphere. This result reflects, at least in part, higher inter-subject variability in the location of the co-activation area in the right hemisphere. Improvement of the group analysis can be achieved by surface-based normalization of individual subject anatomical data, instead of normalizing EPI images to EPI templates. Nevertheless, we were able to identify bilaterally, at the single-subject level, vibrotactile-auditory co-activation in auditory belt areas with good accuracy.

5.2 From Pacinian corpuscles to auditory cortex

Vibrotactile and auditory stimuli have essentially similar temporal patterns, and this similarity may be at the basis of integration processes between the two sensory modalities. Pacinian corpuscles are the only adequate mechanoreceptors able to assess this similarity, as their lowest sensitivity threshold is at 200–300 Hz for skin indentation in the µm range. Study II showed activation of auditory areas by vibrotactile stimulation at relatively early stages of cortical processing. This complements the results obtained in a congenitally deaf subject (Levänen et al., 1998), at the time interpreted by the authors as the result of cross-modal plasticity. Thus, the auditory cortex is implicated in the analysis of some temporal properties of somatosensory stimuli.

Importantly, our results agree with other studies, both in timing and location of areas activated by vibrotactile stimuli (Foxe et al., 2000; Kayser et al., 2005; Murray et al., 2005; Iguchi et al., 2007; Singh et al., 2007). The observed latencies of activation in auditory and SII cortices by vibrotactile stimuli (Study II), peaking at about 100 to 200 ms, were confirmed by Igushi et al. (2007). These findings differ slightly on the timing of audiotactile integration in auditory areas, strongest at ~80 ms and ~50 ms, as identified with EEG by Foxe et al. (2000) and Murray et al. (2005), respectively. These studies do not contradict, but rather complement each other. In Study II, we aimed at finding neuronal dynamics of vibrotactile processing rather than interaction effects.

The results in Study III agree nicely with two fMRI studies. The first study (Kayser et al., 2005), with fMRI and electrophysiological recordings in anaesthetized monkeys, showed audiotactile integration in posterior belt areas, in the same area identified in Study III. In addition, a more recent study (Singh et al., 2007) with deaf and normal-hearing subjects further confirmed the auditory area activated by vibrotactile stimuli.

However, an important question remains open: How does somatosensory or vibrotactile information reach the auditory belt areas? Recent neuroanatomical studies with retrograde tracers in macaque monkey (Hackett et al., 2007; Smiley et al., 2007) have shown thalamic and cortical sources of auditory and somatosensory input to the caudal auditory cortex.

Thalamic projections to caudal auditory areas arose mainly from nuclei of the MGC and multisensory nuclei of the posterior thalamus (Figure 5.1): posterior nucleus, suprageniculate, limitans, and medial pulvinar (Hackett et al., 2007). Interestingly, projections from the ventroposterior complex were absent in caudal auditory belt areas, suggesting that somatosensory relay nuclei do not contribute significantly to somatosensory input (de la Mothe et al., 2006; Hackett et al., 2007).

Similarities in auditory and somatosensory cortical inputs were found for CL and CM (Smiley et al., 2007). Candidate cortical sources of somatosensory input include areas that are primarily somatosensory (retroinsular cortex, granular insula), as well as areas of multisensory integration (temporal parietal occipital and temporal parietotemporal areas). Moreover, the overall pattern of connections suggests that besides CM, auditory-somatosensory integration may be a general feature of caudal auditory belt areas, Tpt, and Ri (Smiley et al., 2007).

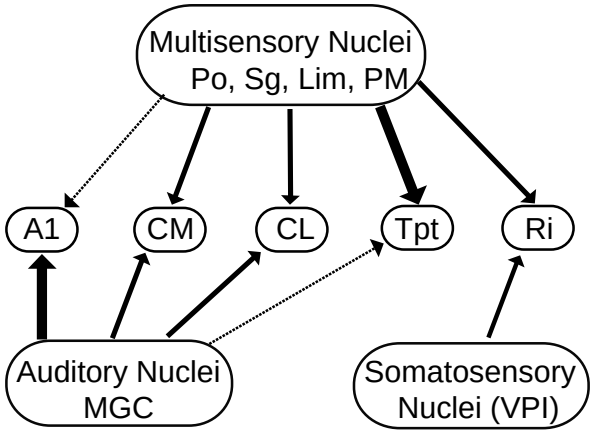

Fig. 5.1 Thalamocortical inputs to A1, CM, CL, Tpt, and Ri. Thick lines denote major connections. MGC = medial geniculate complex; VPI = inferior division of the ventroposterior nucleus; Po = posterior nucleus; Sg = suprageniculate nucleus; Lim = limitans nucleus; PM = medial pulvinar. Adapted from Hackett et al. (2007).

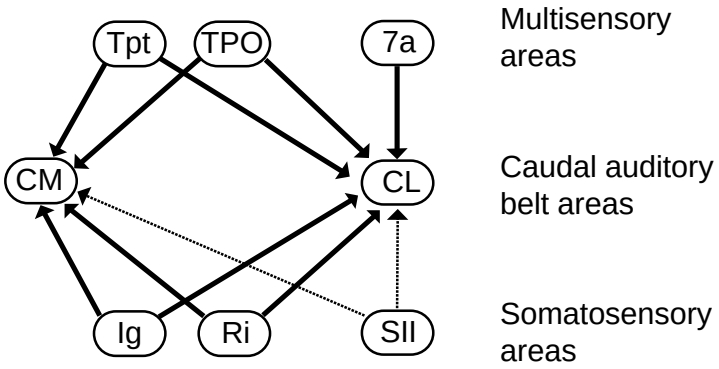

Fig. 5.2 Possible sources of somatosensory input to caudal auditory belt areas (CM and CL) in macaque monkey. Thick lines denote major connections. Tpt = temporal parietotemporal area; TPO = temporal parietal occipital area; 7a = parietal area 7a; Ig =granular insular cortex; Ri = retroinsular area; SII = secondary somatosensory cortex. Adapted from Smiley et al. (2007).

In summary, a growing set of evidence suggests that the neocortex has major multisensory processing features. Caudal auditory cortex and adjacent areas seem to form a network involved in multisensory processing, characterized by weighted inputs from thalamic nuclei and neighboring cortical areas. Whether similar networks and processing frames are found in the human brain is still an open question. Usually homology between different species is not straightforward, but these recent works suggest that vibrotactile input to human auditory areas may project from multisensory thalamic nuclei or adjacent somatosensory and multisensory areas. Nevertheless, understanding the multisensory processing in the human brain still faces many open questions.

5.3 Primary motor cortex vs. mirror-neuron system

Probing the functional state of M1 with MEG

The magnetic μ rhythm is generated in motor (including SMA proper) and somatosensory areas, with ~20-Hz and ~10-Hz components receiving strong contributions from M1 and SI, respectively. Several findings suggest that the ~20-Hz post-movement rebound is associated with increased cortical inhibition and thereby stabilization of the M1

cortex. On the other hand, suppression of the ~20-Hz rhythmic activity is associated with increased excitability of the M1 cortex, which can be due to either an increase in excitatory input or decrease in inhibition. In MEG, the ~20-Hz rebound occurs after both passive movements elicited by electric median nerve stimuli and voluntary finger movements (Salmelin and Hari, 1994; Salenius et al., 1997b). Accordingly, a TMS study showed reduced motor-cortex excitability during the ~20-Hz rebound (Chen et al., 1999).

Coherence is observed between motor-cortex ~20-Hz rhythmic activity and surface electromyogram during isometric contractions (Salenius et al., 1997a; Kilner et al., 2000; Kilner et al., 2003). This cortex-muscle coherence is typically abolished or reduced in the beginning of a movement, and prominent during static phases of motor tasks, such as steady muscle contraction after the end of a phasic movement. Intraoperative cortical stimulation of the cortical site of cortex-muscle coherence, preoperatively determined, supports the generation of the ~20-Hz activity mainly in the M1 cortex (Mäkelä et al., 2001). The increase of the ~20-Hz level after administration of GABAergic benzodiazepine (an inhibitor) (Jensen et al., 2005) and during immobility (for a review, see Niedermeyer, 2005), further supports stabilization of the M1 cortex during enhanced 20-Hz activity. A combined TMS and MEG study in patients with congenital hemiparesis also showed that the ~20-Hz cortex-muscle coherence originated from the contralesional M1 (Gerloff et al., 2006).

Therefore, the ~20-Hz rebound seems to be associated with M1 stabilization and cortical inhibition. Thus, reactivity of the ~20-Hz rhythm is a good probe for the functional state of M1 cortex. Reactivity of the ~10-Hz rhythm may follow similar physiology, thus indicating the functional state of SI cortex.

M1 as part of human mirror-neuron system

The core area, or orchestrator, of the human MNS is the inferior frontal gyrus—Broca's region in the left hemisphere and its right hemisphere homologue. Reactivity of the IFG can be reflected in the functional state of M1, which is anatomically downstream in motor processing. Activation of human M1 cortex during both observation and execution of motor tasks has been extensively demonstrated (Hari et al., 1998a; Nishitani and Hari, 2000; Järveläinen et al., 2001; Babiloni et al., 2002; Nishitani and Hari, 2002; Järveläinen et al., 2004). In this thesis, Study V showed for the first time human M1 reactivity when actions are heard, complementary to the finding of audiovisual mirror-neurons in monkey area F5 (Kohler et al., 2002; Keysers et al., 2003).

Despite major evidence for human M1 reactivity after performed, observed, or heard movements, no studies to date have reported mirror-neurons in monkey area F1 corresponding to the human M1 cortex (Kilner and Frith, 2007). Therefore, lack of agreement exists on whether M1 is part of the MNS. On one hand, M1 activation can be considered as a consequence of reciprocal cortico-cortical connections with premotor areas (Luppino and Rizzolatti, 2000; Rizzolatti and Luppino, 2001; Dum and Strick, 2005), or as a sign of functional activity during action observation, as has been demonstrated with MEG (Hari et al., 1998a; Nishitani and Hari, 2000; Järveläinen et al., 2001; Järveläinen et al., 2004; Nishitani et al., 2004; Kilner and Frith, 2007). Kilner and Frith (2007), in their commentary to Study V, advanced that M1 activity during action observation may be related to the coding of actions in an intrinsic framework, which may also be necessary to decode observed action (Kakei et al., 2001; Kurata and Hoshi, 2002; Kakei et al., 2003; Kilner and Frith, 2007; Umiltà et al., 2007). The work presented in this thesis adds to a set of studies that suggest an active functional role for M1 in action understanding.

5.4 Agency attribution

According to Mead's *"Social Behaviorism"*, the mind and the self are beyond the neurophysiology of the organic individual, but rather emerge out of the dynamic, ongoing social process (Mead, 1934). The interaction of the organism with the social environment structures the self perspective by means of intersubjective and agency processes, as for example verbal and non-verbal communication. On the other hand, the assumption of the Theory of Mind seeks to explain the ability to understand and predict actions and mental states (thoughts, beliefs, feelings) of both the self (1st person) and the other (3rd person). Shared states of mind between the 1st and the 3rd person are assumed to allow the 1st person to covertly mimic the mental activity of the 3rd person.

The discovery of mirror neurons in the macaque monkey provided a neurophysiological model to the understanding of actions performed by others (Gallese et al., 1996; Rizzolatti and Craighero, 2004). Within this framework, the 1st person simulates internally the motor actions performed by the 3rd person, a process at the basis of motor action understanding and even prediction of other people's goal-directed movements (Hari and Nishitani, 2004; Kilner et al., 2004; Rizzolatti and Craighero, 2004). Hereupon, since the human MNS is active during both 1st and 3rd persons' motor actions, it begs the question whether it can disentangle self and other.

Recent fMRI, PET, TMS, behavioral, MEG and EEG studies have approached the problem of agency. Ruby and Decety (2001), by means of PET, showed that during action-simulation tasks both 1st and 3rd person perspectives recruited SMA, the precentral gyrus, the precuneus, and the MT/V5 complex. The 1st person perspective revealed specific activations in the left inferior parietal and somatosensory cortices, suggesting their involvement in the sense of agency.

A transcranial magnetic stimulation study in which subjects performed active and passive finger extension movements while wearing a Cyber Glove assessed the awareness of movement onset by the participants. It showed the importance of the superior temporal lobule, an integration area of visual and somatosensory inputs to motor outputs, for the sense of agency (MacDonald and Paus 2003). Vogeley and colleagues (2004), on the other hand, found by means of fMRI that when subjects count the number of objects presented in a virtual scene in both 1st and 3rd person perspectives, activation in mesial cortical areas increases during the 1st person perspective; this area thereby could play an important role in the definition of self. A later fMRI study (Jackson et al., 2006) compared imitation vs. observation of intransitive hand and foot actions, in both 1st and 3rd person perspectives, and showed that the sensory-motor cortex is involved in the sense of agency.

Finally, similarities between 1st and 3rd person perspectives have been found before and during motor actions, both in behavior and in motor-cortex reactivity. First, in an MEG study made during manipulative finger movements, the motor cortex was activated in both the viewer's and in the actor's brain, although less intensively in the former (Hari et al., 1998a). Second, during attentive observation of well predictable hand movements, the eye fixations of the viewer preceded locations of the actor's hand, similar to the actor's eye fixations (Flanagan and Johansson, 2003). Third, pre-movement EEG activation was identified in the viewer's brain, similar to, although weaker than, in the actor's brain (Kilner et al., 2004).

Concepts of the neural correlates of agency have yet to be fully unified, and the extent of the differences between human MNS and monkey mirror neurons remains open. The experimental condition or life situation defines how the MNS is activated: while observing other people's actions the observer simulates the action without any proprioceptive input, whereas efference copies and proprioceptive input are available during own movements. Modulation of SI and SII activity by imagined and observed movements has previously been shown (Avikainen et al., 2002; Hasson et al., 2004; Möttönen et al., 2005). A possible route

for SI activation, besides direct somatosensory input, is via reciprocal cortical connections between pre- and postcentral cortices. This thesis adds to the importance of proprioceptive input in agency attribution, suggesting that its presence prolongs modulation of the ~10-Hz sensorimotor cortical activity. Testing this hypothesis would be important for better understanding clinical situations in which agency is misattributed.

6 Concluding remarks

This thesis comprises five studies, dealing with behavioral correlates of audiotactile integration (Study I) and information transfer between touch and motor output (Study IV), neuroimaging assessment of brain activation sequences and localization of areas activated by vibrotactile stimuli (Studies II and III), and finally neuromagnetic characterization of rhythmic activity during performed, seen, and heard actions (Study V).

The multimodal approach in this work, from behavior to neuroimaging, has added value. It is of central importance to find behavioral evidence of effects one may want to explore with neuroimaging techniques; as such the experimental paradigms will benefit. Moreover, combining methodological approaches, such as MEG and fMRI, enables complementary information on the underlying brain processes to be gathered, with good temporal and spatial accuracy, respectively.

Auditory areas were shown to participate in processing frequency information conveyed by Pacinian corpuscles. How the information reaches the auditory system of normal-hearing adults is not yet well understood. Future studies may unravel neural correlates of vibrotactile input to the human auditory system.

Motor and sensory properties of actions, whether performed, observed, or heard, modulate the reactivity of the sensorimotor μ rhythm. In addition, distinguishing between self and others may include presence vs. absence of somatosensory and proprioceptive input. Defining how brain processing relates to the sense of agency is of main importance to better understand clinical situations in which agency is misattributed.

In summary, this work presents novel findings on multisensory processing—a small step in the overall understanding of the human brain.

7 Bibliography

Ahveninen J, Jääskeläinen I, Raij T, Bonmassar G, Devore S, Hämäläinen M, Levänen S, Lin F, Sams M, Shinn-Cunningham B, Witzel T, Belliveau J: Task-modulated "what" and "where" pathways in human auditory cortex. Proc Natl Acad Sci USA 2006, 103: 14608–14613.

Alary F, Simões C, Jousmäki V, Forss N, Hari R: Cortical activation associated with passive movements of the human index finger: an MEG study. NeuroImage 2002, 15: 691–696.

Attwell D, Iadecola C: The neural basis of functional brain imaging signals. Trends Neurosci 2002, 25: 621–625.

Avikainen S, Kulomäki T, Hari R: Normal movement reading in Asperger subjects. NeuroReport 1999, 10: 3467–3470.

Avikainen S, Forss N, Hari R: Modulated activation of the human SI and SII cortices during observation of hand actions. NeuroImage 2002, 15: 640–646.

Avikainen S, Wohlschläger A, Liuhanen S, Hänninen R, Hari R: Impaired mirror-image imitation in high-functioning autistic subjects. Curr Biol 2003, 13: 339–341.

Aziz-Zadeh L, Iacobini M, Zaidel E, Wilson S, Mazziota J: Left hemisphere motor facilitation in response to manual action sounds. Eur J Neurosci 2004, 19: 2609–2612.

Babiloni C, Babiloni F, Carducci F, Cincotti F, Cocozza G, Del Percio C, Moretti D V, Rossini P M: Human cortical electroencephalography (EEG) rhythms during the observation of simple aimless movements: A high-resolution EEG study. NeuroImage 2002, 17: 559–572.

Bandettini P, Wong E, Hinks R, Tikofsky R, Hyde J: Time course EPI of human brain function during task activation. Magn Res Med 1992, 25: 390–397.

Bloch F, Hansen W, Packard M: Nuclear induction. Phys Rev 1946, 69: 127.

Bovenzi M, Hand-transmitted Vibration. In: Encyclopaedia of Occupational Health and Safety (ed. Stellman, J. M.), Vol. II, 4th edn, 1998. International Labour Organization.

Brenner D, Williamson S, Kaufman L: Visually evoked magnetic fields of the human brain. Science 1975, 190: 480–482.

Brenner D, Lipton J, Kaufman L, Williamson S: Somatically evoked magnetic fields of the human brain. Science 1978, 199: 81–83.

Buccino G, Binkofski F, Fink G R, Fadiga L, Fogassi L, Gallese V, Seitz R J, Zilles K, Rizzolatti G, Freund H J: Action observation activates premotor and parietal areas in a somatotopic manner: an fMRI study. Eur J Neurosci 2001, 13: 400–404.

Caetano G, Jousmäki V: Evidence of vibrotactile input to human auditory cortex. NeuroImage 2006, 29: 15–28.

Caetano G, Jousmäki V, Hari R: Actor's and observer's primary motor cortices stabilize similarly after seen or heard motor actions. Proc Natl Acad Sci USA 2007, 104: 9058–9062.

Caetano G, Jousmäki V: Kenneth, what's the frequency? Submitted.

Calvert G, Spence C, Stein B, The Handbook of Multisensory Processes, 1st edn, 2004. The MIT Press, Cambridge, Massachusetts.

Caspers S, Geyer S, Schleicher A, Mohlberg H, Amunts K, Zilles K: The human inferior parietal cortex: Cytoarchitectonic parcellation and interindividual variability. NeuroImage 2006, 33: 430–448.

Chen R, Corwell B, Hallett M: Modulation of motor cortex excitability by median nerve and digit stimulation. Exp Brain Res 1999, 129: 77–86.

Cohen D: Magnetoencephalography: Detection of the brain's electrical activity with a superconducting magnetometer. Science 1972, 175: 664–666.

de la Mothe L, Blumell S, Kajikawa Y, Hackett T: Thalamic connections of auditory cortex in marmoset monkeys: core and medial belt regions. J Comp Neurol 2006, 496: 72–96.

Decety J, Chamanide T, Grèzes J, Meltzoff A: A PET exploration of the neural mechanisms involved in reciprocal imitation. NeuroImage 2002, 15: 265–272.

di Pellegrino G, Fadiga L, Fogassi L, Gallese V, Rizzolatti G: Understanding motor events: a neurophysiological study. Exp Brain Res 1992, 91: 176–180.

Dong R, Wu J, Welcome D: Recent advances in biodynamics of human hand-arm system. Ind Health 2005, 43: 449–471.

Dum R, Strick P: Frontal lobe inputs to the digit representations of the motor areas on the lateral surface of the hemisphere. J Neurosci 2005, 9: 1375–1386.

Eickhoff S, Stephan K, Mohlberg H, Grefkes C, Fink G, Amunts K, Zilles K: A new SPM toolbox for combining probabilistic cytoarchitectonic maps and functional imaging data. NeuroImage 2005, 25: 1325–1335.

Eickhoff S, Amunts K, Mohlberg H, Zilles K: The human parietal operculum. II. Stereotaxic maps and correlation with functional imaging results. Cereb Cortex 2006a, 16: 268–279.

Eickhoff S, Schleicher A, Zilles K, Amunts K: The human parietal operculum. I. Cytoarchitectonic mapping of subdivisions. Cereb Cortex 2006b, 16: 254–267.

Eickhoff S, Paus T, Caspers S, Grosbras M-H, Evans A, Zilles K, Amunts K: Assignment of functional activations to probabilistic cytoarchitectonic areas revisited. NeuroImage 2007, 36: 511–521.

Fabri M, Polonara G, Quattrini A, Salvolini U, Del Pesce M, Manzoni T: Role of corpus callosum in the somatosensory activation of the ipsilateral cerebral cortex: an fMRI study of callosotomized patients. Eur J Neurosci 1999, 11: 3983–3994.

Fadiga L, Fogassi L, Pavesi G, Rizzolatti G: Motor facilitation during action observation: A magnetic stimulation study. Eur J Neurosci 1995, 11: 3983–3994.

Falchier A, Clavagnier S, Barone P, Kennedy H: Anatomical evidence of multimodal integration in primate striate cortex. J Neurosci 2002, 22: 5749–5759.

Farrer C, Franck N, Frith C D, Decety J, Georgieff N, d'Amato T, Jeannerod M: Neural correlates of action attribution in schizophrenia. Psychiatry Res 2004, 131: 31–44.

Ferrari P, Gallese V, Rizzolatti G, Fogassi L: Mirror neurons responding to the observation of ingestive and communicative mouth actions in the monkey ventral premotor cortex. Eur J Neurosci 2003, 17: 1703–1714.

Flanagan J, Johansson R: Action plans used in action observation. Nature 2003, 424: 769–771.

Fogassi L, Gallese V, Fadiga L, Luppino G, Matelli M, Rizzolatti G: Coding of peripersonal space in inferior premotor cortex (area F4). J Neurophysiol 1996, 76: 141–157.

Fogassi L, Gallese V, Fadiga L, Rizzolatti G: Neurons responding to the sight of goal directed hand/arm actions in the parietal area PF (7b) of the macaque monkey. Soc Neurosci abstr 1998, 24: 257.255.

Fogassi L, Ferrari P, Gesierich B, Rozzi S, Chersi F, Rizzolatti G: Parietal lobe: From action organization to intention understanding. Science 2005, 308: 662–667.

Forss N, Jousmäki V: Sensorimotor integration in human primary and secondary somatosensory cortices. Brain Res 1998, 781: 259–267.

Forss N, Hietanen M, Salonen O, Hari R: Modified activation of somatosensory cortical network in patients with right-hemisphere stroke. Brain 1999, 122: 1889–1899.

Foxe J J, Morocz A I, Murray M M, Higgins B A, Javitt D C, Schroeder C E: Multisensory auditory–somatosensory interactions in early cortical processing revealed by high–density electrical mapping. Cognit Brain Res 2000, 10: 77–83.

Foxe J J, Wylie G, Martinez A, Schroeder C, Javitt D, Guilfoyle D, Ritter W, Murray M: Auditory-somatosensory multisensory processing in auditory association cortex: an fMRI study. J Neurophysiol 2002, 88: 540–543.

Fu K-M G, Johnston T, Shah A, Arnold L, Smiley J, Hackett T, Garraghty P, Schroeder C: Auditory cortical neurons respond to somatosensory stimulation. J Neurosci 2003, 23: 7510–7515.

Gallese V, Fadiga L, Fogassi L, Rizzolatti G: Action recognition in the premotor cortex. Brain 1996, 119: 593–609.

Garraghty P, Florence S, Tenhula W, Kaas J: Parallel thalamic activation of the first and second somatosensory areas in prosimian primates and tree shrews. J Comp Neurol 1991, 311: 289–299.

Gentilucci M, Fogassi L, Luppino G, Matelli M, Camarda R, Rizzolatti G: Functional organization of inferior area 6 in the macaque monkey. I. Somatotopy and the control of proximal movements. Exp Brain Res 1988, 71: 475–490.

Gerloff C, Braun C, Staudt M, Hegner L Y, Dichgans J, Krägeloh-Mann I: Coherent corticomuscular oscillations originate from primary motor cortex: evidence from patients with early brain lesions. Hum Brain Mapp 2006, 27: 789–798.

Gescheider G, Bolanowski S, Pope J, Verrillo R: A four-channels analysis of the tactile sensitivity of the fingertip: frequency selectivity, spatial summation, and temporal summation. Somato Motor Res 2002, 19: 114–124.

Gescheider G, Bolanowski S, Verillo R: Some characteristics of tactile channels. Behav Brain Res 2004, 148: 35–40.

Geyer S, Schleicher A, Zilles K: Areas 3a, 3b, and 1 of human primary somatosensory cortex. Part 1: Microstructural organization and interindividual variability. NeuroImage 1999, 10: 63–83.

Geyer S, Schormann T, Mohlberg H, Zilles K: Areas 3a, 3b, and 1 of human primary somatosensory cortex. Part 2: Spatial normalization to standard anatomical space. NeuroImage 2000, 11: 684–696.

Gobbelé R, Schürmann M, Forss N, Juottonen K, Buchner H, Hari R: Activation of the human posterior parietal and temporoparietal cortices during audiotactile interaction. NeuroImage 2003, 20: 503–511.

Grafton S, Fadiga L, Arbib M, Rizzolatti G: Premotor cortex activation during observation and naming of familiar tools. NeuroImage 1997, 6: 231–236.

Graziano M, Yap G, Gross C: Coding of visual space by premotor neurons. Science 1994, 11: 1054–1057.

Graziano M, Hu X, Gross C: Visuo-spatial properties of ventral premotor cortex. J Neurophysiol 1997, 77: 2268–2292.

Grefkes C, Geyer S, Schormann T, Roland P, Zilles K: Human somatosensory area 2: Observer-independent cytoarchitectonic mapping, interindividual variability, and population map. NeuroImage 2001, 14: 617–631.

Grèzes J, Costes N, Decety J: The effects of learning and intention on the neural network involved in the perception of meaningless actions. Brain 1999, 122: 1875–1887.

Griffin M J, Handbook of Human Vibration, 1990. Elsevier Academic Press.

Gross J, Kujala J, Hämäläinen M, Timmermann L, Schnitzler A, Salmelin R: Dynamic imaging of coherent sources: Studying neural interactions in the human brain. Proc Natl Acad Sci USA 2001, 98: 688–693.

Guest S, Catmur C, Lloyd D, Spence C: Audiotactile interactions in roughness perception. Exp Brain Res 2002, 146: 161–171.

Guyton A, Hall J, Textbook of Medical Physiology, 9th edn, 1996. WB Saunders Co.

Hackett T, Stepniewska I, Kaas J: Subdivisions of auditory cortex and ipsilateral cortical connections of the parabelt auditory cortex in macaque monkeys. J Comp Neurol 1998, 394: 475–495.

Hackett T, Preuss T, Kaas J: Architectonic identification of the core region in auditory cortex of macaques, chimpanzees, and humans. J Comp Neurol 2001, 441: 197–222.

Hackett T, de la Mothe L, Ulbert I, Karmas G, Smiley J, Schroeder C: Multisensory convergence in auditory cortex, II. Thalamocortical connections of the caudal superior temporal plane. J Comp Neurol 2007, 502: 924–952.

Hämäläinen M, Hari R, Ilmoniemi R, Knuutila J, Lounasmaa O: Magnetoencephalography—Theory, instrumentation, and applications to noninvasive studies of the working brain. Rev Mod Phys 1993, 65: 413–497.

Hari R, Aittoniemi K, Järvinen M, Katila T, Varpula T: Auditory evoked transient and sustained magnetic fields of the human brain. Exp Brain Res 1980, 40: 237–240.

Hari R, Hämäläinen M, Kaukoranta E, Reinikainen K, Teszner D: Neuromagnetic responses from the second somatosensory cortex in man. Acta Neurol Scand 1983a, 68: 207–212.

Hari R, Kaukoranta E, Reinikainen K, Huopaniemi T, Mauno J: Neuromagnetic localization of cortical activity evoked by painful dental stimulation in man. Neurosci Lett 1983b, 42: 77–82.

Hari R: The neuromagnetic method in the study of the human auditory cortex. Adv Audiol 1990, 6: 222–282.

Hari R, Karhu J, Hämäläinen M, Knuutila J, Salonen O, Sams M, Vilkman V: Functional organization of the human first and second somatosensory cortices: a neuromagnetic study. Eur J Neurosci 1993, 5: 724–734.

Hari R, Salmelin R: Human cortical oscillations: a neuromagnetic view through the skull. TINS 1997, 20: 44–49.

Hari R, Forss N, Avikainen S, Kirveskari E, Salenius S, Rizzolatti G: Activation of human primary motor cortex during action observation: A neuromagnetic study. Proc Nat Acad Sci USA 1998a, 95: 15061–15065.

Hari R, Hänninen R, Mäkinen T, Jousmäki V, Forss N, Seppä M, Salonen O: Three hands: fragmentation of human bodily awareness. Neurosci Lett 1998b, 240: 131–134.

Hari R, Forss N: Magnetoencephalography in the study of human somatosensory cortical processing. Philos Trans R Soc London 1999, 354: 1145–1154.

Hari R, Magnetoencephalography in clinical neurophysiological assessment of human cortical functions. In: Electroencephalography: Basic Principles, Clinical Applications and Related Fields (eds. Niedermeyer, E. and Lopes da Silva, F.), 5th edn, 2004, pp. 1165–1197. Lippincott Williams & Wilkins.

Hari R, Nishitani N, In: Functional Neuroimaging of Visual Cognition. Attention and Performance XX (eds. Kanwisher, N. and Duncan, J.), 2004, pp. 463–479. Oxford University Press, Oxford.

Hasson U, Nir Y, Levy I, Fuhrmann G, Malach R: Intersubject synchronization of cortical activity during natural vision. Science 2004, 303: 1634–1640.

Hikosaka K, Iwai E, Saito H, Tanaka K: Polysensory properties of neurons in the anterior bank of the caudal superior temporal sulcus of the macaque monkey. J Neurophysiol 1988, 60: 1615–1637.

Hillebrand A, Barnes G: A quantitative assessment of the sensitivity of the whole-head MEG to activity in the adult human cortex. NeuroImage 2002, 16: 638–650.

Hlushchuk Y, Hari R: Transient suppresion of ipsilateral primary somatosensory cortex during tactile finger stimulation. J Neurosci 2006, 26: 5819–5824.

Holmlund C, Keipi M, Meinander T, Penttinen A: Novel concepts in magnetic shielding. In: *Biomag2000*. J. N. Proc. 12th Int. Conf. on Biomagnetism, R.J. Ilmoniemi, and T. Katila, 2001, Helsinki University of Technology, Espoo, Helsinki, Finland.

Huettel A, Song A, McCarthy G, Functional Magnetic Resonance Imaging, 2004. Sinauer Associates, Sunderland, Massachusetts U.S.A.

Huttunen J, Wikström H, Korvenoja A, Seppäläinen A, Aronen H, Ilmoniemi R: Significance of the second somatosensory cortex in sensorimotor integration: enhancement of sensory responses during finger movements. NeuroReport 1996, 7: 1009–1012.

Hyvärinen J, Poranen A: Function of the parietal associative area 7 as revealed from cellular discharges in alert monkeys. Brain 1974, 97: 673–692.

Iacoboni M, Woods R, Brass M, Bekkering H, Mazziota J, Rizzolatti G: Cortical mechanisms of human imitation. Science 1999, 286: 2526–2528.

Iacoboni M, Koski L, Brass M, Bekkering H, Woods R, Dubeau M, Mazziota J, Rizzolatti G: Reafferent copies of imitated actions in the right superior temporal cortex. Proc Natl Acad Sci USA 2001, 98: 13995–13999.

Iadecola C, Yang G, Ebner T, Chen G: Local and propagated vascular responses evoked by focal synaptic activity in cerebellar cortex. J Neurophysiol 1997, 78: 651–659.

Iadecola C: Intrinsic signals and functional brain mapping: Caution, blood vessels at work. Cereb Cortex 2002, 12: 223–224.

Iguchi Y, Hoshi Y, Nemoto M, Taira M, Hashimoto I: Co-activation of the secondary somatosensory and auditory cortices facilitates frequency discrimination of vibrotactile stimuli. Neurosci 2007, 148: 461–472.

Jackson P, Meltzoff A, Decety J: Neural circuits involved in imitation and perspective-taking. NeuroImage 2006, 31: 429–439.

Järveläinen J, Shürmann M, Avikainen S, Hari R: Stronger reactivity of the human primary motor cortex during observation of live rather than video motor acts. NeuroReport 2001, 12: 3493–3495.

Järveläinen J, Schürmann M, Hari R: Activation of the human primary motor cortex during observation of tool use. NeuroImage 2004, 23: 187–192.

Jensen O, Goel P, Kopell N, Pohja M, Hari R: On the human sensorimotor-cortex beta rhythm: Sources and modeling. NeuroImage 2005, 26: 347–355.

Jiang W, Wallace M, Jiang H, Vaughan J, Stein B: Two cortical areas mediate multisensory integration in superior colliculus neurons. J Neurophysiol 2001, 85: 506–522.

Johansson R, Vallbo Å: Tactile sensitivity in the human hand: relative and absolute densities of four types of mechanoreceptive units in glabrous skin. J Physiol 1979, 286: 283–300.

Johnson K, Yoshioka T, Vega-Bermudez F: Tactile functions of mechanoreceptive afferents innervating the hand. J Clin Neurophysiol 2000, 17: 539–558.

Johnson-Frey S, Maloof F, Newman-Norlund R, Farrer C, Inati S, Grafton T: Actions or hand-object interactions? Human inferior frontal cortex and action observation. Neuron 2003, 39: 1053–1058.

Jousmäki V, Hari R: Parchment-skin illusion: sound-biased touch. Curr Biol 1998, 8: R190.

Kaas J, Hackett T: 'What' and 'where' processing in auditory cortex. Nat Neurosci 1999, 2: 1045–1047.

Kaas J, Hackett T, Tramo M: Auditory processing in primate cerebral cortex. Curr Opin Neurobiol 1999, 9: 164–170.

Kaas J, Hackett T: Subdivisions of auditory cortex and processing streams in primates. Proc Natl Acad Sci USA 2000, 97: 11793–11799.

Kaas J, Collins C, The resurrection of multisensory cortex in primates: connection patterns that integrate modalities. In: The Handbook of Multisensory Processes (eds. Calvert, G., Spence, C., and Stein, B.), 1st edn, 2004. The MIT Press, Cambridge, Massachusetts.

Kakei S, Hoffman D, Strick P: Direction of action is represented in the ventral premotor cortex. Nat Neurosci 2001, 4: 1020–1025.

Kakei S, Hoffman D, Strick P: Sensorimotor transformations in cortical motor areas. Neurosci Res 2003, 46: 1–10.

Kandel E, Schwarts J, Jessel T, Principles of Neural Science, 3rd edn, 1991. Prentice-Hall International Inc.

Kaukoranta E, Hari R, Hämäläinen M, Huttunen J: Cerebral magnetic fields evoked by peroneal nerve stimulation. Somato Res 1986, 3: 309–321.

Kayser C, Petkov C, Augath M, Logothetis N: Integration of touch and sound in auditory cortex. Neuron 2005, 48: 373–384.

Keysers C, Kohler E, Umiltà M, Nanetti L, Fogassi L, Gallese V: Audiovisual mirror neurons and action recognition. Exp Brain Res 2003, 153: 628–636.

Kilner J, Baker S, Salenius S, Hari R, Lemon R: Human cortical muscle coherence is directly related to specific motor parameters. J Neurosci 2000, 20: 8839–8845.

Kilner J, Salenius S, Baker S, Jackson P, Hari R, Lemon R: Task-dependent modulations of cortical oscillatory activity in human subjects during a bimanual precision grip task. NeuroImage 2003, 18: 67–73.

Kilner J, Vargas C, Duval S, Blakemore S, Sirigu A: Motor activation prior to observation of a predicted movement. Nat Neurosci 2004, 7: 1299–1301.

Kilner J, Frith C D: A possible role for primary motor cortex during action obervation. Proc Natl Acad Sci USA 2007, 104: 8683–8684.

Kohler E, Keysers C, Umiltà M, Fogassi L, Gallese V, Rizzolatti G: Hearing sounds, understanding actions: Action representation representation in mirror neurons. Science 2002, 297: 846–848.

Koski L, Wohlschläger A, Bekkering H, Woods R, Dubeau M, Mazziota J, Iacobini M: Modulation of motor and premotor activity during imitation of target-directed actions. Cereb Cortex 2002, 12: 848–855.

Koski L, Iacobini M, Dubeau M, Woods R, Mazziota J: Modulation of cortical activity during different imitative behaviors. J Neurophysiol 2003, 89: 460–471.

Kurata K, Hoshi E: Movement-related neuronal activity reflecting the transformation of coordinates in the ventral premotor cortex of Monkeys. J Neurophysiol 2002, 88: 3118–3132.

Kwong K, Belliveau J, Chesler D, Goldberg I, Weisskoff R, Poncelet B, Kennedy D, Hoppel B, Cohen M, Turner R, Cheng H, Brady T, Rosen B: Dynamic magnetic resonance imaging of human brain activity during primary sensory stimulation. Proc Natl Acad Sci USA 1992, 89: 5675–5679.

Lauritzen M: Reading vascular changes in brain imaging: is dendritic calcium the key? Nat Rev Neurosci 2005, 6: 77–85.

Leinonen L, Nyman G: Functional properties of cells in anterolateral part of area 7 associative face area of awake monkeys. Exp Brain Res 1979, 34: 321–333.

Levänen S, Jousmäki V, Hari R: Vibration-induced auditory-cortex activation in a congenitally deaf adult. Curr Biol 1998, 8: 869–872.

Levänen S, Uutela K, Salenius S, Hari R: Cortical representation of sign language: comparison of deaf signers and hearing non-signers. Cereb Cortex 2001, 11: 506–512.

Lin Y, Simões C, Forss N, Hari R: Differential effects of muscle contraction from various body parts on neuromagnetic somatosensory responses. NeuroImage 2000, 11: 334–340.

Logothetis N, Pauls J, Augath M, Trinath T, Oeltermann A: Neurophysiological investigation of the basis of the fMRI signal. Nature 2001, 412: 150–157.

Luppino G, Rizzolatti G: The organization of the frontal motor cortex. News Physiol Sci 2000, 15: 219–224.

Lütkenhöner B, Lammertmann C, Simões C, Hari R: Magnetoencephalographic correlates of audiotactile interaction. NeuroImage 2002, 15: 509–522.

MacDonald P, Paus T: The role of parietal cortex in awareness of self-generated movements: a transcranial magnetic stimulation study. Cereb Cortex 2003, 13: 962–967.

Maeda F, Kleiner-Fisman G, Pascual-Leone A: Motor facilitation while observing hand actions: specificity of the effects and role of observer's orientation. J Neurophysiol 2002, 87: 1329–1335.

Maeder P, Meuli R, Adriani M, Bellmann A, Fornari E, Thiran J, Pittet A, Clarke S: Distinct pathways involved in sound recognition and localization: a human fMRI study. NeuroImage 2001, 14: 802–816.

Mäkelä J, Kirveskari E, Seppä M, Hämäläinen M, Forss N, Avikainen S, Salonen O, Salenius S, Kovala T, Randell T, Jääskeläinen J, Hari R: Three-dimensional integration of brain anatomy and function to facilitate intraoperative navigation around the sensorimotor strip. Hum Brain Mapp 2001, 12: 180–192.

McGurk H, MacDonald J: Hearing lips and seeing voices. Nature 1976, 264: 746–748.

Mead G H, Mind Self and Society from the Standpoint of a Social Behaviorist, 1934. University of Chicago Press, Chicago.

Morosan P, Rademacher J, Schleicher A, Amunts K, Schormann T, Zilles K: Human primary auditory cortex: cytoarchitectonic subdivisions and mapping into a spatial reference system. NeuroImage 2001, 13: 684–701.

Morosan P, Schleicher A, Amunts K, Zilles K: Multimodal architectonic mapping of human superior temporal gyrus. Anat Embryol 2005, 210: 401–406.

Möttönen R, Järveläinen J, Sams M, Hari R: Viewing speech modulates activity in the left SI mouth cortex. NeuroImage 2005, 24: 187–192.

Mukamel R, Gelbard H, Arieli A, Hasson U, Fried I, Malach R: Coupling between neuronal firing, field potentials, and fMRI in human auditory cortex. Science 2005, 309: 951–954.

Murakami S, Okada Y: Contributions of principal neocortical neurons to magnetoencephalography and electroencephalography signals. J Physiol 2006, 575: 925–936.

Murata A, Fadiga L, Fogassi L, Gallese V, Raos V, Rizzolatti G: Object representation in the ventral premotor cortex (area F5) of the monkey. J Neurophysiol 1997, 78: 2226–2230.

Murray E, Mishkin M: Relative contributions of SII and area 5 to tactile discrimination in monkeys. Behav Brain Res 1984, 11: 67–83.

Murray M M, Molholm S, Michel C M, Heslenfeld D J, Ritter W, Javitt D C, Schroeder C E, Foxe J J: Grabbing your ear: rapid auditory-somatosensory multisensory interactions in low-level sensory cortices are not constrained by stimulus alignment. Cereb Cortex 2005, 15: 963–974.

Niedermeyer E, The normal EEG of the waking adult. In: Electroencephalography: Basic Principles, Clinical Applications and Related Fields (eds. Niedermeyer, E. and Lopes da Silva, F.), 5th edn, 2005, pp. 167–192. Lippincott Williams & Wilkins.

Niessing J, Ebisch B, Schmidt K, Niessing M, Singer W, Galuske R: Hemodynamic signals correlate tightly with synchronized gamma oscillations. Science 2005, 309: 948–951.

Nishitani N, Hari R: Temporal dynamics of cortical representation for action. Proc. Natl. Acad. Sci. USA 2000, 97: 913–918.

Nishitani N, Hari R: Viewing lip forms: Cortical dynamics. Neuron 2002, 36: 1211–1220.
Nishitani N, Avikainen S, Hari R: Abnormal imitation-related cortical activation sequences in Asperger's syndrome. Ann Neurol 2004, 55: 558–562.
Ogawa S, Lee T, Kay A, Tank D: Brain magnetic resonance imaging with contrast dependent on blood oxygenation. Proc Natl Acad Sci USA 1990, 87: 9868–9872.
Ogawa S, Tank D, Menon R, Ellermann J, Kim S, Merkke H, Ugurbil K: Intrisic signal changes accompanying sensory stimulation: Functional brain mapping with magnetic resonance imaging. Proc Natl Acad Sci USA 1992, 89: 5951–5955.
Okano K, Tanji J: Neuronal activities in the primate motor fields of the agranular frontal cortex preceding visually triggered and self-paced movements. Exp Brain Res 1987, 66: 155–166.
Paetau R, Kajola M, Hari R: Magnetoencephalography in the study of epilepsy. Neurophysiol Clin 1990, 20: 169–187.
Patuzzo S, Fiaschi A, Manganotti P: Modulation of motor cortex excitability in the left hemisphere during action observation: a single- and paired-pulse transcranial magnetic stimulation study of self- and non-self-action observation. Neuropsychol 2003, 41: 1272–1278.
Penfield W, Jasper H, Epilepsy and the Functional Anatomy of the Human Brain, 1954. Boston, MA: Little, Brown & Co.
Pons T, Garraghty P, Friedman D, Mishkin M: Physiological evidence for serial processing in somatosensory cortex. Science 1987, 237: 417–420.
Poremba A, Saunders R, Crane A, Cook M, Sokoloff L, Mishkin M: Functional mapping of the primate auditory system. Science 2003, 299: 568–572.
Purcell E, Torrey H, Pound R: Resonance absorption by nuclear magnetic moments in a solid. Phys Rev 1945, 69: 37–38.
Rabi I, Zacharias J, Millman S, Kusch P: A new method of measuring nuclear magnetic moment. Phys Rev 1938, 53: 318.
Rademacher J, Morosan P, Schormann T, Schleicher A, Werner C, Freund H, Zilles K: Probabilistic mapping and volume measurement of human primary auditory cortex. NeuroImage 2001, 13: 669–683.
Rademacher J, Bürgel U, Zilles K: Stereotaxic localization, intersubject variability, and interhemispheric differences of the human thalamocortical system. NeuroImage 2002, 17: 142–160.
Raij T, Uutela K, Hari R: Audiovisual integration of letters in the human brain. Neuron 2000, 28: 617–625.
Rauschecker J, Tian B: Mechanisms and streams for processing of "what" and "where" in auditory cortex. Proc Natl Acad Sci USA 2000, 97: 11800–11806.
Ridley R, Ettlinger G: Impaired tactile learning and retention after removals of the second somatic sensory projection cortex (SII) in the monkey. Brain Res 1976, 109: 656–660.
Rivier F, Clarke S: Cytochrome oxidase, acetylcholinesterase, and NADPH-Diaphorase staining in human supratemporal and insular cortex: evidence for multiple auditory areas. NeuroImage 1997, 6: 288–304.
Rizzolatti G, Camarda R, Fogassi L, Gentilucci M, Luppino G, Matelli M: Functional organization of inferior area 6 in the macaque monkey. II. Area F5 and the control of distal movements. Exp Brain Res 1988, 71: 491–507.
Rizzolatti G, Fadiga L, Gallese V, Fogassi L: Premotor cortex and the recognition of motor actions. Cogn Brain Res 1996a, 3: 131–141.
Rizzolatti G, Fadiga L, Matelli M, Bettinardi V, Paulesu E, Perani D, Fazio F: Localization of grasp representation in humans by PET: Observation versus execution. Brain Res 1996b, 111: 246–252.
Rizzolatti G, Arbib M: Language within our grasp. Trends Neurosci 1998, 21: 188–194.
Rizzolatti G, Luppino G, Matelli M: The organization of the cortical motor system: new concepts. Electoencephalogr Clin Neurophysiol 1998, 106: 283–296.
Rizzolatti G, Fogassi L, Gallese V: Neurophysiological mechanisms underlying the understanding and imitation of action. Nat Rev Neurosci 2001, 2: 661–670.
Rizzolatti G, Luppino G: The cortical motor system. Neuron 2001, 31: 889–901.
Rizzolatti G, Craighero L: The mirror-neuron system. Ann Rev Neurosci 2004, 27: 169–192.
Rockland K, Ojima H: Multisensory convergence in calcarine visual areas in macaque monkey. Int J Psychophysiol 2003, 50: 19–26.
Romanski L, Bates J, Goldman-Rakic P: Auditory belt and parabelt projections to the prefrontral cortex in the rhesus monkey. J Comp Neurol 1999, 403: 141–157.
Ruben J, Schwiemann J, Deuchert M, Meyer R, Krause T, Curio G, Villringer K, Kurth R, Villringer A: Somatotopic organization of human secondary somatosensory cortex. Cereb Cortex 2001, 11: 463–473.
Ruby P, Decety J: Effect of subjective perspective taking during simulation of action: a PET investigation of agency. Nat Neurosci 2001, 4: 546–550.
Salenius S, Portin K, Kajola M, Salmelin R, Hari R: Cortical control of human motoneuron firing during isometric contraction. J Neurophysiol 1997a, 77: 3401–3405.

Salenius S, Schnitzler A, Salmelin R, Jousmäki V, Hari R: Modulation of human cortical rolandic rhythms during natural sensorimotor tasks. NeuroImage 1997b, 5: 221–228.

Salmelin R, Hari R: Spatiotemporal characteristics of sensorimotor neuromagnetic rhythms related to thumb movement. Neurosci 1994, 60: 537–550.

Salmelin R, Hämäläinen M, Kajola M, Hari R: Functional segregation of movement-related rhythmic activity in the human brain. NeuroImage 1995, 2: 237–243.

Salmelin R, Kujala J: Neural representation of language: Activation vs. long-range connectivity. Trends Cogn Sci 2006, 10: 519–525.

Salmelin R: Clinical neurophysiology of language: The MEG approach. Clin Neurophysiol 2007, 118: 237–254.

Schmuel A, Augath M, Oeltermann A, Logothetis N: Negative functional MRI response correlates with decreases in neuronal activity in monkey visual area V1. Nat Neurosci 2006, 9: 569–577.

Schnitzler A, Salenius S, Salmelin R, Jousmäki V, Hari R: Involvement of primary motor cortex in motor imagery: A neuromagnetic study. NeuroImage 1997, 6: 201–208.

Schroeder C, Lindsley R, Specht C, Marcovici A, Smiley J, Javitt D: Somatosensory input to auditory association cortex in the macaque monkey. J Neurophysiol 2001, 85: 1323–1327.

Schroeder C, Foxe J: The timing and laminar profile of converging inputs to multisensory areas of the macaque neocortex. Cogn Brain Res 2002, 14: 187–198.

Schroeder C, Smiley J, Fu K-M G, McGinnis T, O'Connell M, Hackett T: Anatomical mechanisms and functional implications of multisensory convergence in early cortical processing. Int J Psychophysiol 2003, 50: 5–17.

Schürmann M, Caetano G, Jousmäki V, Hari R: Hands help hearing: Facilitatory audiotactile interaction at low sound intensity levels. J Acoust Soc Am 2004, 115: 830–832.

Schürmann M, Caetano G, Hlushchuk Y, Jousmäki V, Hari R: Touch activates human auditory cortex. NeuroImage 2006, 30: 1325–1331.

Simões C, Hari R: Relationship between responses to contra- and ipsilateral stimuli in the human second somatosensory cortex SII. NeuroImage 1999, 10: 408–416.

Simões C, Mertens M, Forss N, Jousmäki V, Lütkenhoner B, Hari R: Functional overlap of finger representations in human SI and SII cortices. J Neurophysiol 2001, 86: 1661–1665.

Simões C, Jensen O, Parkkonen L, Hari R: Phase locking between human primary and secondary somatosensory cortices. Proc Natl Acad Sci USA 2003, 100: 2691–2694.

Singh M, Sungkarat W, Bernstein L E, Auer Jr E T: Vibrotactile activation of the auditory cortices in deaf versus hearing adults. NeuroReport 2007, 18: 645–648.

Smiley J, Hackett T, Ulbert I, Karmas G, Lakatos P, Javitt D, Schroeder C: Multisensory convergence in auditory cortex, I. Cortical connections of the caudal superior temporal plane in macaque monkeys. J Comp Neurol 2007, 502: 894–923.

Smith A, Williams A, Singh D: Negative BOLD in the visual cortex: evidence against blood stealing. Hum Brain Mapp 2004, 21: 213–220.

Stein B, Meredith M, The Merging of the Senses, 1993. Cambridge, MA: MIT Press.

Stein B: Neural mechanisms for synthesizing sensory information and producing adaptive behaviors. Exp Brain Res 1998, 123: 124–135.

Tardif E, Clarke S: Intrisic connectivity of human auditory areas: a tracing study with Dil. Eur J Neurosci 2001, 13: 1045–1050.

Tarkiainen A, Liljeström M, Seppä M, Salmelin R: The 3D topography of MEG source localization accuracy: effects of conductor model and noise. Clin Neurophysiol 2003, 114: 1977–1992.

Teyler T, Cuffin B, Cohen D: The visual magnetoencephalogram. Life Sci 1975, 17: 683–692.

Thulborn K, Waterton J, Matthews P, Radda G: Oxygenation dependence of the transverse relaxation time of water protons in whole blood at high field. Biochim Biophys Acta 1982, 714: 265–270.

Turman A, Ferrington D, Ghosh S, Morley J, Rowe M: Parallel processing of tactile information in the cerebral cortex of the cat: effect of reversible inactivation of SI on responsiveness of SII neurons. J Neurophysiol 1992, 67: 411–429.

Umiltà M, Kohler E, Gallese V, Fadiga L: "I know what you are doing": a neurophysiological study. Neuron 2001, 32: 91–101.

Umiltà M, Brochier T, Spinks R L, Lemon R: Simultaneous recording of macaque premotor and primary motor cortex neuronal populations reveals different functional contributions to visuomotor grasp. J Neurophysiol 2007, 98: 488–501.

Uusitalo M A, Ilmoniemi R J: Signal-space projection method for separating MEG or EEG into components. Med & Biol Eng & Comput 1997, 35: 135–140.

Uutela K, Hämäläinen M, Somersalo E: Visualization of Magnetoencephalographic data using minimum current estimates. NeuroImage 1999, 10: 173–180.

Van Essen D C, Dierker D: On navigating the human cerebral cortex: Response to "in praise of tedious anatomy". NeuroImage 2007, 37: 1050–1054.

Vogeley K, May M, Ritzl A, Falkai P, Zilles K, Fink G R: Neural correlates of first-person perspective as one constituent of human self-consciousness. J Cogn Neurosci 2004, 16: 817–827.

von Békésy G, Experiments in Hearing, 1960. McGraw-Hill, New York.

von Schiller P: Die Rauhigkeit als intermodale Erscheinung. Z Psychol Bd 1932, 127: 265–289.

Wallace M, Meredith M, Stein B: Converging influences from visual, auditory, and somatosensory cortices onto output neurons of the superior colliculus. J Neurophysiol 1993, 69: 1797–1809.

Wallace M, Stein B: Development of multisensory neurons and multisensory integration in cat superior colliculus. J Neurosci 1997, 17: 2429–2444.

Wallace M, Meredith M, Stein B: Multisensory integration is the superior colliculus of the alert cat. J Neurophysiol 1998, 80: 1006–1010.

Wallace M, Stein B: Sensory and multisensory responses in the newborn monkey superior culliculus. J Neurosci 2001, 21: 8886–8894.

Wansapura J, Holland S K, Dunn R S, Ball W: NMR relaxation times in the human brain at 3.0 Tesla. J Magn Res Imag 1999, 9: 531–538.

Wessinger C, van Meter J, Tian B, van Lare J, Pekar J, Rauschecker J: Hierarchical organization of the human auditory cortex revealed by functional magnetic resonance imaging. J Cogn Neurosci 2001, 13: 1–7.

Wilkinson L, Meredith M, Stein B: The role of anterior ectosylvian cortex in cross-modality orientation and approach behavior. Exp Brain Res 1996, 112: 1–10.

Zilles K, Palomero-Gallagher N: Cyto-, myelo-, and receptor architectonics of the human parietal cortex. NeuroImage 2001, 14: S8–S20.